# UNIVERSITÀ DEGLI STUDI DI CATANIA

*Dipartimento di Ingegneria Civile e Architettura*

*Dottorato di Ricerca in Valutazione e Mitigazione dei Rischi Urbani e Territoriali*

XXXVII cicle


# INTEGRATED ASSESSMENT OF LANE SUPPORT SYSTEM: A MULTI-SOURCE APPROACH USING ADAS, ROAD, ENVIRONMENTAL MEASUREMENTS, AND HUMAN DATA


Dottorando

Omid Ghaderi

Advisor:
Prof. Salvatore Cafiso

Co-advisor:
Dr. Giuseppina Pappalardo

Coordinator:
Prof. Antonino Cancelliere



CATANIA

Ph. D. attended during 2022/2025

# Acknowledgements

This PhD journey has been one of the most transformative and meaningful chapters of my life—intellectually rigorous, emotionally intense, and deeply fulfilling. It is the result not only of years of dedication and hard work, but also of the support, guidance, and kindness of many individuals and institutions to whom I owe my sincerest gratitude.

I would first like to express my profound appreciation to my supervisor, Professor Salvatore Cafiso, for his exceptional mentorship, professional guidance, and continuous encouragement throughout the course of my PhD. His deep expertise and leadership in the field provided me with a solid foundation, while his personal support and friendly demeanor created a collaborative and welcoming environment. Working under his supervision has been both an honor and a privilege.

I am sincerely grateful to Professor Antonino Cancelliere, my PhD coordinator, for his support and constructive feedback during these years. A special thanks goes to Professor Giuseppina Pappalardo, whose active involvement in shaping the research plan and managing project activities greatly contributed to the quality and structure of this work. Her technical expertise, commitment, and continuous support were truly invaluable

I also wish to thank Professors Riccardo Caponetto, Alessandro Di Graziano, and Michele Mangiameli, with whom I had the opportunity to collaborate during various academic activities. Their professional advice, insightful discussions, and encouragement helped me acquire essential research and academic skills. Their support enriched my PhD experience and contributed significantly to my development as an independent researcher.

I would also like to extend my sincere thanks to Professor Massimo Cuomo and Professor Giuseppe Inturri for their kindness and friendly encouragement throughout my time at the University of Catania. Their warm attitude and respectful support, even outside the scope of direct collaboration, meant a great deal to me.

My sincere appreciation goes to Professor Haneen Farah, who warmly welcomed me during my academic internship at TU Delft. Her scientific

mentorship, generous hospitality, and personal support had a profound impact on me. She was not only a brilliant academic host, but also a supportive friend whose kindness and encouragement gave me strength and confidence during a pivotal stage of my work. I am also grateful to Professor Marjan Hagenzieker, co-director of the Traffic and Transportation Safety Lab (TTSLab) at TU Delft, for her warm welcome and continued support during my stay.

I am especially thankful to the members and friends at TTSLab — Nagarjun, Siri, Sina, Yiyun, Vincent, and Yongqi — for the scientific discussions and shared experiences in the lab. I also wish to thank my friends at TU Delft — Konstantinos, Ricardo, Saman, Elif, Sara, Mahsa, and Monique — for their friendship and support, which made my time in the Netherlands both enjoyable and memorable. My heartfelt appreciation also extends to the Faculty of Civil Engineering and Geosciences at TU Delft, whose academic environment enriched my research experience.

In addition to my academic internship, I would like to acknowledge ITER – Infrastructure and Transport Engineering S.r.l., where I completed a professional internship. I am thankful to its management and team members for the valuable learning opportunities and support provided during my time there.

I gratefully acknowledge the University of Catania, particularly the Department of Civil Engineering and Architecture (DICAR), for their continuous institutional support and for providing access to essential datasets, including ADAS and human driving perception data. I also thank Azienda Nazionale Autonoma delle Strade (ANAS) for supplying the lane marking data, which formed a core part of this research.

I am especially thankful to Engineer Giovanni Andrea Dimauro and Engineer Daniele Bordonaro, whose collaboration in data preparation and fusion was instrumental in building a robust, high-value dataset.

I also thank my fellow PhD colleagues and officemates — Federica, Roberto, Martina, Michela, Giovanni, Francesco, Andrea, Zahra, Soroush, Fatima, Alice, Alessandro, and Shahin — for their camaraderie, shared ideas, and everyday support through the highs and lows of this academic journey. Your presence made this experience far more enjoyable, both professionally and personally.

Beyond the academic realm, I would like to acknowledge my beloved country, Iran—a land with a profound legacy of scientific excellence and intellectual achievement. As the birthplace of countless pioneers in science, medicine, mathematics, and engineering, Iran has contributed greatly to global knowledge. Coming from a highly academic family rooted in such a heritage has been one of the greatest motivations in my scientific journey.

My deepest gratitude belongs to my family, whose unconditional love, patience, and sacrifices have made this achievement possible. To my very kind and beautiful mother, thank you for your endless love and emotional strength, which have supported me through every stage of life. To my supportive father, your encouragement and belief in my abilities have shaped my confidence and determination. To my dear brother Amin, thank you for being a constant source of positivity and motivation. And to my dearest brother, Dr. Amir Ghaderi, your scientific insight, thoughtful advice, and heartfelt support have played a major role in my academic success. I am deeply proud to walk this path with you beside me.

This work is not merely the outcome of individual effort, but the shared result of kindness, knowledge, and inspiration offered by a remarkable circle of people. To each of you, I extend my heartfelt thanks.

Omid Ghaderi
Spring 2025

# Copyright Notice

INTEGRATED ASSESSMENT OF LANE SUPPORT SYSTEM: A MULTI-SOURCE APPROACH USING ADAS, ROAD, ENVIRONMENTAL MEASUREMENTS, AND HUMAN DATA

by
Omid Ghaderi

© 2025 Omid Ghaderi
All rights reserved.

No part of this dissertation may be reproduced, stored in a retrieval system, or transmitted in any form or by any means, electronic, mechanical, photocopying, recording, or otherwise, without the prior written permission of the author, except where permitted by law.

This dissertation was submitted to Università di Catania in partial fulfillment of the requirements for the degree of PhD Degree.

# Index

*Acknowledgements* ..... *C*

*Copyright Notice* ..... *G*

*Index* ..... *I*

*Figure Index* ..... *P*

*Table Index* ..... *S*

*Abbreviations and Acronyms* ..... *U*

*Research highlights* ..... *W*

*Abstract* ..... *AA*

*Riassunto* ..... *CC*

*1 Chapter 1: Introduction and Literature Review* ..... *2*

1.1 Background and Motivation ..... 3

1.2 Problem Statement ..... 6

1.3 Research Objectives ..... 7

1.4 Scope of research ..... 8

1.5 Key Concepts and Definitions ..... 9

1.5.1 Lane Markings definitions and functions ..... 9

1.5.2 Types of Lane Markings (Geometrical Classification) 10

1.5.3 Lane Marking Performance Criteria & Metrics 11

1.5.4 Lane marking Retroreflectivity (RL) ..... 12

1.5.5 Evaluation of Pavement Marking Retroreflectivity ..... 15

1.5.6 ANAS DELPHI Car ..... 19
1.5.7 Retroreflectivity Thresholds ..... 21
1.5.8 Maintenance Thresholds by Road Agencies..... 24
1.5.9 Relationship Between RL and Road Safety..... 25

1.6 Advanced Driver Assistance Systems (ADAS) and Autonomous Vehicles (AVs)..... 26
1.6.1 Definition of Advanced Driver Assistance Systems (ADAS) ..... 26
1.6.2 Levels of Vehicle Automation..... 29

1.7 Lane Support Systems (LSS) and Their Role in ADAS 32
1.7.1 Types of Lane Support Systems ..... 32
1.7.2 Importance of LSS for Road Safety..... 33
1.7.3 Regulatory Framework and Lane Support Systems (LSS) Reliability ..... 33

1.8 Operational Design Domain (ODD) for LKA ..... 35
1.8.1 Definition and Importance of ODD..... 35
1.8.2 Definition of Lane Support Systems (LSS)..... 35
1.8.3 Operational Design Domain (ODD) Taxonomy 41
1.8.4 ODD Testing and Validation..... 42
1.8.5 Infrastructure Impact on LKA Operational Design Domain (ODD)..... 45
1.8.6 ADAS and Pavement Marking Reflectivity. .... 46
1.8.7 Challenges in Lane Marking Detection for ADAS Systems..... 51

1.9 State-of-the-Art and Empirical Evidence ..... 51
1.9.1 Lane Marking Quality Assessment and Detection Techniques 52
1.9.2 Empirical Studies on Lane Markings and LKA

Performance 66

1.10 Summary and Research Gaps ..... 69

1.11 Structure of the Dissertation ..... 70

***2 Chapter 2: Methodology ..... 74***

2.1 Database ..... 74

2.1.1 Mobileye 6.0 Data ..... 76

2.1.2 Road Geometry ..... 78

2.1.3 Driver perception of lane marking quality ..... 79

2.2 Data fusion ..... 80

2.3 Aggregation Datasets ..... 85

2.4 Data stratification ..... 87

2.5 Data Cleaning ..... 88

2.6 Project 1: Lane marking quality assessment ..... 91

2.6.1 Features selection ..... 91

2.6.2 Database Balancing ..... 94

2.6.3 Model Selection ..... 97

2.6.4 Statistical Classification Models ..... 98

2.6.5 Machine Learning Models ..... 99

2.6.6 Deep Learning Models ..... 102

2.7 Project 2: Monitoring Lane Marking Retroreflectivity Using ADAS Sensor Data ..... 105

2.7.1 Data Preparation and Dataset Derivation ..... 105

2.7.2 Exploratory Analysis ..... 105

2.7.3 Regression Modelling ..... 111

2.7.4 Classification Modelling ..... 111

2.7.5 Environmental Conditions Integration ..... 112

2.8 Project 3: Human–ADAS Lane Marking Quality

assessment 113
2.8.1 Analytical Framework ..... 114

***3 Chapter 3: Results ..... 122***

3.1 Analysis and Results of Project 1: Lane marking quality assessment ..... 122
3.1.1 Model Validation ..... 128
3.1.2 SHAP (SHapley Additive exPlanations) analysis (class 1): 134

3.2 Analysis and Results of Project 2: Monitoring Lane Marking Retroreflectivity Using ADAS Sensor Data ..... 140
3.2.1 Regression Analysis ..... 141
3.2.2 Classification Analysis ..... 143

3.3 Analysis and Results of Project 3: Lane Marking perception and assessment by Human vs. ADAS ..... 149
3.3.1 Frequency Analysis of Lane Marking Quality under Varying Environmental Conditions ..... 149
3.3.2 Spearman's Rank Correlation Between Human and System Assessments ..... 153
3.3.3 Descriptive Statistics and Group Comparison 155
3.3.4 One-Way ANOVA and Box's M Test ..... 157
3.3.5 Discriminant Function Analysis ..... 158

***4 Chapter 4: Discussion ..... 166***

4.1 Interpretation and Discussion of Project 1: Lane Marking Quality Assessment ..... 166
4.1.1 Overview of Predictive Performance ..... 166
4.1.2 SHAP Interpretability and Feature Interactions 167
4.1.3 Implications for Road Design and Maintenance 169

4.2 Interpretation and Discussion of Project 2: Monitoring Lane Marking Retroreflectivity Using ADAS Sensor Data ..... 170
4.2.1 Model Behaviour under Filtering Strategies... 170
4.2.2 Dataset-Specific Analysis and Use Case Relevance 171
4.2.3 Environmental Conditions and General Model Reflections 172

4.3 Interpretation and Discussion of Project 3: Human vs. ADAS Lane Marking Quality Perception ..... 173
4.3.1 Perception Biases under Varying Environmental Conditions 173
4.3.2 Quantitative Agreement Analysis and Condition-Dependent Behavior ..... 174
4.3.3 Infrastructure and Design Recommendations. 174

4.4 Cross-Project Synthesis and Implications ..... 175
4.4.1 Converging Influences: Geometry, Retroreflectivity, and Environmental Factors ..... 175
4.4.2 Complementarity Between Measurement, Machine, and Human Perspectives..... 176
4.4.3 Implications for ADAS Development and Infrastructure Planning ..... 177

***5 Chapter 5: Conclusions and Recommendations..... 182***

5.1 General Overview and Chapter Structure..... 182

5.2 Lane Support System Performance under ODD Variability 182

5.3 Monitoring Lane Marking Retroreflectivity Using ADAS Sensor Data..... 184

5.4 Driver vs. ADAS Perception of Lane Marking Quality 185

5.5 Cross-Project Insights and Future Directions ..... 187

***References*** ***..... 190***

***Appendix*** ***..... 208***

O

# Figure Index

Figure 1 30 meters geometry (FHWA 2022).....14
Figure 2 Pavement marking with known retroreflectivity levels [21] .....14
Figure 3 ANAS DELPHI Car[30] .....20
Figure 4 ODD Taxonomy (BSI PAS 1883:2020) .....42
Figure 5 Data acquisition; a) University of Catania Aran 9000 Car, b) Mobileye 6 full protocol, c) ANAS DELPHI Car [139] .....75
Figure 6 Schematic of data collection from different sources.....76
Figure 7 Mobileye survey for right and left lane.....81
Figure 8 a) Geometric parameters extraction in GIS environment and geometric curvature from Civil 3D, b) Road Track construction.....82
Figure 9 ANAS points and buffering .....83
Figure 10 Intersection and aggregation of ANAS buffers, Mobileye data and geometry for right and left lane.....83
Figure 11 Data labeling based on road geometry .....85
Figure 12 The effect of Right (+) and left (-) curvature on curvature parameter & quality scores (dark green is highest and red for lowest quality) by Mobileye. .....86
Figure 13 Curvature parameter on open street map (QGis); a) Trajectory Curvature (1/R), b) Mobileye Curvature.....86
Figure 14 Data stratification; a) LDWoff base; b) Lane marking width base; c) Speed base.....88
Figure 15 Pearson Correlation of Features .....90
Figure 16 Percentages of LSS fail for different marking detection scores.....91
Figure 17 Catboost Feature Importance Analysis for different outcomes: a) Qmin, b) Qmode, c) Qmax.....93
Figure 18 Resampling Strategy, a) Normalized confusion matrix before resampling. b) Normalized confusion matrix after resampling with 50% SMOTE. c) Normalized confusion matrix after resampling

with 100% SMOTE. ..... 97
Figure 19 Correlation heatmap ..... 107
Figure 20 Network graph (TR=0.3) ..... 108
Figure 21 XGBoost feature importance analysis for general dataset (Removed rain) ..... 109
Figure 22 XGBoost feature importance. a) Daytime. b) Nighttime 111
Figure 23 Overall model accuracy ..... 123
Figure 24 Comparison of classes F1-Scores by different models .. 124
Figure 25 Comparison of classes precision by different models .... 124
Figure 26 Comparison of classes recall by different models ..... 125
Figure 27 K-Fold cross validation ..... 129
Figure 28 Learning curves ..... 130
Figure 29 Validation Curves ..... 130
Figure 30 Normalized confusion matrix for AutoML-LGBM ..... 131
Figure 31 LightGBM model accuracy for three SMOTE strategies ..... 133
Figure 32 LightGBM model F1-score for different classes based on three SMOTE strategies ..... 133
Figure 33 a) SHAP Summary Plot (Beeswarm) for Critical Condition (Class 1) (Light: Day=1, Night=0; Env.: Dry=1, Rain=2; Wet=3) b) Shap summary bar plot (with mean SHAP value) ..... 136
Figure 34 SHAP Dependence Plots for critical system condition (class 1) ..... 138
Figure 35 Model's R Square for different conditions ..... 142
Figure 36 Model's MAPE for different conditions ..... 142
Figure 37 RLavg F1-Scores for RL Classes under Each Filtering Condition (for Thresholds A and B) ..... 144
Figure 38 RL3 F1-Scores for RL Classes under Each Filtering Condition (for Thresholds A and B) ..... 144
Figure 39 RLmin F1-Scores for RL Classes under Each Filtering Condition (for Thresholds A and B) ..... 144
Figure 40 Overall Accuracy for RLavg, RL3, and RLmin under Each

Filtering Condition for thresholds A& B. ..... 145
Figure 41 Environmental Analysis – F1-Scores and general model accuracy for RLavg dataset for Day/Night and Dry–Wet vs. Dry Conditions. ..... 147
Figure 42 Environmental Analysis – F1-Scores and general model accuracy for RL3 dataset for Day/Night and Dry–Wet vs. Dry Conditions. ..... 148
Figure 43 Environmental Analysis – F1-Scores and general model accuracy for RLmin dataset for Day/Night and Dry–Wet vs. Dry Conditions. ..... 148
Figure 44 Frequency distribution of lane marking quality classes under different conditions: LSS (Quality) vs. Human (Mode) perception. ..... 152
Figure 45 Spearman's Rank Correlation for different conditions .. 155

# Table Index

Table 1 Lane marking Visibility Metrics ..... 12
Table 2 Relationship Between RL, Qd, Cr and Visibility ..... 12
Table 3 Proposed MUTCD Minimum Retroreflectivity (MUTCD) 22
Table 4 Proposed MUTCD minimum retroreflectivity values for longitudinal pavement markings ..... 22
Table 5 Recommended RL levels for dry condition by CEN..... 23
Table 6 Recommended RL levels for wet and rain conditions by CEN ..... 23
Table 7 Overview of different levels of automation based on SAE 31
Table 8 Lane Support Systems categories ..... 32
Table 9 Environmental Challenges..... 51
Table 10 Infrastrutture Challenges ..... 51
Table 11 Mobileye® CAN messages parameters and definitions for LKA system..... 78
Table 12 Alignment parameters ..... 79
Table 13 Surveyed Road Sections under different environmental conditions ..... 84
Table 14 Summary statistic parameters..... 89
Table 15 Correlation matrix ..... 154
Table 16 summary statistics of Groups means ..... 157
Table 17 Equality of Group Means test..... 158
Table 18 Tests null hypothesis of equal population covariance matrices ..... 158
Table 19 Summary of Canonical Discriminant Functions ..... 159
Table 20 Wilks' Lambda estimates..... 160
Table 21 Functions at Group Centroids..... 160
Table 22 Classification Results ..... 161
Table 23 Standardized Canonical Discriminant Function Coefficients

.....162
Table 24 Structure Matrix .....162
Table 25 RLmin datasets summary statistics under different segmentation.....209
Table 26 RLmin environmental datasets summary statistics .....210
Table 27 RL3 datasets summary statistics under different segmentation.....211
Table 28 RL3 environmental datasets summary statistics.....212
Table 29 RLavg datasets summary statistics under different segmentation.....213
Table 30 RLavg environmental datasets summary statistics.....214

# Abbreviations and Acronyms

| Abbreviation | Full Term |
|---|---|
| **ADAS** | Advanced Driver-Assistance Systems |
| **ADS** | Automated Driving Systems |
| **AF** | Agreement Factor |
| **ANAS** | Agenzia Nazionale Autonoma delle Strade (Italian Road Agency) |
| **ARAN** | Automatic Road Analyzer |
| **AVs** | Autonomous Vehicles |
| **AutoML** | Automated Machine Learning |
| **CAN** | Controller Area Network |
| **CV** | Coefficient of Variation |
| **CatBoost** | Categorical Boosting |
| **DDT** | Dynamic Driving Task |
| **DFA** | Discriminant Function Analysis |
| **DL** | Deep Learning |
| **EFB** | Exclusive Feature Bundling |
| **FCNN** | Fully Connected Neural Network |
| **GIS** | Geographic Information System |
| **GNSS** | Global Navigation Satellite System |
| **GOSS** | Gradient-based One-Side Sampling |
| **GPS** | Global Positioning System |
| **L1** | Lasso Regularization (L1 norm) |
| **L2** | Ridge Regularization (L2 norm) |
| **LDW** | Lane Departure Warning |
| **LGBM** | Light Gradient Boosting Machine |
| **LKA** | Lane Keeping Assistance |
| **LSS** | Lane Support System |
| **MLP** | Multi-Layer Perceptron |
| **ODD** | Operational Design Domain |
| **OEMs** | Original Equipment Manufacturers |
| **OMLP-N** | Ordinal Multi-Layer Perceptron Network |
| **ORF** | Ordinal Random Forest |
| **OSM** | OpenStreetMap |
| **PCI** | Pavement Condition Index |
| **PDRF** | Probabilistic Driving Risk Field |
| **QGIS** | Quantum Geographic Information System |
| **QoS** | Quality of Service |
| **RL** | Retroreflectivity Level |
| **RLw** | Wet Retro-Reflectance of Lane Markings |
| **SAE** | Society of Automotive Engineers |
| **SHAP** | SHapley Additive exPlanations |
| **SMOTE** | Synthetic Minority Over-Sampling Technique |
| **SVM** | Support Vector Machines |
| **TPOT** | Tree-based Pipeline Optimization Tool |
| **UI** | User Interface |

# Research highlights

- Comprehensive analysis of the Operational Design Domain (ODD) for Lane Support Systems (LSS) based on real-world experimental driving data.
- Development of a multi-source dataset combining Mobileye vision-based ADAS outputs, GNSS/INS positioning, OpenStreetMap (OSM) geometry, and ANAS retroreflectivity (RL) measurements.
- Advanced machine learning methodologies (AutoML-LGBM, CatBoost, and SHAP) applied for lane marking quality classification and model interpretability.
- Comparative evaluation of statistical, machine learning, and deep learning models, demonstrating superior predictive performance of AutoML-LGBM and CatBoost algorithms.
- SHAP-based interpretability analysis, identifying critical factors (e.g., retroreflectivity, curvature, lane width) affecting LSS lane detection under varying road and environmental conditions.
- Investigation of geometric road features (curvature, lane width, shoulder width) and their impact on LSS detection performance, supported by SHAP dependence plots.
- Assessment of LSS limitations under adverse environmental conditions, including rain, nighttime driving, and segments with low retroreflectivity markings.
- GIS-based data fusion framework implemented for synchronizing and aligning heterogeneous spatial datasets, enabling enhanced analysis precision.
- Monitoring of lane marking retroreflectivity (RL) through ADAS sensor data, using regression and classification models to estimate RL without direct physical measurements.

- Evaluation of filtering strategies (curvature filtering, coefficient of variation filtering) to improve model accuracy in retroreflectivity prediction.
- Environmental impact analysis on RL prediction models, showing better performance under dry daytime conditions and emphasizing the need for adaptive calibration.
- Comparative analysis of driver perception versus ADAS evaluation of lane marking quality under real-world conditions, highlighting condition-dependent divergences.
- Spearman correlation and discriminant analysis, revealing the key factors (lane width, retroreflectivity, lighting) contributing to perception mismatches between human drivers and the ADAS.
- Proposal of policy recommendations for road maintenance, suggesting optimal lane marking retroreflectivity thresholds (>150 mcd/m²/lx) to enhance both LSS and driver safety.
- Introduction of a machine learning-driven evaluation framework for LSS performance, adaptable for future studies on autonomous vehicle perception and infrastructure interaction.

Z

# Abstract

The effectiveness of Lane Support Systems (LSS) in Advanced Driver-Assistance Systems (ADAS) is highly dependent on their Operational Design Domain (ODD), particularly factors such as lane marking quality, road geometry, and environmental conditions. This dissertation evaluates LSS performance through a multi-project investigation based on real-world experimental data collected using a vision-based ADAS (Mobileye 6.0), GNSS/INS sensors, OpenStreetMap (OSM) geometry, and ANAS retroreflectivity (RL) measurements, integrated via GIS-based data fusion techniques.

In the first project, a comprehensive machine learning framework was developed, leading to the selection of AutoML-LGBM and CatBoost models for lane marking quality classification, supported by SHAP analysis for feature interpretability. Results show that retroreflectivity, road curvature, lane width, and environmental factors (e.g., rain and nighttime driving) significantly impact LSS lane detection reliability. In the second project, regression and classification models were employed to estimate lane marking retroreflectivity using ADAS sensor outputs, demonstrating that ADAS data can effectively approximate physical RL measurements when supported by appropriate segmentation and calibration strategies. The third project investigated the agreement between human driver assessment and ADAS-based lane marking quality evaluation, revealing a significant, although moderate correlation, but identifying divergences under specific environmental and geometric conditions, particularly in low-visibility scenarios.

Together, the findings provide engineering, operational, and policy recommendations to improve road standards, particularly lane marking retroreflectivity thresholds, and to enhance ADAS calibration

strategies. The proposed data-driven framework contributes to safer autonomous driving technologies and more reliable ADAS deployment under real-world operational conditions.

*Keywords*:
*Lane Support System (LSS); Operational Design Domain (ODD); Machine Learning in ADAS; Lane Marking Detection; Road Geometry and Retroreflectivity; Autonomous Vehicles and Safety; Retroreflectivity Estimation; Human–Machine Perception Comparison*

# Riassunto

L'efficacia dei Lane Support Systems (LSS) nei sistemi avanzati di assistenza alla guida (ADAS) dipende fortemente dal loro Operational Design Domain (ODD), in particolare da fattori quali la qualità della segnaletica orizzontale, la geometria stradale e le condizioni ambientali. Questa tesi valuta le prestazioni degli LSS attraverso un'indagine articolata in più progetti, basata su dati sperimentali reali raccolti mediante un sistema ADAS basato su visione (Mobileye 6.0), sensori GNSS/INS, geometrie stradali da OpenStreetMap (OSM) e misurazioni di retroriflettanza (RL) fornite da ANAS, integrati tramite tecniche di fusione dati basate su GIS.

Nel primo progetto, è stato sviluppato un quadro completo di Machine Learning (ML), che ha portato alla selezione dei modelli AutoML-LGBM e CatBoost per la classificazione della qualità della segnaletica orizzontale, supportati da un'analisi SHAP per l'interpretabilità delle variabili. I risultati mostrano che la retroriflettanza, la curvatura stradale, la larghezza della corsia e i fattori ambientali (ad esempio pioggia e guida notturna) influenzano significativamente l'affidabilità del rilevamento delle corsie da parte degli LSS. Nel secondo progetto, sono stati utilizzati modelli di regressione e classificazione per stimare la retroriflettanza della segnaletica orizzontale utilizzando i dati dei sensori ADAS, dimostrando che tali dati possono approssimare efficacemente le misurazioni fisiche di RL, se supportati da adeguate strategie di segmentazione e calibrazione. Il terzo progetto ha analizzato la concordanza tra la valutazione dei conducenti umani e quella basata su ADAS della qualità della segnaletica orizzontale, rivelando una correlazione significativa, seppur moderata, e identificando divergenze in condizioni ambientali e geometriche specifiche, in particolare in scenari a bassa visibilità.

*CC*

Nel complesso, i risultati forniscono raccomandazioni ingegneristiche, operative e normative per migliorare gli standard stradali, in particolare le soglie di retroriflettanza della segnaletica, e per ottimizzare le strategie di calibrazione degli ADAS. Il quadro metodologico proposto, basato sui dati, contribuisce allo sviluppo di tecnologie di guida autonoma più sicure e a una distribuzione più affidabile degli ADAS in condizioni operative reali.

*Parole chiave*:
*Sistema di Supporto alla Guida in Corsia (LSS); Dominio Operativo Progettuale (ODD); Apprendimento Automatico negli ADAS; Rilevamento della Segnaletica Orizzontale; Geometria Stradale e Retro-riflettanza; Veicoli Autonomi e Sicurezza; Stima della Retro-riflettanza; Confronto tra Percezione Umana e Macchina*

# Chapter 1: Introduction and Literature Review

# 1 Chapter 1: Introduction and Literature Review

The development of automated driving systems (ADS) offers significant potential for more efficient, eco-friendly, and safe mobility. To achieve these benefits, advanced driver-assistance systems (ADAS) must be analyzed, and road standards and maintenance must be adapted to support vehicle automation. Various sensors and detection systems aid drivers in safe navigation, evaluating the accuracy and reliability of these systems and their Operational Design Domain (ODD) is essential. The ODD defines the specific conditions under which an ADS operates, playing a crucial role in the safety and effectiveness of ADSs [1]. A vehicle's ODD varies by service type, automation level, and sensor equipment. Numerous initiatives aim to detail the ODD for ADS, often through creating ODD taxonomies that outline operational parameters. These taxonomies ensure clarity and consistency among manufacturers, developers, regulators, and insurers, aiding in safety case development by categorizing the operational limits and expected performance of ADS. Thus [1] proposed a generic taxonomy build on the definition by the Society of Automotive Engineers (SAE) [2] with three main (A) and three complementary (B) categories which includes all the identified features:

- 1A) Physical infrastructure: roadway type, roadway surface, roadway edge, roadway geometry, junctions, temporary structures, fixed surrounding structures, special structures, signage.
- 2A) Environmental conditions: precipitation, particulates, illumination, temperature, weather-induced roadway conditions (e.g., slippery road).
- 3A) Traffic conditions: traffic density, road users (type, speed), road users' behaviour (e.g., accidents).
- 1B) Scenery: specific zones, regions/states, interference zones, geo-fencing.

- 2B) Digital infrastructure: type of information, radio access technology (e.g., 5G cellular network).
- 3B) Vehicle capabilities: maximum/authorized speed, maneuvers, vehicle dimensions.

In parallel, the ISO 34503:2023 standard [3] introduces a formal, internationally harmonized taxonomy for describing ODDs. It categorizes ODD elements into six major domains: Operating environment, Geographical area, Time-of-day restrictions, Traffic conditions, Roadway types and features, and other constraints. This standardized structure complements the SAE-based approaches by offering a globally accepted framework for regulatory, certification, and interoperability purposes. The ISO taxonomy supports consistent documentation of ODD across different vehicle platforms and regulatory contexts, contributing to safety assurance and transparent communication among stakeholders.

## *1.1 Background and Motivation*

Road markings are among the most fundamental traffic control devices used worldwide. They provide critical guidance to drivers about road alignment, vehicle positioning, and safe manoeuvring particularly under low-visibility conditions such as nighttime driving or inclement weather. Historically, lane markings were simple painted lines, but over time they have evolved into sophisticated systems that utilize high-performance retroreflective materials. These materials are designed to enhance visibility by reflecting light from vehicle headlamps back to the driver, improving lane clarity and reducing the risk of run-off-road or head-on collisions.

Before the emergence of automated systems, another critical intervention for lane departure prevention was the implementation of rumble strips. These passive safety features, often installed along

roadway shoulders or centerlines, consist of grooves or raised patterns that produce auditory and tactile vibrations when driven over. This sensory feedback alerts drivers especially those who are drowsy or distracted of unintended lane departures. Although rumble strips do not actively influence vehicle trajectory, they represent an early form of lane departure mitigation and are still widely used today, particularly on rural highways and high-speed roads [4]. In this sense, they can be viewed as precursors to more sophisticated systems like Lane Keeping Assistance (LKA), offering a physical form of lane-keeping support before digital automation became prevalent.

In parallel, recent decades have seen profound advancements in vehicle automation, culminating in systems broadly referred to as Advanced Driver Assistance Systems (ADAS). Among these, Lane Support Systems (LSS) which encompass functionalities like Lane Departure Warning (LDW) and Lane Keeping Assistance (LKA) are particularly significant for preventing unintentional lane departures. These systems rely heavily on camera-based sensors and computer vision algorithms to "read" lane markings. Consequently, if lane markings are faded, obscured, poorly maintained, or lack sufficient retroreflectivity, the reliability of ADAS features can drop markedly. Effective lane markings thus serve a dual purpose: they enhance the safety of human drivers while also providing robust cues for automated vehicles to detect and track roadway boundaries.

Despite the growing implementation of ADAS in modern vehicles, significant challenges persist. Inconsistencies in pavement marking standards, coupled with varying climate and maintenance practices, can undermine the performance of camera-based lane detection systems. This shortfall is critical not only for present-day ADAS-equipped vehicles but also for higher levels of vehicle automation now being trialed on public roads. As the technological capability of autonomous vehicles (AVs) expands, the road

infrastructure in particular, the quality and uniformity of lane markings must also adapt to ensure that both human-driven and partially/fully automated vehicles can operate safely and efficiently.

Motivated by these challenges, this research investigates the complex interplay between lane marking attributes, roadway geometry, and environmental factors on the performance of vision-based Lane Support Systems. Key metrics such as pavement marking retroreflectivity, width, and visibility under varying weather and lighting conditions are examined to determine their impact on LSS reliability. The overarching goal is to identify thresholds and guidelines for lane marking quality that can sustain effective lane detection across a wide range of operational design domains (ODDs), supporting both driver safety and the growing automation needs of the automotive industry.

By integrating real-world experimental data, machine learning techniques, and advanced sensor fusion, this dissertation aims to advance both the theoretical understanding and practical applications of lane marking quality for modern vehicles. Ultimately, these insights will contribute to developing guidelines and policies for more consistent and higher-visibility pavement markings, thereby improving road safety for today's drivers while paving the way for safer deployment of tomorrow's autonomous vehicles.

In the context of ensuring road readiness for autonomous vehicles, this dissertation also explores the potential of using in-vehicle ADAS systems specifically Mobileye's Lane Keeping Assistance (LKA) to estimate pavement marking retroreflectivity (RL). Traditional RL measurements require costly and disruptive procedures, prompting interest in whether ADAS outputs can serve as a practical alternative. One of the projects within this dissertation investigates how Mobileye's lane detection quality relates to actual RL measurements across varied road geometries, lighting conditions, and

environmental scenarios. By combining Mobileye outputs with contextual roadway data and machine learning techniques, the study aims to assess whether ADAS-equipped vehicles can indirectly support large-scale RL monitoring, offering a cost-effective tool for road agencies and infrastructure planners.

The third study in this thesis focuses on the alignment between human drivers and Advanced Driver Assistance Systems (ADAS) in evaluating lane marking quality. As systems like Mobileye's Lane Support System (LSS) increasingly support driving tasks, understanding how well their outputs correspond to human perception becomes critical. In this project, the subjective assessments of drivers during real-world road surveys are compared with Mobileye's lane marking classifications and with retroreflectivity (RL) measurements obtained from the ANAS dataset. The objective is to evaluate the level of agreement and identify environmental and geometric factors such as lighting, weather, curvature, and lane geometry that influence misalignment. Statistical and discriminant modelling methods are used to investigate these relationships, offering practical implications for both ADAS calibration and road infrastructure design.

## *1.2 Problem Statement*

Despite their potential to reduce road accidents and improve traffic management, the performance of LSS is highly dependent on a variety of factors, including road conditions, environmental factors, and dynamic traffic elements. Inconsistent road markings, adverse weather conditions, and variable traffic densities can severely undermine the efficacy of these systems. Thus, a systematic analysis to ascertain the specific Operational Design Domains (ODD) under which LSS can operate reliably is essential. Understanding these influences will enable the development of more robust systems that

can perform optimally across a broader range of scenarios.

In addition to understanding LSS performance limits, it is also vital to explore how such systems can be leveraged to monitor lane marking retroreflectivity (RL) on a wide scale, reducing the need for costly, disruptive measurement procedures using specialized vehicles. This brings forward the second dimension of this research, where we assess whether Mobileye's sensor-based outputs can effectively predict RL values, enabling more efficient maintenance strategies for road agencies.

Moreover, beyond the technological lens, there remains an underexplored aspect of how human drivers perceive lane markings compared to ADAS systems. Understanding the alignment or misalignment between driver perception, system detection, and physical RL values is essential for developing systems that are not only functionally accurate but also aligned with real-world user expectations and safety needs. Thus, the problem is threefold: defining LSS's operational boundaries, exploring its potential as a retroreflectivity proxy, and bridging the gap between human and machine perception.

## *1.3 Research Objectives*

The research objectives are as follows including main objective and secondary objectives:

- **Primary research objectives:**

1 Evaluating the impact of the Physical infrastructure factors (e.g. lane marking quality, road geometry) in different environmental conditions on LSS performance and reliability of the system.

2 Developing an ADAS data-driven framework for lane marking quality assessment.

3 Assessing the feasibility of predicting lane marking retroreflectivity (RL) from ADAS outputs and contextual roadway data and developing classification models to detect low RL segments.

4 Evaluating the alignment between driver perception and ADAS assessments of lane marking quality across diverse conditions using correlation and discriminant analysis.

5 Identifying the environmental and geometric conditions under which human and system assessments agree or diverge, informing future ADAS calibration and infrastructure design.

- **Secondary objectives:**

1. Applying advanced machine learning models to predict and analyze LSS performance: Utilizing advanced algorithms to handle large datasets and improve prediction accuracy under varied operational conditions.
2. Conducting SHAP-based interpretability analysis to determine key influencing factors for LSS performance.
3. Proposing engineering and policy recommendations for improved lane marking standards.

## *1.4 Scope of research*

This dissertation will focus on the detailed evaluation of LSS performance through the utilization of a comprehensive dataset that includes road geometric parameters, lane marking quality metrics, driving conditions, and environmental factors. GIS data fusion and Advanced machine learning techniques will be employed to analyze these data, aiming to enhance the predictive capabilities and understand the critical factors influencing the operational efficiency of LSS.

Beyond modelling the operational performance of LSS, this

dissertation also explores how sensor-based lane detection outputs can be applied to estimate marking retroreflectivity (RL), a key parameter for roadway safety and compliance. Furthermore, a human-centered analysis is incorporated, comparing the perceived visibility of lane markings by drivers to both the system assessments and objective RL values. These multi-perspective insights aim to provide a richer understanding of ADAS performance, both as a perception-based driver aid and as a potential tool for infrastructure monitoring.

## 1.5 Key Concepts and Definitions

### 1.5.1 Lane Markings definitions and functions

The visibility of pavement markings is crucial for ensuring a safe travel environment and helping drivers recognize the road path, particularly at night. The presence and consistency of longitudinal pavement markings offer ongoing guidance to drivers regarding roadway alignment, vehicle positioning, and other important driving tasks like steering and braking. These markings are vital for conveying information about the road layout and vehicle placement [5]. It's essential to maintain pavement markings to ensure they remain visible and retroreflective for the safety of all motorists.

Longitudinal pavement markings play a vital role in communicating regulations, guidance, or warnings to drivers, providing essential information about road geometry [6]. They help define lane boundaries, aiding drivers in selecting the correct path and keeping their vehicles within the designated lanes [7]. It's clear that these markings improve visibility for driving both day and night, enhancing a driver's ability to make informed decisions [8], [9]. One way to potentially reduce accidents is by offering better continuous information to drivers through wider or higher-quality longitudinal pavement markings, such as those that are more retroreflective or

brighter. Therefore, it's crucial to examine the link between the characteristics of pavement markings and single-vehicle roadway departure crashes, as well as to explore safety improvements that come with installing brighter or wider markings. Ensuring that pavement markings remain visible can help decrease crashes during both daytime and nighttime; however, their retroreflectivity is especially important at night. Thus, maintaining a safe level of retroreflectivity for pavement markings is essential.

### *1.5.2 Types of Lane Markings (Geometrical Classification)*

Pavement markings are generally divided into three primary categories: longitudinal, transverse, and temporary. Key characteristics of longitudinal pavement markings include their color (either white or yellow) and pattern (which can be double or single, broken or solid). These features should be clearly defined according to their specific location and intended purpose.

- **Longitudinal Markings:**

Longitudinal markings are continuous lines found on roads that help drivers understand how to use the roadway. Essentially, these markings indicate the separation between the travel lane and oncoming traffic, the edge of the road, adjacent lanes, or areas for turning. These pavement markings can take the form of edge lines, lane lines, or centerlines/skip lines, which serve as passing or no-passing indicators[10].

- **Transverse Pavement Markings:**

Transverse pavement markings refer to all markings that are installed across the pavement, from one side to the other, or

perpendicular to the centerline of the road. According to the Manual on Uniform Traffic Control Devices (MUTCD), this term encompasses various types of markings, including word and symbol markings, shoulder markings, stop line markings, crosswalk markings, speed measurement markings, parking markings, and transverse median markings.

- **Temporary Pavement Markings:**

Temporary pavement markings serve as a temporary alternative to permanent traffic markings. They are applied and kept up during construction phases in work zones for maintenance or utility projects.

### *1.5.3 Lane Marking Performance Criteria & Metrics*

Two key criteria are often used to assess the performance of pavement markings over time are visibility and durability. Visibility pertains to how bright the markings are, while durability refers to their ability to withstand damage from traffic, snowplowing, and environmental factors [11]. In daylight, drivers primarily identify pavement markings through color contrast, whereas at night, they rely on the luminous contrast between the markings and the dark road surface, which is influenced by the retroreflectivity of the pavement markings.

Lane markings must meet minimum performance standards to ensure visibility and durability. Retroreflectivity (RL), luminance coefficient (Qd) and contrast ratio are three key parameters defining lane marking effectiveness. Table 1 list the definitions of these parameters and Table 2 shows the relationship between RL, Qd, Cr and visibility.

**Table 1 Lane marking Visibility Metrics**

| Performance Metric | Definition |
|---|---|
| Retroreflectivity (RL) | Measures night-time visibility by reflecting light back to the driver. |
| Luminance Coefficient (Qd) | Evaluates daytime contrast and visibility. |
| Contrast Ratio (CR) | Determines visibility against pavement background. |

**Table 2 Relationship Between RL, Qd, Cr and Visibility**

| Condition | Effect on RL | Effect on Qd | Effect on Contrast Ratio (CR) |
|---|---|---|---|
| Dry Road | High RL | High Qd | High CR (clear lane markings) |
| Wet Road | Low RL (water disperses reflection) | Moderate Qd | Low CR (water reduces contrast) |
| Worn Markings | Low RL | Low Qd | Very Low CR (poor visibility) |

### *1.5.4 Lane marking Retroreflectivity (RL)*

The term retroreflectivity refers to how light from vehicle headlights illuminates the visible pavement markings and then reflects back to the driver's eyes. These retroreflected light rays provide crucial information to roadway users in low-light conditions, such as roadway alignment, vehicle position, and other driving-related factors [12]. Retroreflectivity is quantified in millicandelas per square meter per lux (mcd/m²/lux), which is known as the coefficient of retroreflected luminance (RL) [13]. This reflective property makes the markings appear bright at night, indicating their visibility in darkness [14]. Faster recognition of pavement markings is associated with their RL levels, which can differ in brightness [15]. Keeping an adequate RL level is crucial for reducing nighttime accidents and fatalities, especially in dark and adverse weather conditions [8]. Improving safety on rural roads is a key reason for investigating the relationship between RL and crashes. Lower RL values may heighten the risk of single-vehicle run-off-road (ROR) crashes, which are more common

in rural areas [16].

In previous studies, the retroreflectivity of pavement markings has been recognized as a crucial factor in assessing the performance and cost-effectiveness of pavement marking materials [17]. The evaluation of retroreflectivity can be conducted through either an objective method (quantitative) using retroreflectometers or a subjective method (qualitative) involving visual inspections [18]. Objective measurements of pavement marking performance tend to be favoured over subjective evaluations due to their greater accuracy and the capacity to gather extensive data more quickly.

Different standards have been established to measure the retroreflectivity of pavement markings using retroreflectometers, depending on the driver's viewing geometry, such as the 12-meter and 30-meter geometries. The American Society for Testing and Materials (ASTM) has standardized the "30-meter geometry" for this purpose, based on the belief that 30 meters is the maximum distance from which drivers can clearly see pavement markings at night. As a result, most retroreflectometers currently utilize the 30-meter geometry for measuring pavement marking retroreflectivity [19], [20]. Retroreflectivity acts as a proxy for visibility and quantitatively assesses how effectively a material, like a pavement marking, returns light to the source at the specified geometry. Following shows the 30 meters geometry (Figure 1). Also Figure 2 shows Pavement marking with known retroreflectivity levels from a 30-meters distance from the observer, representing the standard 30-meter measurement geometry used as a standard for pavement marking retroreflectivity.

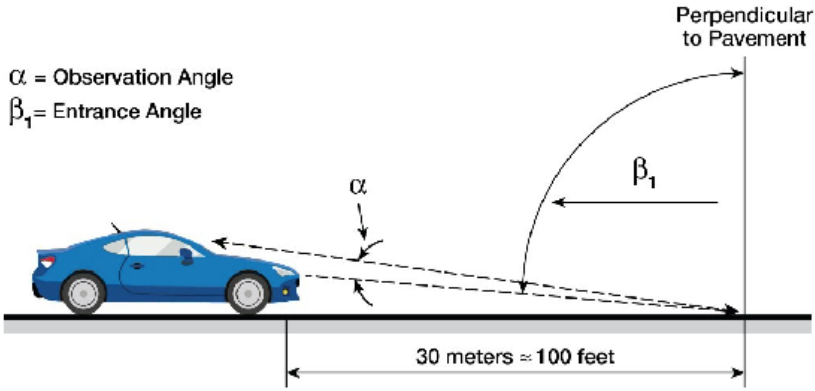


**Figure 1 30 meters geometry (FHWA 2022)**

**Figure 2 Pavement marking with known retroreflectivity levels** [21]

*Note: These markings are 30-meters from the observer, representing the standard 30-meter measurement geometry used as a standard for pavement marking retroreflectivity.*

The service life of pavement markings refers to the duration during which they can be considered "serviceable" and effectively serve road users. However, the longevity of various materials can differ significantly; each type of pavement marking material possesses distinct characteristics that can change based on factors such as the pavement surface, climate, and operating conditions.

### *1.5.5 Evaluation of Pavement Marking Retroreflectivity*

Retroreflectivity serves as a surrogate measure for visibility and is a quantitative measure of the efficiency of a material (e.g., a pavement marking) at returning light back toward the light source at the prescribed geometry. Pavement marking performance evaluation is crucial for ensuring road safety. Different methods are employed to assess retroreflectivity, including subjective visual inspections, handheld retroreflectometers, and mobile machine-based measurements.

- **Visual Inspection:** Subjective assessments of retroreflectivity (RL) are carried out by visually inspecting pavement markings to ensure they are sufficiently visible. However, a significant drawback of these visual inspections is their subjective nature, as results can vary widely among different evaluators. The perceived brightness of pavement markings can be affected by the contrast between the markings and the pavement surface. For instance, a marking on a darker pavement may seem brighter than one on a lighter surface, even if both have the same RL. As a result, numerous studies have pointed out that visual inspections are susceptible to human error, challenging to verify, and often yield inconsistent outcomes [22], [23]. These markings are generally rated on a scale from 1 to 5, where 1 signifies poor condition and 5 denotes excellent condition. Benz et al. [22] conducted an extensive study in Texas to explore how well subjective evaluations of RL matched actual measured RL. The study utilized various trend analyses to assess how closely subjective ratings corresponded with RL trends, taking into account factors such as marking color, line type, and pavement type.

- **Handheld Retroreflectometers:** Handheld retroreflectometers offer a more objective way to measure retroreflectivity by directing a controlled beam of light at the marking and assessing the intensity of the light that is reflected. These devices are popular because they are portable and easy to use; however, they often necessitate stopping traffic or working in dangerous road conditions, which can make the process time-consuming and labor-intensive.
- **Mobile Retroreflectometers:** To address the challenges of visual and handheld assessments, mobile retroreflectometers have been created. These systems, mounted on vehicles, measure retroreflectivity while driving at regular traffic speeds. Mobile retroreflectometers allow for the efficient and safe collection of extensive retroreflectivity data without the need for road closures. The American Society for Testing and Materials (ASTM) has established the "30-meter geometry" for these measurements, defining 30 meters as the maximum distance at which drivers can clearly see pavement markings at night [19], [20]. Oracheff et al. [24] investigated the application of mobile retroreflectivity units (MRUs) for assessing the retroreflectivity of raised pavement markers (RPMs), aiming to supplement the conventional visual inspection methods used by the Florida Department of Transportation. By modifying the Laserlux G7 MRU system originally designed for line-stripe pavement markings the authors were able to derive regression models correlating RL values ($mcd/m^2/lux$) with the industry-standard RI values (mcd/lux) for RPMs. Their study demonstrated that the enhanced MRU could measure RPM retroreflectivity with a mean error of ±13.5% and detect RPMs with 98% accuracy during high-speed surveys. The methodology enabled simultaneous assessment of both RPMs and standard pavement markings, offering a network-level solution with improved repeatability and reproducibility. This research

contributes to retroreflectivity assessment techniques by enabling automated, objective evaluations of RPM quality at highway speeds.

Different methods like photometric analysis that use cameras and image processing can be utilized to assess luminance and contrast. Also advanced systems like LIDAR and AI-based evaluations providing real-time lane marking assessments are increasingly used to provide continuous and large-scale monitoring of lane marking conditions.

Chou et al. [25] developed a cost-effective real-time assessment system using a stereo camera and a machine vision algorithm to measure the dry retroreflectivity (RL) of broken lane line markings on in-service roads. The system integrates vehicle headlights as the illumination source and photogrammetry to maintain standard measuring conditions in accordance with EN 1436 specifications. The algorithm processes images to calculate centroid positions of markings, controls measuring conditions, estimates illumination, and computes luminance values. The system demonstrated an average absolute error of 6.1% across 47 marking samples, with RL values ranging from 65 to 570 mcd/m²/lux. This approach enables simultaneous evaluation of left and right lane markings in a single vehicle pass at speeds up to 100 kph. The method significantly reduces equipment cost compared to commercial retroreflectometers and offers flexibility in adapting to different vehicles and camera sets, making it a promising alternative for routine pavement marking retroreflectivity assessments.

Brinster et al. [26] investigated the effectiveness of mobile LiDAR intensity data for classifying and inventorying durable tape pavement markings. Their study focused on assessing preformed tape retroreflectivity along a 73-mile segment of I-74 in Indiana, where various types of markings (including recessed tape and waterborne

paint) had been applied. A strong correlation was observed between LiDAR intensity and retroreflectivity, with regression models yielding a coefficient of determination ($R^2$) up to 0.76. The researchers demonstrated that LiDAR can effectively distinguish between marking types and detect degraded areas by segmenting the data into 0.1-mile intervals. This technique provides transportation agencies with a scalable and non-intrusive method to maintain accurate inventories of high-cost markings and plan maintenance accordingly. Their results emphasize the potential of LiDAR as a screening tool to support large-scale monitoring of pavement marking retroreflectivity.

#### *1.5.5.1 ASTM Retroreflectivity Standards*

##### 1.5.5.1.1 ASTM E1710 Retroreflectivity in Dry Conditions

ASTM E1710 is the standard test method for measurement of retroreflective pavement marking materials with CEN-prescribed geometry using a portable retroreflectometer [27]. As discussed before CEN specifies the entrance and observation angles corresponding to the 30-m geometry. These angles are an entrance angle of 88.76 degrees and an observation angle of 1.05 degrees. These are the same required angles for all retroreflectivity measurements of pavement markings. These angles represent a viewing distance of 30 m by a driver whose eyes are 1.2 m above the road surface, with headlights 0.65 m above the road surface. The actual value measured is the coefficient of retroreflected luminance, commonly referred to as retroreflectivity. The units of measure are expressed in millicandelas per square meter per lux($mcd/m^2/lux$).

##### 1.5.5.1.2 ASTM E2177 Standard Condition of Wetness (Recovery)

ASTM E2177 is the standard test method for measuring the coefficient

of retroreflected luminance (RL) of pavement markings in a standard condition of wetness [28]. The test method has the same requirements as the dry retroreflectivity test method, except with the inclusion of water. This test method is often referred to as the "recovery" or "bucket" method. The wetting requirements for the test are 3 L of water poured from a bucket over the measurement area within a 3- to 5-second span of time. The retroreflectometer is then placed on the marking, and a retroreflectivity reading is measured 45 seconds after pouring the water.

#### 1.5.5.1.3 ASTM E2832 Standard Condition of Continuous Wetting

ASTM E2832 is the standard test method for measuring the coefficient of retroreflected luminance of pavement markings in a standard condition of continuous wetting (RL-2) [29]. The test method has many more requirements than the dry or recovery retroreflectivity test methods. The biggest requirement is the need for the continuous wetting spray box. The box is designed to provide a consistent and uniform water application rate of 2 in/hr over the measurement area. This water application rate was found to have reasonable correlation with visibility results in human factors testing, and it was a rate that could be consistently sprayed.

### *1.5.6 ANAS DELPHI Car*

The DELPHI (Delineation Photometric Instrument) is a state-of-the-art mobile laboratory designed to measure the nighttime retroreflection (RL) of various types of horizontal road markings, including edge lines and dashed markings by Italian road agency and management. This system ensures that road safety performance standards are met by assessing the visibility and effectiveness of lane

markings during nighttime driving. DELPHI works by illuminating road markings and analyzing their reflective properties from a perspective that mimics a driver's view at night. It can conduct continuous measurements at speeds over 90 km/h, enabling large-scale evaluations without disrupting traffic. Italian National Autonomous Road Agency (ANAS) gathered high-precision data on the retroreflectivity index (RL) and GNSS position using the DELPHI system, with measurements statistically compiled to include mean, maximum, minimum, and standard deviation every 50 meters along the right side of the lane. In 2023, over 36,000 km of horizontal road markings were monitored, marking an increase of about 10% from the previous year [30]. This extensive data collection is essential for road maintenance planning, allowing transportation authorities to pinpoint areas that need repainting, evaluate compliance with safety regulations, and optimize resource allocation for better roadway visibility. Figure 3 shows the ANAS DELPHI Car with installed sensors.

**Figure 3 ANAS DELPHI Car**[30]

### 1.5.7 Retroreflectivity Thresholds

To ensure the quality of pavement marking retroreflectivity, it's essential to establish a minimum standard value. This minimum retroreflectivity value indicates the lowest level of pavement marking retroreflectivity that is acceptable on roads, serving as a safety measure for drivers.

#### 1.5.7.1 MUTCD Retroreflectivity Standards

Transportation agencies like the American Association of State Highway and Transportation Officials (AASHTO), the Federal Highway Administration (FHWA), and State Departments of Transportation (DOTs) have worked diligently to create detailed standard specifications, manuals, and procedures aimed at ensuring the proper application and upkeep of pavement markings [31]. In this context, the FHWA seeks to improve safety by establishing minimum retroreflectivity (RL) levels in the Manual on Uniform Traffic Control Devices (MUTCD), which helps meet the nighttime visibility needs of drivers on public roads.

On August 5, 2022, the FHWA introduced a new regulation that sets national standards for minimum RL levels of longitudinal marking lines across all roads, with variations based on posted speed limits [32]. According to this regulation, roads with posted speed limits of 35 mph(≈56Km/Hr) or higher must maintain a minimum RL of 50 mcd/m²/lux, while no minimum is required for roads with speed limits below 35 mph. Additionally, it is advised to keep a minimum RL of 100 mcd/m²/lux for freeways where the posted speed limit is 70 mph((≈113Km/Hr) or more. These regulations and guidelines are applicable under dry conditions and do not account for factors such as ambient lighting, roads with fewer than 6000 annual average daily

traffic (ADT), dashed extension lines, curb markings, parking spaces, and shared-use paths. Table 3 and Table 4 shows the presented minimum retroreflectivity values for longitudinal lane marking by MUTCD.

**Table 3 Proposed MUTCD Minimum Retroreflectivity (MUTCD)**

| | Standard | | Guidance |
|---|---|---|---|
| Speed Limit (mph) *Km/Hr | < 35(56.3*) | ≥ 35(56.3*) | ≥ 70(112.65*) |
| RL (mcd/ m²/lux) | n/a | 50(80.47*) | 100(160.93*) |

**Table 4 Proposed MUTCD minimum retroreflectivity values for longitudinal pavement markings**

| Road Type | Posted Speed (mph) | | |
|---|---|---|---|
| | ≤30(48.3*) | 35-50 (56.3-80.5*) | ≥ 55(88.5*) |
| Two-lane roads with centerline marking only | N/A | 100 | 250 |
| All other roads | N/A | 50 | 100 |

### *1.5.7.2 European Committee for Standardization (CEN) Retroreflectivity Standards*

The European Committee for Standardization (CEN) has established a standard document, EN 1436, which focuses on road marking materials [33]. This document details the test methods and performance criteria for various classifications of pavement markings. CEN EN 1436 serves as the European standard for assessing pavement marking performance. It specifies performance standards for white and yellow markings under both daytime and nighttime conditions, considering dry, wet, and rainy scenarios.

The retroreflectivity values outlined in CEN EN 1436 represent the maintained levels throughout the functional life of each marking class. However, the specific duration of a marking's functional life for

the various classes is not specified.

Table 5 provides the classification levels for permanent and provisional markings under dry conditions and Table 6 presents the CEN EN 1436 performance levels for various marking classifications for rain and wet conditions.

**Table 5 Recommended RL levels for dry condition by CEN**

| | | Class | Minimum Retroreflectivity (mcd/m2/lux) |
|---|---|---|---|
| Permanent | White | R0 | No performance required |
| | | R2[a] | RL ≥100 |
| | | R3[a] | RL ≥150 |
| | | R4[a] | RL ≥200 |
| | | R5[a] | RL ≥300 |
| | Yellow | R0 | No performance required |
| | | R1[a] | RL ≥80 |
| | | R3[a] | RL ≥150 |
| | | R4[a] | RL ≥200 |
| provisional | | R0 | No performance required |
| | | R3[a] | RL ≥150 |
| | | R5[a] | RL ≥300 |

Note: class R0 applied when the visibility of road marking is achieved without retroflection under vehicle headlamp lighting conditions.

[a] In some countries these classes cannot be maintained for a limited period of the year during which the probability of poor performance of road marking is high due to the presence of water, dust, mud, etc.

**Table 6 Recommended RL levels for wet and rain conditions by CEN**

| Conditions of Wetness | | Conditions of Rain | |
|---|---|---|---|
| Class | Minimum Retroreflectivity (mcd/m2/lux) | Class | Minimum Retroreflectivity (mcd/m2/lux) |
| RW0 | No performance required | RR0 | No performance required |
| RW1 | RL ≥ 25 | RR1 | RL ≥ 25 |
| RW2 | RL ≥ 35 | RR2 | RL ≥ 35 |
| RW3 | RL ≥ 50 | RR3 | RL ≥ 50 |
| RW4 | RL ≥ 75 | RR4 | RL ≥ 75 |
| RW5 | RL ≥ 100 | RR5 | RL ≥ 100 |

### *1.5.8 Maintenance Thresholds by Road Agencies*

In addition to standardized minimum retroreflectivity values defined by international bodies such as the MUTCD and CEN, various national and regional road authorities have established their own performance-based thresholds for pavement marking maintenance. These thresholds are often tailored to local traffic conditions, climate, and policy priorities, and they play a crucial role in contract enforcement, safety assurance, and budget planning. This section presents selected examples of retroreflectivity thresholds applied by agencies in Australia, New Zealand, the United Kingdom, and the United States based on their technical specifications and empirical studies.

Across various regions, road authorities have established performance-based retroreflectivity thresholds to guide the maintenance of pavement markings, reflecting differences in climate, traffic conditions, and infrastructure policies. In Australia and New Zealand, agencies follow the Austroads ATS 4110:2021 specification, which mandates an initial dry retroreflectivity of at least 350 mcd/m²/lux for white and 200 mcd/m²/lux for yellow markings within the first 30 days after application. A second test conducted after one year requires reduced thresholds of 200 mcd/m²/lux (white) and 150 mcd/m²/lux (yellow), with intervention triggered if annual readings fall below 150 and 100 mcd/m²/lux, respectively. Moreover, for pale pavement surfaces, markings must exceed pavement luminance by at least 150 mcd/m²/lux to ensure visual contrast [34]. Similarly, Highways England adopts a risk-based methodology in its CS 126 manual, where retroreflectivity thresholds are 100 mcd/m²/lux in lit and 150 in unlit areas for standard markings, and even lower for "line type b" in critical zones—80 mcd/m²/lux (lit) and 120 (unlit). Wet

retroreflectivity must exceed 35 mcd/m²/lux, aligning with preview time models designed to maintain safety under varying environmental and geometric conditions [35]. In contrast, a Caltrans [36] review in the United States reveals a broader variability among states. Initial thresholds ranged from 130 to 700 mcd/m²/lux for white and 100 to 700 mcd/m²/lux for yellow markings, depending on materials and local policies. States like Delaware, Georgia, and Minnesota reported higher standards for preformed tapes, while Georgia and Nebraska adopted a 180-day monitoring period, and Pennsylvania DOT enforced performance maintenance for up to three years in test deck applications. Retroreflectivity compliance in the U.S. is generally verified through 30-meter retroreflectometers, and failure to meet standards may trigger reapplication or payment reductions under warranty or contract terms [36].

### *1.5.9 Relationship Between RL and Road Safety*

Different studies conducted to analyze the relationship of RL and road safety and threshold levels for RL and crashes.

Dravitzki et al. [37] explored the connection between reflectivity (RL) and crash trends in dark conditions, including nighttime and curves. Their research revealed that maintaining a minimum RL of 70 mcd/m²/lx did not lead to any significant changes in crash trends.

Smadi et al. [16] examined nighttime crashes involving lane departures that were not caused by collisions with animals, objects, vehicle interactions, or mechanical failures. They found that lower RL levels were linked to a higher likelihood of crashes in segments with RL values of ≤70 mcd/m²/lx.

Donnell et al. [38] investigated nighttime crashes, including sideswipe and run-off-road (ROR) incidents involving fixed objects in

non-work zones, while excluding cases involving alcohol use or wet conditions. Their results indicated that increasing RL on two-lane highways could help reduce the occurrence of target crashes. Although the findings for yellow centerlines (YCL) showed marginal significance, those for white right edgelines (WREL) were not statistically significant.

Carlson et al. [39] concentrated on nighttime single-vehicle crashes at non-intersections during non-winter months. They discovered that higher RL was associated with a decrease in expected crash frequency, with variations in datasets within the RL range of ≤150-200 mcd/m²/lx across different marking positions.

Avelar and Carlson [40] investigated single-vehicle, sideswipe, and ROR crashes at night. Their analysis indicated that segments with higher RL had fewer crashes compared to those with lower retroreflectivity, a trend that was consistent for both white right edgelines (WREL) and yellow centerlines (YCL).

## *1.6 Advanced Driver Assistance Systems (ADAS) and Autonomous Vehicles (AVs)*

### *1.6.1 Definition of Advanced Driver Assistance Systems (ADAS)*

Advanced Driver Assistance Systems (ADAS) have been extensively researched and progressively implemented to enhance driving safety, optimize vehicle control, and minimize driver fatigue and human errors [41]. These systems rely on cameras, radar, LiDAR, ultrasonic sensors, and AI-driven software to observe the surroundings, identify hazards, and deliver real-time driver support. ADAS encompasses various technologies, including adaptive cruise control (ACC), anti-lock braking systems (ABS), lane support system (LSS), automatic parking, blind spot monitoring, collision avoidance systems, parking sensors, tire pressure monitoring, and turning

assistance. The integration and application of these individual technologies contribute to the development of intelligent vehicles and advanced traffic models.

A key factor in further improving road safety is the development and implementation of ADAS in vehicles. These systems are designed to detect and avoid hazardous traffic situations by utilizing sensor data and vehicle states to control movement. As more complex and safety-critical ADAS are developed, new testing methods must be considered to ensure their reliability and effectiveness. Over recent years, significant progress has been made, marking the emergence of a new era with the introduction of ADAS, which has contributed to reducing road traffic fatalities [42], as conventional safety systems have reached their full potential [43].

Ebinger et al. [44] conducted two field studies to examine drivers' trust in and preference for individual subsystems of partially automated driving namely adaptive cruise control (ACC), lane-keeping assist (LA), and lane change assist (LC). Their results consistently indicated that trust and preference among drivers were functionally specific. According to both studies, drivers expressed the highest trust and usage duration for ACC, followed by LA, and lastly LC, which was often perceived as unreliable or unnecessary. Despite more interaction difficulties reported with ACC, it remained the most favoured function, suggesting that perceived usefulness outweighed usability concerns. The authors emphasized the importance of calibrated, function-specific trust for safe and effective human-automation interaction in partially automated vehicles.

The concept of systems that aid the driver through autonomous intervention is already well established. These systems, collectively referred as driver assistance systems (DAS), have been in development since 1978, when the first electronic anti-lock braking system (ABS) was introduced. Since then, advancements such as

electronic stability control (ESC) and traction control system (TCS) have been integrated into modern vehicles to further enhance safety.

#### 1.6.1.1 ADAS Functions

Knapp et al. [45] characterized ADAS functions by their ability to:

- Detect and evaluate the vehicle environment.
- Support the driver in the primary driving task.
- Provide active support for lateral and/or longitudinal control with or without warnings.
- Enable direct interaction between the driver and the system.
- Utilize complex signal processing.

In addition to improving road infrastructure and driver education, which are conventional methods of reducing traffic fatalities, Human error has a main contribution in traffic accidents. Consequently, driver assistance systems are essential for improving road safety by addressing the primary cause of traffic incidents. While passive safety systems such as seat belts and airbags primarily mitigate the consequences of accidents, studies indicate that these systems have reached their full potential [43]. Therefore, the development of new active safety systems, such as ADAS, is necessary to further enhance road safety.

According to the European Road Safety Observatory (ERSO) [46], ADAS can be defined as "vehicle-based intelligent safety systems that could improve road safety in terms of crash avoidance, crash severity mitigation, protection, and post-crash phases." ADAS functions can thus be categorized as integrated in-vehicle or infrastructure-based systems that contribute to multiple crash phases.

Studies suggest that the implementation of ADAS can lead to a reduction in vehicular accidents by up to 40% [47] while significantly

enhancing driver reaction times in critical situations. Research also highlights that the combination of multiple ADAS functionalities enhances overall road safety and traffic management. The capabilities of ADAS range from basic driver warnings, such as Lane Departure Warning (LDW), to proactive intervention systems like Lane Keeping Assist (LKA) and Adaptive Cruise Control (ACC). The overarching objective of ADAS is to diminish accident risks, streamline traffic movement, and lay the groundwork for fully autonomous vehicles.

### *1.6.2 Levels of Vehicle Automation*

Different organizations have defined the level of driving automation differently, where the definition of each level differs slightly, and the total number of levels are not the same. However, the same structure is used, where low levels correspond to high human responsibilities, and with increasing automation levels, the safety responsibilities shift from the driver to the system.

#### *1.6.2.1 Society of Automotive Engineers (SAE)*

SAE International is a global association of engineers and technical experts in various industries, with a primary focus on the automotive industry. In 2014, SAE introduced six levels of driving automation in the issued SAE Standard J3016 [48], which remains widely used as a global reference for defining vehicle automation levels (Table 7):

- **Level 0**: No automation; the human driver is responsible for all driving tasks.
- **Level 1**: Driver assistance; either steering or speed control is automated.

- **Level 2**: Partial automation; both steering and speed control are automated under certain conditions, requiring driver supervision
- **Level 3**: Conditional automation; the vehicle takes full control under specific conditions, but the driver must be ready to intervene.
- **Level 4**: High automation; the vehicle operates autonomously within limited driving scenarios, though a driver may intervene.
- **Level 5**: Full automation; the vehicle independently performs all driving tasks under any scenario without human intervention.

A key aspect of these different levels of driving automation is the transition from Level 2 to Level 3, where the driver's role shifts from safety control to supervisory control due to Level 3's definition, in which the system is responsible for monitoring the driving environment. Research highlights that transitioning from Level 2 to Level 3 is crucial since driver responsibility shifts from direct control to supervisory control. Studies emphasize the importance of accurately defining the Operational Design Domain (ODD) to ensure safe vehicle operation.

**Table 7 Overview of different levels of automation based on SAE**

| | **Human driver monitors the driving environment** | | | **Automated driving system ("system") monitors the driving environment** | | |
|---|---|---|---|---|---|---|
| **SAE Level** | 0 | 1 | 2 | 3 | 4 | 5 |
| **Driver Role** | Full manual control | Driver assistance | Partial automation | Conditional automation | High automation | Full automation |
| **System Capabilities** | No ADAS features | Some driving modes | Some driving modes | Some driving modes | Some driving modes | All driving modes |
| **Execution of Steering and Acceleration/Deceleration** | Human driver | Human driver and system | System | System | System | System |
| **Monitoring of Driving Environment** | Human driver | Human driver | Human driver | System | System | System |
| **Fallback Performance of Dynamic Driving Task** | Human driver | Human driver | Human driver | Human driver | System | System |

Each level of automation is designed to work in specific conditions referred to as the Operational Design Domain (ODD); this includes geographic, environmental, traffic, road geometry, speed and/or temporal dimensions. SAE level 2, the execution of both the lateral and longitudinal vehicle motion control tasks are performed by an automation system with the expectation that the driver supervises the driving automation system. A well-researched problem at this level of automation, is the task of transition of control from the system to the driver when the automated system cannot handle the driving situation. Drivers of level 2 vehicles are responsible to monitor the driving environment at all times. If the ODD is not accurately defined and made clear to the drivers, this could make the drivers more vulnerable to accidents, as they could have misconceptions about capabilities of the system [2].

Annual road safety statistics published by the European Commission in the year 2015, reported that over 90% of the traffic

accidents were caused by human errors [49]. In addition to this, drivers in contrast to pilots, vary widely in their abilities, seldom have extensive training, and cannot be expected to understand complex literature (technical information about systems in the owners' manual) about the automated driving features in their own vehicle [50], [51].

## 1.7 Lane Support Systems (LSS) and Their Role in ADAS

### 1.7.1 Types of Lane Support Systems

LSS technologies can be categorized into three types based on intervention levels:

- **Warning-Based Systems:** These systems provide alerts but do not actively correct vehicle trajectory. They include systems that use audible, visual, or haptic feedback to warn the driver about potential lane departure.
- **Intervention-Based Systems:** These systems provide limited assistance by applying torque to the steering wheel or braking specific wheels to help maintain lane positioning.
- **Control-Based Systems:** These systems take continuous control of the steering to keep the vehicle cantered in the lane, reducing the driver's workload and improving stability.

Table 8 summarized these three categories.

**Table 8 Lane Support Systems categories**

| System category | System Type | Functionality |
|---|---|---|
| Warning-Based Systems | Lane Departure Warning (LDW) | Alerts the driver if the vehicle drifts out of the lane without signaling. |
| Intervention-Based Systems | Lane Keeping Assist (LKA) | Actively steers the vehicle to maintain lane position. |
| Control-Based Systems | Lane Centering Assist (LCA) | Continuously keeps the car centered within the lane. |

### 1.7.2 Importance of LSS for Road Safety

Lane departure crashes contribute significantly to road fatalities worldwide. ADAS, specifically Lane Support Systems (LSS), plays a crucial role in mitigating these crashes. Research has demonstrated that unintentional lane departure is a major contributor to serious accidents, particularly due to driver distraction, fatigue, and inattention. Various studies have analysed crash data to establish the effectiveness of LSS in reducing lane departure crashes. For example, the introduction of electronic stability control (ESC) has helped reduce loss-of-control crashes, but drift-out-of-lane incidents remain a critical issue. The integration of lane support technologies, therefore, is essential in enhancing road safety and reducing fatalities.

Unintentional lane departures are among the leading causes of traffic accidents. The European Transport Safety Council (ETSC) states that Lane Keeping Assist (LKA) can reduce single-vehicle road departures by up to 50%, making it a critical feature for future autonomous vehicles. However, LKA performance is directly dependent on the visibility and quality of lane markings, as faded or missing markings reduce system effectiveness [52], [53].

### 1.7.3 Regulatory Framework and Lane Support Systems (LSS) Reliability

#### 1.7.3.1 EU Regulation and Mandatory Lane Support

The significance of lane markings escalated further when the European Union issued Regulation 2019/2144, mandating that newly produced vehicles include a Lane Support System (LSS) from July 2024, EU regulation 2019/2144 [54], mandates the Lane Support System (LSS) as a required ADAS, even at the lowest automation levels (L1+). This system, providing both Lane Departure Warning (LDW) and Lane Keeping Assistance (LKA), allows automated

vehicles to detect lane markings accurately warning the driver in case of departure at L1 and supporting the Dynamic Driving task (DDT) at L2+. The implementation of these new regulations will increase the presence of vehicles with LSS in traffic, making their accuracy and reliability in detecting road markings and lane edges vital for safety. Understanding the set of operating conditions (TOD) in which LSS will be expected to operate is crucial for OEMs to enhance these systems, for road operators to update standards and maintenance, and to predict driving fallback when the system is going out of its ODD. However, this legislative push also highlights the dependence of LKA on high-contrast, well-maintained markings that cameras can detect consistently.

#### *1.7.3.2 Potential Failure Modes and System Dependencies*

Numerous external factors can undermine LSS accuracy. The performance of Lane Support Systems (LSS) can be compromised by missing, unclear, obscured, or noncompliant road markings [55]. Environmental conditions like inadequate lighting, frequent occlusion, sun glare, rain, and snow reduce the detection rate due to low lane marking visibility [56]. Additionally, factors such as road deposits and time decay affect marking quality, necessitating routine monitoring [57]. Austroads reports [58] that the performance of LSS is also influenced by road geometry and pavement conditions, along with marking characteristics like width, reflectivity, and consistency features such as variation, position, format, and continuity.

Taken together, these studies imply that for LSS to reach acceptable levels of reliability, road agencies and OEMs must coordinate not just on vehicle sensor calibration but also on infrastructure consistency especially marking retroreflectivity and uniformity.

## 1.8 Operational Design Domain (ODD) for LKA

### 1.8.1 Definition and Importance of ODD

The Operational Design Domain (ODD) specifies the conditions under which an automated driving system is designed to function. These conditions encompass geographic, environmental, traffic, road geometry, and speed-related constraints [59]. SAE defines ODD as "the operating conditions under which a given driving automation system or feature thereof is specifically designed to function, including, but not limited to, environmental, geographical, and time-of-day restrictions, and/or the requisite presence or absence of certain traffic or roadway characteristics" [60]. In other words, ODD defines the domain over which the automated vehicle (AV) can operate safely [61], outlining the specific operating environment for which the system is designed.

ODD plays a critical role in defining the limitations and capabilities of vehicles equipped with Lane Keeping Assist (LKA). If the ODD is not well-defined, drivers may overestimate system capabilities, leading to safety concerns[2]. By definition, the ODD for Level 5 AVs is unlimited since these vehicles are fully automated and designed to handle any driving scenario. However, for Levels 1 to 4, the ODD is restricted and varies based on the system's characteristics, which can change depending on the original equipment manufacturer (OEM).

### 1.8.2 Definition of Lane Support Systems (LSS)

As a key component of Advanced Driver Assistance Systems (ADAS), lateral driving assistance systems are available in multiple forms, including Lane Keeping Assistance System (LKAS, also

referred to as Lane Departure Prevention/Avoidance, LDP/LDA), Lane Change Assist (LCA, also recognized as Blind Spot Warning/Intervention, BSW/BSI), and Collision Avoidance (FCA), among others [62], [63]. Among these, LKAS is specifically designed to counteract unintended lane departures caused by driver fatigue or lapses in concentration. It is a critical lateral driving assistance system that mitigates lane departure tendencies by employing steering assist control to maintain the vehicle within its designated lane.

Lane Keeping Assistance Systems (LKAS) are categorized based on their mode of intervention. One type is limited to warning the driver about potential lane departures through mechanisms such as shoulder belt vibrations or machine vision-based Lane Departure Warning (LDW) [63]. LDW alerts the driver when an unintentional deviation from the lane occurs, typically due to inattention. A camera-based system detects lane markings and warns the driver using visual, audible, or haptic alerts[64].

Lane Support Systems (LSS) encompass various in-vehicle technologies designed to prevent unintentional lane departures by detecting lane markings using cameras and sensors. LSS includes both Lane Departure Warning (LDW) and Lane Keeping Assist (LKA). While LDW functions as an alert system to notify the driver of unintended lane deviations, LKA actively assists the driver by applying limited steering torque or braking to maintain lane position. The primary distinction between LDW and LKA is that LDW issues a warning, whereas LKA intervenes to keep the vehicle in its lane. The main advantage of LSS is its ability to reduce the likelihood of lane departure crashes caused by driver fatigue, distraction, or inattention [53], [65]. Current research efforts in lane-keeping assistance technology predominantly focus on refining and advancing active intervention systems to enhance safety and improve the reliability of lane support mechanisms.

#### *1.8.2.1* Crash Situations Related to Lane Departure

It is logical that drivers leave the lane either intentionally or unintentionally. Overtaking, avoidance manoeuvres or lane changes are common types of intentional lane departure. However, there are multiple causes of unintentional lane departure as well. Staying in lane is important as it generally is a precondition for safe driving. From a vehicle dynamics perspective, unintentional lane departure may be the result of either loss of control or drift-out-of-lane, where driver fatigue, distraction or unawareness are typical causes of unintentional drift-out-of-lane.

#### *1.8.2.2* *Early Countermeasures for Unintentional Lane Departure*

Before the introduction of advanced in-vehicle technologies such as Lane Departure Warning (LDW), Lane Keeping Assist (LKA), and Lane Support Systems (LSS), rumble strips were among the first and most widely implemented countermeasures to prevent unintentional lane departures. Installed along the edge or centerline of a lane, rumble strips produce tactile vibration and audible noise to alert distracted or drowsy drivers drifting out of lane. Their safety effectiveness has been demonstrated in several studies, with reductions in run-off-road crashes ranging from 18% to 79% depending on the type and implementation [66], [67]. A meta-analysis by Høye [68] reported that centerline rumble strips reduced head-on and opposite-direction crashes resulting in injury by up to 37%. Despite some limitations such as unsuitability for areas near residential zones due to noise, and risks posed to cyclists, rumble strips have played a crucial role in lane departure crash prevention. Interestingly, in-vehicle LSS technologies at SAE Level 1 and 2 have shown comparable safety benefits, potentially addressing lane drift

incidents regardless of road location. However, unlike rumble strips, LSS performance can be compromised by poor road markings or challenging environmental conditions [69]. Therefore, both systems can be considered complementary, with physical interventions like rumble strips offering passive, location-bound safety, while LSS provides active, vehicle-specific support across the network.

Additionally, a reliability-based assessment of shoulder rumble strips on Italian freeways confirmed not only their safety performance but also their cost-effectiveness. Rumble strips demonstrated a mean CMF of 0.83 (i.e., 17% crash reduction) with a high benefit–cost ratio of 18.0, emphasizing their economic and operational value [70]. Although their application in Italy has been limited, international experience supports their use on rural freeways with AADT ranging from 6,000 to 37,000 vehicles per day [66]. These findings reinforce the important role that rumble strips have historically played in guiding driver behavior and preventing lane departure, particularly in settings where in-vehicle technology is either unavailable or unreliable. Their passive nature ensures broad effectiveness across all vehicles, making them especially valuable in road environments with high variability in infrastructure or maintenance.

Historically, rumble strips have offered a reliable, location-specific safety intervention against unintentional lane departures, reducing Run-off-Road and opposite-direction crashes by approximately 20% under optimal installation conditions [71]. These tactile and auditory warnings act universally on all vehicles, independent of make or model. However, the evolution of vehicle automation has introduced Lane Support Systems (LSS) as a more dynamic and scalable solution. Unlike rumble strips, LSS can prevent lane departures regardless of road location, provided that the system functions correctly. Still, performance issues can arise due to poor road markings or tight curves, where LSS fault probabilities

significantly increase, for example, when retroreflectivity (Qd) drops below 153 mcd/m²/lx or curve radius falls below 141 m, fault rates climb to 11–18%, compared to a baseline of 3% [71]. Therefore, while LSS systems promise broader applicability, their effectiveness remains heavily dependent on infrastructure quality, reinforcing the value of legacy treatments like rumble strips, particularly on lower-quality or rural roads.

#### *1.8.2.3 In-Vehicle Systems*

In the last ten years, new innovative lane keeping support solutions have been developed and sold by the automotive industry, where the vehicle interprets the road environment by camera. Lane support systems (LSS) such as LDW and LKA represent in-vehicle technology detecting the travel lane by its lane markings and road edge lines. As mentioned in the previous section the system issues a warning by vibrating the steering wheel or driver's seat, or through audible and visual signalling. While both the LDW and LKA systems warn drivers, without necessarily any action having to be taken by the driver, LKA systems actively assist drivers through an automatic limited steering torque, or by applying gentle brake pressure on the appropriate wheels, as the vehicle is about to drift beyond the edge line of the current lane of travelling. Lane support systems require lane markings to be present and visible, i.e., not worn or covered by snow, or an outline contrasting significantly, such as a verge. They do not operate at low speeds, typically being activated at about 64 km/h (40 mph). There are other technical limitations to lane support systems as they do not function properly if the curve radius of the road is small or during heavy precipitation [72], [73]. Other factors, such as adverse lighting as well as temporary lane markings at construction zones, could also cause the system to fail. Hence, some limitations are effects

of technical issues while others the effect of attempting to avoid frequent warning signals in situations where the driver is deemed to be in control of the vehicle. In reducing the warning frequency, industry is trying to minimise the number of users disconnecting the system as well as attempting to avoid drivers becoming complacent to accurate warnings, which comes at a potential cost of reduced efficiency. It is crucial that system designs are aimed at optimising efficiency by maximising true positives while simultaneously minimising false positives [74], [75]. Consequently, enhanced lane detection has a potential to improve lane support efficiency.

The LDWS involves three sub-systems: driver, vehicle and road. The system makes use of the relation of the three to determine the vehicle-road relationship. Firstly, the vehicle-road state is obtained through computer vision. Through analyzing the relationship between vehicle and road, the lane departure detection approach works. In order for the electronic system or controller of the ADAS to determine which lane the vehicle is on; sensors and cameras are needed to take snapshots of the road. Cameras might be additional hardware mounted on the host vehicle or they may be built-in the vehicle. For example, a single digital camera and a laser range finder has been used in [76] to identify the lane segments and categorize them as the master and slave lane boundaries. Another paper has used a built-in forward-looking camera for distraction-free driving. An advantage of any ADAS feature is that they can be integrated to increase road safety. (Salari & Ouyang [77] integrated the Lane Departure Warning System (LDWS) with another Advanced Driver Assistance System (ADAS) feature, the Forward Collision Warning System. This camera-based driving technology demonstrated improved capabilities in analyzing captured video and alerting the driver when the host vehicle is too close to the preceding vehicle. Lane Keeping Assist in opposition with the LDWS

being a mere warning, the second half of this project proposal is the Lane Keeping Assist System (LKAS). It is an ADAS feature that detects the driver's steering effort and decides to assist with right or left steering to avoid the line boundaries. The general set-up of this system is divided into two parts: the camera for lane detection and the controls system for the steering reaction force. The main purpose of the camera is to detect the white line for the current position of the vehicle. One disadvantage of not using LDWS with LKAS is poor lane detection. In [78], the authors mentioned issues such as dirty lanes or places where the dynamic range of the image varies greatly.

### *1.8.3 Operational Design Domain (ODD) Taxonomy*

The Operational Design Domain (ODD) defines the specific conditions under which an Automated Driving System (ADS) is designed to operate safely. To standardize the specification of these conditions, the British Standards Institution (BSI) published PAS 1883:2020 [59], titled "Operational Design Domain (ODD) taxonomy for an automated driving system (ADS) Specification." PAS 1883:2020 establishes a hierarchical taxonomy for ODDs, promoting consistency in their definition to ensure safe deployment of ADS. This taxonomy categorizes ODD attributes into three primary elements:

- **Scenery:** Encompasses static aspects of the environment, such as road types, infrastructure, and geographical features.
- **Environment:** Includes dynamic environmental conditions like weather, lighting, and time-of-day factors.
- **Dynamic Elements:** Pertains to movable objects within the operational area, including other vehicles, pedestrians, and animals.

By providing a structured approach to defining these elements, PAS 1883:2020 aids manufacturers, regulators, and stakeholders in

aligning on the operational parameters of ADS, thereby enhancing safety and reliability in automated vehicle deployment.

Building upon the foundations of PAS 1883:2020, the International Organization for Standardization (ISO) published ISO 34503 [3], which offers a global specification for ODD taxonomy, further harmonizing the framework for defining operating conditions of automated driving systems worldwide. Figure 4 shows the ODD Taxonomy by BSI.

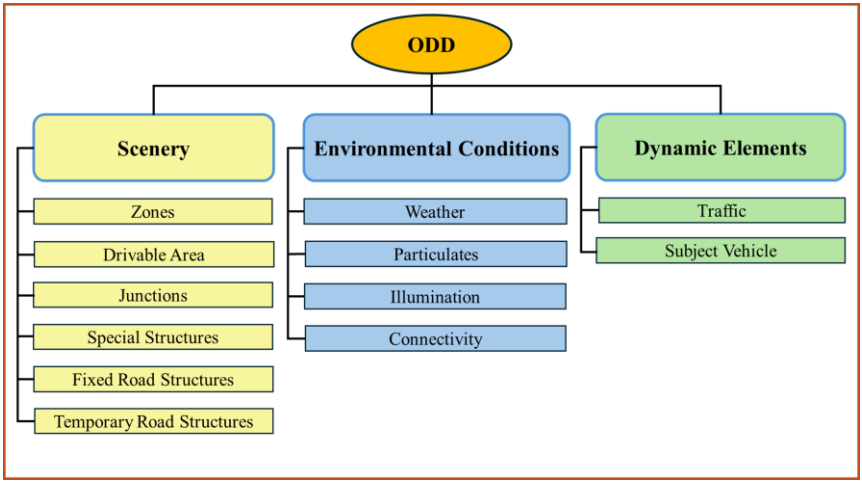


**Figure 4 ODD Taxonomy (BSI PAS 1883:2020)**

### *1.8.4 ODD Testing and Validation*

Different OEMs competing against each other to be the leading brand in AV technology results in a wide variety of defined ODD. Each OEM specifies the ODD differently in the same level of automation, resulting in a mismatch in the expected capabilities by the driver and actual capabilities of the system defined in the OEM manual. Multiple studies have conducted real-world tests to evaluate

ODD compliance and system performance. The research emphasizes the need for standardizing ODD definitions to improve reliability and prevent driver confusion.

Farah et al. [79] proposed an analytical approach to evaluate the Operational Design Domain (ODD) for Lane Keeping Assist (LKA). To examine the system's performance across various ODD classifications (inside the ODD, outside the ODD, and indeterminate) a field test was conducted under diverse road types and conditions. The findings revealed inconsistencies between the ODD defined in the OEM manual and the driver's interpretation in all test scenarios.

García & Camacho-Torregrosa [80] conducted on-road pilot tests to evaluate lane-keeping systems, assessing their performance across lane widths ranging from 2.28 m to 3.80 m. The study found that the system was unable to function on lane widths of 2.50 m or less, while it consistently operated on lanes 2.75 m or wider. Although the field tests indicated that the system could still function in lanes narrower than 2.5 m, the researchers concluded that further reductions in lane width would not be feasible given the current state of vehicle automation technology. Similarly, Marr et al. [81] emphasized that lane widths below 2.8 m pose significant challenges for vehicle machine vision systems, particularly in the absence of edge markings.

In another study, García et al. [82] tested a Level 2 vehicle on various horizontal curves, revealing a strong correlation between the system's maximum attainable speed and the curve geometry. This newly identified speed, referred to as "automated speed," was often lower than both the design speed and the operating speed. The study also highlighted a clear relationship between vehicle speed and system disengagements. Furthermore, the system's performance could not be assessed at speeds exceeding the legal limit or on curves sharper than 170 m when traveling as slow as 50 km/h. The findings concluded that for curves sharper than 550 m, the automated speed remains lower

than the design speed.

Chai et al. [83] developed a surrogate evaluation model to assess the reliability of lane detection in automated vehicles operating within complex road environments. The study identified key environmental and infrastructure-related parameters such as road curvature, lighting conditions, and lane marking visibility as critical influences on perception performance. Using data from a front-mounted monocular camera and applying RANSAC for lane detection, the authors classified detection outcomes and analyzed failure causes, including incomplete markings and lane occlusion. A machine learning approach employing XGBoost with recursive feature elimination (RFE) was used to model detection reliability based on ten selected features. Notably, the radius of curvature was found to be the most significant factor, with detection performance sharply declining at radii below 500 meters. The model also highlighted the combined influence of curvature, lighting, and marking quality, providing valuable insights into the operational design domain (ODD) for lane keeping and ADAS reliability evaluations.

Field tests conducted by Reddy et al. [84] identified key factors influencing lane-keeping performance and examined the impact of vehicle speed and visibility conditions on system effectiveness. The study found that lane width, curve type, weather conditions, lighting conditions, and speed were the primary factors affecting performance. The highest lane-keeping accuracy was observed on lanes wider than 2.50 m, while speeds exceeding 90 km/h led to reduced performance. Additionally, the research highlighted that curves are critical sections where lane assistance systems are more likely to fail.

Seppelt et al. [85] introduced the concepts of static and dynamic Operational Design Domains (ODD), categorizing identified conditions and elements accordingly. Static ODD refers to roadway

and environmental conditions that remain fixed at specific locations, while dynamic ODD encompasses conditions that require real-time monitoring through onboard sensing to detect changes over time. Autonomous vehicles primarily rely on four types of sensor technologies for perception: radar, lidar, vision, and infrared (IR).

The camera sensor is the most widely used sensor in lane-keeping systems. Xing et al. [86] examined two primary vision-based approaches for lane detection: conventional computer vision and deep learning. The computer vision-based algorithm, which relies on image processing for lane tracking, is more computationally efficient than the deep learning-based approach, which utilizes deep neural networks for lane detection. However, the study reported that computer vision-based algorithms struggle to detect lane markings in challenging driving scenarios, such as curves.

Camera sensors can provide either mono or stereo vision. They enable object mapping ahead of the vehicle and measure the distance between the vehicle and detected objects. Additionally, cameras can determine whether an object is stationary or in motion. Stereo cameras also support various Advanced Driver Assistance System (ADAS) features, such as Traffic Sign Assist (TSA) [87]. TSA can recognize and extract critical information from traffic signs, such as speed limits, and communicate it to the driver.

For Adaptive Cruise Control (ACC) and Autonomous Emergency Braking Systems (AEBS), camera sensors measure the distance to the leading vehicle to help prevent rear-end collisions. Similarly, in Lane Keeping Assist (LKA) and Lane Departure Warning (LDW) systems, cameras detect lane markings and provide visual or auditory warnings to assist drivers with warnings to change the lanes.

### *1.8.5 Infrastructure Impact on LKA Operational Design Domain*

*(ODD)*

#### 1.8.5.1 *Defining ODD Requirements*

The Operational Design Domain (ODD) for LKA comprises roadway elements (lane widths, marking condition, curvature), traffic conditions, and the range of permissible weather/lighting scenarios. Research indicates that while certain minimum reflectivity thresholds (e.g., ~80–120 mcd/m²/lux) suffice for human visibility, higher or more consistent RL values may be required for cameras that lack the adaptive sensitivity of human vision. As road agencies adopt more robust marking standards, LKA could function over a broader range of environmental contexts without frequent false alarms or dropouts.

#### 1.8.5.2 *Infrastructure and Maintenance Strategies*

Achieving a broader and safer ODD for LKA systems demands collaboration across sectors:

1. **Infrastructure Updates**: Standardizing lane marking materials that retain high RL despite traffic wear or extreme climates.
2. **Regular Condition Monitoring**: Employing advanced sensing, UAV-based or LiDAR-based surveys [88], [89], [90] for cost-effective, large-scale marking inspections.
3. **Driver Education and Regulatory Alignment**: Clarifying the limits of LKA functionality, so drivers understand how marking deficiencies or harsh weather can compromise ADAS performance [79].

Such multi-pronged efforts underscore the shared responsibility among automotive OEMs, road authorities, and policymakers.

### 1.8.6 *ADAS and Pavement Marking Reflectivity.*

In general, research points out that ideal road marking should be "readable" by both human drivers and machine-vision systems [91], [92], [93], [94]. In recent years, the retroreflectivity (RL) of pavement markings has become an important factor in improving how infrastructure works with advanced driver assistance systems (ADAS) and automated driving systems (ADS) [95]. Autonomous vehicle (AV) systems include various safety features aimed at preventing accidents; however, the success of these features largely hinges on the level of automation. Advanced safety systems are especially crucial in vehicles that have partial driving automation. Despite their potential to enhance safety, the widespread use of these technologies is still limited due to the higher costs associated with ADAS-equipped vehicles. It is well known that RL is a vital parameter for pavement marking recognition by machine vision (MV) systems in AVs that use driver assistance technologies [96], [97]. Maintaining an adequate level of RL is critical for all vision-based MV systems to ensure effective nighttime guidance.

Lane Departure Warning (LDW), Lane Keeping Assistance (LKA), and Lane Centering Assistance (LCA) are key ADAS technologies that depend significantly on the visibility of lane markings. Their effectiveness is closely tied to the characteristics of pavement markings, particularly the retroreflectivity level (RL).

In Europe, high-quality road markings are recommended to meet specific performance standards, with a minimum reflectivity of 150 mcd/lux/m² in dry conditions and a width of 150 mm for all roads. In wet conditions, the minimum required reflectivity is 35 mcd/lux/m² [98], [99]. It is widely acknowledged in the literature that maintaining road markings at a high standard and conducting frequent maintenance can help mitigate the challenges faced by camera-based vision systems in automated vehicles.

However, road markings are not always clearly visible in real-

world environments, as factors such as shadows can reduce their clarity [100]. Many trials of automated driving have either failed or required disengagement due to poorly maintained or inconsistent road markings [101]. Consequently, various studies have focused on developing algorithms capable of real-time lane boundary recognition and vehicle guidance to enhance automated driving performance [86], [102].

Recent studies have assessed the performance and safety effectiveness of Lane Support Systems (LSS) across different geometric and environmental conditions, providing valuable insights into their Operational Design Domain (ODD). Cafiso et al. [69] conducted experimental tests and logistic regression analysis on two-lane rural roads, reporting a 2.6% fault occurrence rate. The study found that faults were particularly sensitive to the luminance coefficient of lane markings under diffuse lighting (Qd) and the inverse of the horizontal curvature radius (1/R) [71].

Further research by Pappalardo et al. [88] examined Lane Departure Warning (LDW) performance on two-lane rural roads under different weather conditions. Using on-road testing and Generalized Estimating Equations (GEE), the study identified a significant rise in LDW faults during rainfall, whereas wet pavement alone had no substantial impact on system performance. The findings highlighted the critical role of wet retro-reflectance of lane markings (RLw) and the horizontal curvature radius (1/R) in defining the ODD for LDW, reinforcing the need for well-maintained road infrastructure to ensure optimal system functionality.

Babić et al. [103] conducted an on-road investigation to assess how the retroreflectivity of road markings influences the performance of machine-vision-based lane support systems (LSS) under dry nighttime conditions. Using a Mobileye 630 system and a dynamic retroreflectometer, they tested four rural road segments in Croatia,

categorizing retroreflectivity values and associating them with detection quality and view range. The findings showed a strong positive correlation between retroreflectivity and both detection quality and view range. Specifically, it was determined that a minimum retroreflectivity of 55 mcd/lx/m² is required to achieve a level 2 detection quality, while 88 mcd/lx/m² is needed for level 3. Based on these results, the authors recommend maintaining lane marking retroreflectivity at or above 100 mcd/lx/m² to ensure robust performance of LSS in diverse conditions. This study emphasizes the importance of maintaining sufficient retroreflectivity levels to enhance the operational reliability of vision-based ADAS technologies. However, this research was conducted under dry conditions, and the quality of detection is greatly influenced by the type of sensors employed. Furthermore, related studies have focused on digital image sensors tailored for camera-based applications, which can capture high-quality images even in low-light situations [96], [97], [103].

In terms of how RL affects ADAS technologies, research shows that the performance of LDW systems improves with higher RL values [104]. Importantly, lower RL levels can significantly diminish the effectiveness of LDW systems during moderate to heavy rainfall. Conversely, in dry conditions and light rain at night, LDW systems can still function well even with relatively low RL levels, such as 100 mcd/m²/lx. Besides RL, the performance of motor vehicle systems is also affected by the color of pavement markings, as greater contrast improves detection [105].

Jeong et al. [106] investigated the influence of road marking retroreflectivity on the detection accuracy of lane departure warning systems (LDWS) under varying environmental conditions. Through controlled experiments at the Yeoncheon SOC Demonstration Research Center, the authors evaluated LDWS recognition rates

across different levels of marking wear, rainfall intensities, and lighting conditions. The findings highlighted that reduced retroreflectivity significantly decreased LDWS recognition performance, particularly at night and under rainfall exceeding 20 mm/h. Critical retroreflectivity thresholds were identified for white, yellow, and blue markings to maintain a lane recognition rate above 70%, essential for the reliable operation of vision-based systems. Furthermore, the study proposed a simulation framework for optimizing road marking maintenance strategies, balancing safety with economic considerations by modelling degradation patterns and repainting costs. The results emphasized the inadequacy of current road marking standards for autonomous systems and suggested the need for updated retroreflectivity guidelines tailored to machine-vision requirements.

Storsæter et al. [107] investigated how snow coverage affects the performance of camera-based lane detection systems and evaluated whether yellow road markings offer better visibility than white markings in snowy conditions. Using images captured under laboratory, test track, and real-world conditions, the authors assessed the visibility of yellow and white road markings in different color spaces (RGB, HSL, HSV, and YUV). Their analysis showed that yellow markings generally offer better contrast than white markings in snowy scenes, especially in the HSV-S, HSL-S, YUV-U, and YUV-V channels. These findings suggest that road marking color and maintenance policies can significantly influence lane detection reliability in automated driving systems. The study emphasizes the need to consider infrastructure design particularly road marking color and visibility under adverse weather as a critical factor in supporting both human and automated driving.

Several studies indicate that contrast might, in some instances, be a more crucial factor than RL for accurate lane marking recognition

[69], [95]. This highlights the need to consider both RL and contrast when assessing the visibility and effectiveness of pavement markings in enhancing ADAS functionality.

### 1.8.7 Challenges in Lane Marking Detection for ADAS Systems

Despite technological advancements, LSS and LKA systems face real-world challenges that limit lane detection accuracy. These challenges fall into three main categories: environmental, infrastructural, and technical.

#### 1.8.7.1 Environmental, Infrastructure & Technical Challenges

**Table 9 Environmental Challenges**

| Weather Condition | Impact on LKA & ADAS |
|---|---|
| Heavy Rain & Wet Roads | Reduces lane contrast and reflectivity. |
| Fog & Low Visibility | Weakens lane marking recognition. |
| Snow & Ice | Completely obscures lane markings. |
| Glare & Sunlight Reflection | Causes overexposure in camera-based systems. |

**Table 10 Infrastrutture Challenges**

| Road Condition | Effect on LKA Detection |
|---|---|
| Faded Markings | Reduces contrast, making tracking difficult. |
| Poor Road Contrast | Light-colored pavements reduce system effectiveness. |
| Temporary Construction Markings | Can confuse LKA algorithms. |

There are several challenges like as poor detection by camera-based systems due to low light condition. LiDAR & Radar cannot reliably detect painted markings. Also, ADAS systems may misinterpret road edge, cracks or dirt as lane marking.

## 1.9 State-of-the-Art and Empirical Evidence

In the previous sections (1.1–1.8), essential definitions, concepts, and context regarding Lane Support Systems (LSS), lane marking quality, and Operational Design Domain (ODD) were provided. This section offers a more detailed examination of current research literature relevant to the themes of lane marking quality assessment, lane support system technologies, and their interactions under various conditions. Specifically, current review synthesizes existing findings on: (1) the state-of-the-art methods for assessing lane marking quality; (2) regulatory developments concerning Lane Support Systems; (3) empirical evidence linking lane marking attributes to the reliability of lane keeping systems; and (4) how infrastructure quality directly influences the Operational Design Domain (ODD) of these advanced vehicle systems. The review presented here will lay the groundwork for identifying existing knowledge gaps and setting the stage for the methodological and analytical approaches described in subsequent chapters.

### *1.9.1 Lane Marking Quality Assessment and Detection Techniques*

#### *1.9.1.1 Lane Marking Fundamentals*

Lane markings fulfil a dual role of improving road safety for human drivers and providing critical visual cues for in-vehicle cameras and sensors. Their overall effectiveness hinges on core attributes such as retroreflectivity (RL), which aids nighttime detection by reflecting vehicle headlamp illumination back toward the driver or camera, and contrast between markings and the pavement surface, which is often measured through coefficients like Qd (luminance under diffuse lighting). Degradation from weather, heavy traffic, or suboptimal maintenance can obscure markings, thereby undermining human perception and machine-based detection.

#### *1.9.1.2 Lane Marking Detection and Quality Assessment*

Recent literature exhibits a variety of approaches to evaluating lane marking conditions. Multiple studies leverage image processing and machine learning to automate inspections; for instance, Sapkal et al. [108] presented a comprehensive review of lane detection methods utilized in advanced driver-assistance systems (ADAS) such as Lane Keeping Assistance Systems (LKAS) and Lane Departure Warning Systems (LDWS). The study categorized existing techniques into conventional image-processing-based methods and deep learning approaches. Traditional models were described to rely heavily on edge detection, color transformation, and geometric modelling, including methods such as Hough Transform, RANSAC, and Kalman filtering. In contrast, deep learning models including encoder-decoder frameworks like SegNet and UNet demonstrated superior performance under challenging conditions such as poor visibility, degraded markings, and road curvature. The paper also reviewed generative models (e.g., GANs) and dual-view CNNs that combine perspective and bird's-eye views for enhanced accuracy. Among the tested models using the TuSimple dataset, UNet achieved higher accuracy compared to SegNet. The review further detailed publicly available benchmark datasets and highlighted persistent challenges such as robustness under adverse environmental conditions, poor lane visibility, and the need for fusion with other sensing modalities to overcome limitations inherent to camera-based systems. Liu [109] presented a lane detection framework that utilizes deep learning, incorporating a full-reference quality-aware discriminative gradient model. This method employs a gradient-guided convolutional neural network (CNN) to identify lane presence by taking advantage of the high gradient values at lane edges compared to the surrounding areas. Furthermore, a recurrent neural network (RNN) was introduced to model the spatial distribution of detected lanes, addressing challenges

related to lighting and visual obstructions. Experimental tests on the TuSimple dataset revealed that this approach surpasses traditional algorithms, achieving greater detection accuracy while remaining resilient to noise. Similarly, Pollard et al. [110] introduced an enhanced lane marking extraction technique that combines multiple extraction algorithms to improve detection accuracy in challenging situations. This method merges high-contrast pixel detection to minimize false positives with lower-contrast pixel identification to decrease false negatives. Tests using both real-world and synthetic images confirmed the robustness of their approach in enhancing lane marking detection for Advanced Driver Assistance Systems (ADAS). Dewangan and Sahu [111] developed a low-cost, vision-based Lane Detection Model (LDM) using computer vision and image processing techniques to enhance the lane-keeping capabilities of intelligent vehicle systems. Their approach utilized a Raspberry Pi prototype equipped with a monocular camera and Arduino microcontroller to detect lane markings in real time through inverse perspective mapping, binary thresholding, and edge detection. The system was evaluated on both straight and curvy lane scenarios, demonstrating the ability to maintain vehicle alignment within lane boundaries and to respond adaptively to detected deviations. Experimental results indicated a high lane detection accuracy rate of 98.57%, highlighting the practical viability of low-cost embedded vision solutions for advanced driver assistance systems (ADAS). The study also provided a detailed comparison with state-of-the-art methods, underscoring the importance of integrating efficient image processing strategies for robust lane detection in dynamic driving environments Xiao et al. [112] proposed a structure-prior deep neural network to improve the accuracy and efficiency of lane detection by incorporating the structural continuity of lane markings. The model introduces a Recurrent Slice Convolution Module (RSCM) that processes lane

features by learning both horizontal and vertical structural dependencies, enhancing the semantic interpretation of elongated lane markings. Additionally, a novel distance-based loss function was introduced to ensure geometrically consistent predictions. Experimental evaluations on standard datasets such as CULane and TuSimple demonstrated that the method achieved competitive detection performance with reduced computational complexity compared to state-of-the-art approaches. This study highlights the importance of structural representation of lane markings for reliable system-based lane detection in advanced driver-assistance systems. Al Mamun et al. [113] proposed a deep learning-based approach for lane marking detection utilizing a customized encoder-decoder E-Net architecture trained with differential and cross-entropy loss functions. The model was developed using the TuSimple dataset, which contains diverse environmental conditions including different traffic scenarios, weather types, and lighting variations. Their framework aims to overcome the limitations of traditional handcrafted feature-based methods that suffer from high computational cost and poor performance under challenging conditions. By applying binary and instance segmentation, the model achieves more accurate lane localization and reduced false positive and negative rates. With a maximum accuracy of 96.61% and an F1 score of 96.34%, this method outperformed several state-of-the-art techniques in lane detection, demonstrating its robustness and suitability for advanced driver-assistance systems (ADAS) applications. Zhang et al. [114] conducted a comprehensive survey on deep learning methods applied to lane marking detection, emphasizing the evolution from handcrafted feature-based techniques to deep neural network architectures. The authors categorized detection strategies based on their focus on spatial structure, scene priors, and positional regularity. The review covered various network architectures such as FCN, U-Net, SCNN, and

SpinNet, along with optimization strategies including cross-entropy, regression, and adversarial losses. The study also highlighted the role of attention mechanisms and LSTM structures in enhancing detection accuracy, especially in complex or occluded road scenes. Additionally, the paper provided an in-depth analysis of datasets commonly used in lane detection research, such as CULane and TuSimple, and evaluated methods based on both detection performance and real-time processing capability. This work offers valuable insight into the architectural considerations and evaluation metrics critical to lane marking detection using deep learning. Sheng et al. [115] conducted a comprehensive comparative analysis of lane marking detection methods, evaluating the performance of four advanced techniques—SCNN, LaneATT, InSPyReNet, and RESA—using a consistent dataset collected from UK motorways. The study tested these methods under diverse conditions, including optimal lighting, faded markings, night-time, adverse weather, and traffic congestion. Among them, InSPyReNet and RESA exhibited superior accuracy and robustness across most scenarios. Notably, the study emphasized the importance of retroreflectivity in enhancing lane marking visibility under challenging conditions and highlighted its correlation with detection performance and road safety. The research contributes valuable insights into the role of lane marking features such as color, shape, and reflectivity on automated vehicle sensing systems, aligning with current efforts in improving real-time lane marking quality assessment using camera-based ADAS technologies. Lin et al. [116] developed a lane detection framework that integrates deep neural networks and temporal information to enhance the identification of lane markings under complex urban conditions. The proposed method combines a 3D ResNet50 backbone with existing lane detection networks such as PolyLaneNet and PINet, allowing the use of image sequences instead of single frames to incorporate

temporal dependencies. The model employs time-space split convolution and LeakyReLU activation to improve detection stability and accuracy. Experimental validation on benchmark datasets, including TuSimple, CULane, and a custom urban dataset from Taipei, demonstrated that the enhanced PINet model achieved an accuracy of 91.34%, confirming the effectiveness of temporal data in improving real-time lane detection under challenging driving environments. Chai et al. [117] developed an efficient lane detection model combining a row-anchor-based architecture with a Transformer encoder–decoder structure to enhance the extraction of global features in complex driving scenarios. The proposed method integrates a Poolformer encoder to reduce computational complexity while maintaining high performance and employs an auxiliary segmentation branch during training to improve feature fusion. A novel loss function incorporating structural and expectation loss components was also introduced to preserve the continuity of lane predictions. Evaluated on the TuSimple dataset, the model achieved 96.16% accuracy and a processing speed of 129 FPS, demonstrating a strong balance between accuracy and real-time performance. The study contributes to the advancement of lane detection algorithms used in ADAS applications, particularly for consistent lane tracking under varying visibility conditions. Srivastava and Maiti [118] proposed a robust vision-based lane detection and tracking framework designed to function under diverse road and illumination conditions. Their method utilizes a two-stage feature extraction process, combining adaptive thresholding at the sub-image level with artifact removal using vertical aggregation and Hough transform at the regional level. To enhance detection robustness, they integrated a Kalman filter-based tracking module, with dynamically adjusted parameters based on measurement reliability. A dynamic area of interest (DAOI) is defined for each frame, and a frame coherence strategy periodically verifies lane

position through full-frame detection, supported by a moving average window estimator. The system effectively adapts to lane transitions and occlusions and demonstrates superior detection performance across challenging urban and highway environments in both Indian and Caltech datasets, achieving up to 99.55% accuracy. Getahun and Karimoddini [119] proposed an integrated vision-based control framework for autonomous lane keeping, comprising a robust lane detection algorithm and a nonlinear model predictive controller (MPC). The system uses monocular camera input to extract lane markings through advanced image pre-processing techniques, including Gabor filtering, and estimates the ego-lane center. The controller utilizes a kinematic model to generate lateral and longitudinal control commands for smooth vehicle path tracking. The approach was implemented and tested on a Lincoln MKZ hybrid vehicle under various real-world road conditions, demonstrating reliable performance in maintaining lane centering, including scenarios with missing lane boundaries, shadows, and road texture changes. Fakhari and Anwar [120] introduced a robust lane detection framework for Lane Keeping Assist Systems (LKAS) utilizing Multiple Model Adaptive Estimation (MMAE) to integrate two computer vision-based detection algorithms. This method employs front and rear camera data, where the front-facing models generate real-time lane offset estimates and the rear camera provides a time-delayed reference. The MMAE framework probabilistically evaluates each model's reliability under various environmental and road conditions, ensuring dynamic switching between models for optimal accuracy. Through simulations in the AirSim environment, the study demonstrated that this adaptive approach significantly enhances lane offset prediction, particularly in scenarios involving sharp curves, shadow occlusions, wet pavement, and degraded markings. The integration of model uncertainty in steering control via a PID

controller allowed for consistent lane keeping performance, outperforming individual models and matching the reliability levels of multi-sensor fusion systems.

Yuan et al. [121] proposed a novel approach for lane detection and estimation utilizing a Surround View Camera System (SVS) without the need for additional hardware. Their method involves processing distorted mono-camera images through neural network-based semantic segmentation, followed by spatial and temporal filtering of lane-relevant data using a truncated Gaussian random field and fading memory model, respectively. The processed data is then used for adaptive polynomial fitting to estimate lane geometry and vehicle orientation. The study demonstrated promising performance in a real-world parking lot scenario, highlighting the potential of SVS-based systems in supporting advanced lane keeping capabilities in automated vehicles. Zhang et al. [122] proposed an improved sliding window algorithm for lane detection that integrates steering wheel angle sensor data and binocular camera input to enhance performance on curves with high curvature. Traditional lane detection algorithms, including sliding window methods, perform adequately on straight roads and gentle curves but often fail on sharper curves. The authors introduced a fusion method using the steering wheel angle from the previous frame to predict the search center for the next sliding window, improving robustness even when lane markings are dashed or partially occluded. Their system also utilizes perspective transformation and binary image processing to increase detection accuracy and applies the least squares method for fitting lane lines. Experimental validation in simulation environments demonstrated significant improvements in tracking lane lines in high-curvature and visually challenging conditions.

Jabłoński et al. [123] presented a novel real-time hardware-in-the-loop (HiL) simulation framework designed for the development

and validation of Advanced Driver Assistance Systems (ADAS). The system integrates the CARLA 3D simulator with a real-time automation platform, Morphee, and facilitates closed-loop testing with actual sensors like the Mobileye 6 camera. The setup supports camera-based lane-keeping systems by simulating various road scenarios and capturing real-time data through CAN communication. Their experimental configuration demonstrated the lane detection capability of Mobileye 6 and enabled real-time computation of vehicle trajectory based on lane model parameters. The system's high sampling frequency (1 kHz) and synchronization with a CANoe-based FPGA clock allowed for precise temporal validation. This HiL platform enables testing of lane-keeping algorithms in both open and closed-loop scenarios without physical vehicle deployment, thus enhancing safety and cost-efficiency in system validation processes.

Vidya Sagar and Prabhakar [124] proposed an Enhanced Lane Departure Warning System (ELDWS) that combines Phase Stretch Transform for edge detection, a Curved and Straight Lane Detector (C&S) for accurate lane identification, and a modified Kalman filter for robust lane tracking. The system is designed to maintain high performance under diverse lighting and weather conditions, addressing limitations of conventional methods that rely on clear markings and favorable environments. Their approach was validated using both custom and benchmark datasets, achieving a lane detection accuracy of 97.83% on straight roads and 97.33% on curved roads in daytime scenarios. For lane departure detection, the system demonstrated an accuracy of 95.81% during the day and 84.6% at night. These results indicate that integrating adaptive edge detection with dynamic tracking enhances the accuracy and reliability of lane departure estimation for ADAS-equipped vehicles.

Jeong [125] proposed an interactive Lane Keeping Assist System (LKAS) based on a Long Short-Term Memory Recurrent

Neural Network (LSTM-RNN), which integrates lane marker geometry, ego-vehicle dynamics, and surrounding vehicle interactions to determine steering wheel inputs. The model was trained using data collected from a front camera, LiDAR, and DGPS sensors mounted on a test vehicle. The study demonstrated that incorporating temporal and contextual driving information leads to improved lane keeping performance, especially in scenarios involving adjacent vehicles. Comparative simulations revealed that the proposed algorithm outperforms conventional LKAS approaches that only rely on lane marker detection, highlighting the value of incorporating environmental interactions into lateral control strategies for autonomous and advanced driver-assist systems (ADAS).

Beyond camera-based methods, LiDAR and UAV platforms have also emerged for marking assessment. Jung et al. [89] created a strong and efficient method for extracting lane markings from mobile LiDAR point clouds. Their approach tackles issues like varying noise, faded markings, and different road conditions by breaking down LiDAR data into smaller segments, converting it into a local coordinate system, and using constrained RANSAC segmentation to extract the road surface. The road markings are then refined through image processing techniques, such as segmentation, morphological filtering, and noise removal using Dip test statistics. The study showed that the method is effective across various datasets, achieving F1 scores ranging from 89% to 97%, highlighting its reliability in different road environments. By contrast, Rahnamayiezekavat et al. [90] presented a UAV-based platform for the automated assessment of pavement marking integrity. Their system captures high-resolution images using a UAV equipped with an optical camera, which are then analyzed through digital image processing techniques. A case study in a public parking area highlighted the platform's ability to detect worn pavement markings and aid in data-driven maintenance decisions.

Alzraiee et al. [126] created a deep learning framework for identifying pavement marking defects with Faster R-CNN. This study tackled the challenges of manual inspections by utilizing a photogrammetry dataset from Google Maps, annotating 1,040 images to train the model. The resulting model detected defects with confidence levels between 43% and 99%, showcasing its potential for automated assessments of pavement markings. Li et al. [127] created a lane marking quality assessment (LMQA) framework designed to assess the adequacy of road markings for autonomous driving. This approach employs an inspection vehicle outfitted with a GPS receiver, a frontal-view camera, and a LiDAR system. It introduces three essential metrics for evaluating lane marking quality: correctness, shape consistency, and visibility contrast. A dual-modal algorithm that combines camera and LiDAR data was developed to calculate these metrics, effectively identifying irregularities in lane markings and proving useful for assessing road infrastructure. Collectively, these studies confirm that multisensor data fusion (e.g., combining GPS, cameras, and LiDAR) can dramatically enhance the reliability and scalability of pavement marking quality evaluations. Jang et al. [128] developed a system for constructing lane-level road marking (RM) maps using monocular cameras, presenting a cost-effective alternative to high-end mobile mapping systems (MMS) equipped with 3D LiDAR and RTK GPS. The proposed method utilizes a deep learning network named RMNet to perform pixel-level segmentation of road lanes (RLs) and symbolic road markings (SRMs), allowing for the creation of high-definition maps. Their mapping pipeline includes inverse perspective mapping, error correction through weighted iterative closest point (ICP) matching, and graph-based optimization with loop closure detection. The system was trained on a newly developed dataset called SeRM, which includes over 25,000 pixel-wise annotated images. Unlike previous approaches focused on curve

fitting for lane detection in Lane Keeping Systems (LKS), this method emphasizes pixel-level semantic segmentation, making it suitable for detailed mapping tasks. The resulting maps exhibit structural similarity to high-definition LiDAR-generated maps and demonstrate the feasibility of using standard vision systems for high-resolution mapping in autonomous driving contexts. Barandiarán Martirena et al. [129] developed a method for automated annotation of lane markings using low-density LIDAR point clouds and odometry information. The technique involves processing vehicle trajectory blocks, detecting lane marking candidates using virtual scan lines and dynamic thresholding, and classifying markings as solid or dashed. A notable aspect of the work is the use of 3D polylines to represent centerlines and widths of markings, enabling lateral localization suitable for applications such as lane-keeping assist systems. The study reported high accuracy (F-measure of 0.92 for lines and 0.94 for dashed segments) with a processing time of 4 seconds per 100 meters of road, and a 60% reduction in manual annotation time.

Parallel research also explores environmental and material factors. For example, Burghardt et al. [130] examined the impact of road markings on microplastic pollution, focusing on the contribution of glass beads and the estimation of abrasion-related loss. This study questioned previous high estimates of microplastic emissions from road markings by taking into account the frequency of marking renewals and the maintenance of retroreflectivity. The findings suggested that emissions were lower than earlier reports indicated, except in Nordic countries where severe winter conditions lead to increased wear. Formosa et al. [131] investigated how lane marking quality affects the functioning of autonomous vehicles, stressing the importance of road infrastructure for AV safety. The research utilized an instrumented vehicle to gather data on active motorways and a controlled motorway

facility, simulating inputs from AV sensors. Findings revealed that lane departure warning (LDW) systems accurately detected lane changes 95% of the time when lane markings were 50% faded, but this accuracy dropped to only 54% when markings were 75% faded. The study underscored the necessity for high-definition lane-based digital maps to alleviate the adverse effects of worn lane markings. Hadhrami et al. [132] conducted an extensive review of lane marking detection algorithms designed for all-weather conditions, emphasizing the challenges posed by fog, rain, haze, and snow on detection accuracy. The paper discusses the importance of classifying different lane marking types such as solid, dashed, and their combinations for improving ADAS decision-making processes. A contour-angle-based method is proposed for marking classification, capable of distinguishing between subtle variations like solid-dashed and dashed-solid marking. Their proposed system demonstrates high classification accuracy (above 93%) across various marker types in different weather scenarios. This work highlights the gap in lane marking classification research compared to lane detection, reinforcing the need for robust methods to support lane-keeping assist systems. Storsæter et al. [133] investigated the potential of advanced driver assistance systems (ADAS), specifically lane departure warning (LDW) systems, to monitor the quality of pavement markings in real-world conditions. In their study, data collected from an in-vehicle LDW system were compared with retroreflectivity measurements obtained from a mobile retroreflectometer mounted on the same vehicle. The experiment spanned over 200 kilometers across various road classes and lighting conditions in Norway. The results indicated that the retroreflectivity values could predict the detection performance of the LDW system with an accuracy ranging from 92% to 98%. Furthermore, binary logistic regression revealed that contrast was a more significant predictor of lane detection success than

retroreflectivity itself, and that speed of the vehicle also played a key role. These findings highlight the potential of using ADAS sensor outputs, as complementary tools for road marking management and suggest the need for quality metrics beyond traditional RL values to assess visibility for machine perception systems. Teo et al. [134] proposed a Gabor filtering-based method to enhance lane detection performance under challenging conditions such as shadows, faded lane markings, and inconsistent road textures. The approach involves a three-stage process that includes Gabor-based texture analysis, adaptive Canny edge detection, and probabilistic Hough transformation to identify lane candidates robustly. Their method integrates real-time implementation on a Raspberry Pi 3B and achieves a lane detection accuracy of 93.67% and a lane departure warning accuracy of 95.24% using a dataset recorded on Malaysian roads under varying environmental conditions. Compared with traditional inverse perspective methods and the GVP approach, their solution showed superior performance, especially in urban environments with low-quality markings and shadow interference. The study also emphasizes the system's computational efficiency and suitability for low-cost, real-time ADAS applications. Tikar and Patil [135] proposed a fast-response driver assistance framework capable of performing efficient lane detection and collision avoidance under diverse environmental conditions, including poor lighting and missing lane markings. Their system applies to a spatial domain image enhancement technique and a dynamic algorithm that draws virtual lane markers when physical markings are absent. The method segments regions of interest using white and yellow intensity filters and estimates vehicle departure using Euclidean distances between detected lane lines and a reference point. The proposed system showed lane detection accuracy above 98% across various scenarios and demonstrated superiority over traditional approaches like Hough and

Gabor transforms in both performance and robustness, particularly when dealing with lane occlusion or degraded visibility.

### 1.9.2 Empirical Studies on Lane Markings and LKA Performance

#### 1.9.2.1 Influence of Geometry, Weather, and Lighting

Empirical data consistently show that LKA systems degrade when road curvature is high, or lane widths are below commonly recommended thresholds. Recent studies have evaluated LSS performance and safety effectiveness under various geometric and environmental conditions, revealing key insights into their ODD. Cafiso et al. [69] analyzed two-lane rural roads using experimental tests and logistic regression, finding a 2.6% fault occurrence rate. Faults were highly sensitive to the luminance coefficient of lane markings under diffuse lighting (Qd) and the horizontal curvature radius (1/R) [71].

Nighttime and inclement weather can compound these problems. In a broad field study examining environmental variation, Reddy et al. [84] evaluated LSSs under various environmental and road conditions. Detection performance significantly worsened at night under streetlights and during rainy weather, with the lowest detection rates under these conditions. Additionally, LKA systems positioned vehicles more to the left in narrow lanes and on left curves. These findings emphasize the need to consider road geometry and environmental factors in designing and deploying lane assistance systems to ensure their reliability and safety.

Babić et al. [103] explored the differences in lane marking detection quality and view range between daytime and nighttime conditions using the Mobileye 630 system. Their on-road tests conducted on rural roads in Croatia found that nighttime conditions enhanced lane marking detection, boosting confidence levels by 5%

to 8% and decreasing instances of "nothing detected" by 12%. However, the view range was 16% longer during the day due to better ambient lighting.

Pappalardo et al. [88] evaluated LDW performance on two-lane rural roads under various weather conditions. The study, using on-road testing and Generalized Estimating Equations (GEE) found a significant increase in LDW faults during rain, while wet pavement alone did not notably affect performance. The importance of wet retro-reflectance of lane markings (RLw) and horizontal curvature radius (1/R) in defining the ODD for LDW was emphasized, advocating for robust road infrastructure and maintenance.

Sultana et al. [136] proposed a real-time and robust vision-based lane detection and tracking algorithm that addresses a wide range of real-world challenges, including illumination changes, weather-induced occlusions, and lane-like visual noise. Their approach introduces a comprehensive intensity threshold range (CITR) to enhance the performance of the Canny edge detector, allowing for the accurate detection of blurred, eroded, and low-intensity lane markings. Additionally, a geometric verification step based on angle and length constraints is used to differentiate true lane markings from visual distractions such as guardrails or vehicle edges. The method includes a simple but effective tracking system that predicts the horizontal position of lane markings in subsequent frames, enhancing reliability even when markings are partially or fully invisible. Experimental validation using DSDLDE and SLD datasets demonstrated a detection accuracy of 97.55% with an average processing time of 22.33 milliseconds per frame, outperforming several existing approaches in terms of both robustness and computational efficiency.

Lehoczky et al. [137] conducted an in-depth study assessing the readiness of Slovak road infrastructure for the deployment of

intelligent transportation systems, including Lane Keeping Assist (LKA) and Intelligent Speed Assist (ISA). The authors emphasized the critical role of well-maintained and visible road markings and signage for the effective functioning of ADAS technologies. Using an onboard sensor platform integrating camera, LIDAR, GNSS, and network modules, the research team recorded and analyzed various road conditions across Slovakia. Their observations revealed significant disparities in lane marking quality, especially in rural and secondary roads, where markings were often faint or missing. Inconsistent temporary markings and outdated signage were also found to cause detection issues for LKA systems, underlining the necessity for infrastructure standardization and maintenance. These findings highlight the infrastructural challenges that impact the reliability of automated driving systems and the importance of retroreflectivity and visibility in lane markings.

#### *1.9.2.2 Discrepancies Between Manufacturer ODDs and Real-World Conditions*

Some studies focus on human factors, showing that drivers often overestimate their vehicle's lane-keeping capabilities. Farah et al. [79] assessed the ODD for LKA-equipped vehicles with 19 participants, focusing on objective risk via the Probabilistic Driving Risk Field (PDRF) and subjective risk evaluations of driver behaviour, trust, and situational awareness. The study found significant gaps between the manufacturer's ODD and drivers' understanding, highlighting the urgent need for better communication about the role of road infrastructure particularly the necessity for high-quality, well-maintained markings in preventing system disengagements or false positives.

## 1.10 Summary and Research Gaps

Existing research consistently highlights the central role of lane marking retroreflectivity, marking width, and road geometry in enabling reliable LKA performance. Studies have explored the degradation of marking visibility under adverse weather, nighttime conditions, and high traffic, underscoring how suboptimal markings lead to higher fault rates or deactivations in ADAS. Yet, many field investigations rely on isolated segments or controlled experiments, limiting the breadth of insight into real-world operation over extended road sections and diverse weather conditions.

In this dissertation, we address these gaps by:

1. Collecting Comprehensive On-Road Data: We integrate Mobileye ADAS outputs with retroreflectivity measurements (RL) from the ANAS DELPHI car, road geometry from OpenStreetMap (OSM), and environmental parameters (rain, day/night) across multiple highways in Italy.
2. Analyzing Detection Quality at Scale: Our dataset encompasses thousands of lane segments under various weather/light conditions, enabling robust statistical analysis of ODD constraints particularly for lane marking width, curvature, and RL thresholds.
3. Employing Advanced Classification and Interpretability Techniques: After balancing the dataset via SMOTE to handle class imbalances, we adopt LightGBM, CatBoost, and other ordinal classification methods to model lane-marking quality. Moreover, we incorporate a Shapley Additive exPlanations (SHAP) framework to interpret the influence of each feature on the predicted detection score. SHAP leverages cooperative game theory to quantify how much each parameter (e.g., curvature, weather, RL) contributes to a particular class outcome. This

interpretability step ensures not only high predictive accuracy but also a transparent understanding of which road or environmental factors degrade or enhance LKA detection.

4. Assessing the feasibility of predicting lane marking retroreflectivity (RL) from ADAS outputs and contextual roadway data and developing classification models to detect low RL segments.
5. Evaluating the alignment between driver perception and ADAS assessments of lane marking quality across diverse conditions using correlation and discriminant analysis.
6. Identifying the environmental and geometric conditions under which human and system assessments agree or diverge, informing future ADAS calibration and infrastructure design.

By employing a multi-source data fusion and machine learning pipeline, this study offers a large-scale empirical examination of how physical infrastructure features and marking retroreflectivity interact with vision-based LSS detection. Unlike previous work that may focus narrowly on a single condition or technology, the proposed methodology covers a broad swath of real-world operational scenarios. The following methodology chapter will detail how these data were acquired, processed, and modelled, ultimately guiding infrastructure recommendations to support safer, more reliable ADAS/LKA functionalities in everyday driving conditions.

## *1.11 Structure of the Dissertation*

The dissertation is structured into several chapters to facilitate a systematic exploration of the research objectives:

- **Introduction and Literature Review:** Outlines the research problem, significance, and objectives. This chapter provides a thorough review of existing research on LSS, machine learning

applications in traffic systems, and regulatory and safety standards affecting LSS implementation.

- **Methodology:** Describes the data collection processes, machine learning models used, and the analytical techniques employed to evaluate LSS performance.
- **Data Collection and Analysis:** Details the specific data used, how it was processed, and the initial findings from the data analysis.
- **Results and Discussion:** Discusses the results of the analysis, interprets the significance of these results, and explores the implications for LSS technology.
- **Conclusions and Recommendations:** Summarizes the findings, suggests practical applications of the research, and proposes areas for further study.

# Chapter 2: Methodology

# 2 Chapter 2: Methodology

The methodological structure of this dissertation reflects its multi-project design, encompassing three interconnected research efforts focused on evaluating and improving the performance of Lane Support Systems (LSS). The first part of the chapter outlines the data acquisition and processing procedures, including the integration of Mobileye ADAS sensor outputs, retroreflectivity measurements from ANAS, road geometry from OpenStreetMap, and human perception ratings. This unified dataset forms the foundation for all three projects.

Subsequently, each project is addressed in a dedicated section. Project 1 focuses on ODD by developing a classification framework for lane marking quality as detected by LSS. Project 2 investigates whether LSS data can be used to estimate physical retroreflectivity levels (RL), traditionally measured by specialized instruments. Project 3 evaluates the agreement between driver perception and Mobileye detection to analyse consistency or discrepancies between human and automated driving needs.

This chapter details the analytical frameworks, modelling approaches, and preprocessing techniques applied to each of these projects.

## 2.1 Database

Data used in this research have been made available and collected by different sources. the Dept. of Civil Engineering and Architecture provided the ADAS data, collected by the Mobileye 6.0 (Intel®) full protocol, a cutting-edge vision-based ADAS, installed on the Automatic Road Analyzer (ARAN 9000). Mobileye systems support real-time driving by providing video and/or audio warnings for frontal collisions, safety distance, pedestrian collisions, lane departure, speed limits, and road sign recognition. Mobileye is

connected with a custom-designed data logger to record and synchronize data with other sensors, including a high-accuracy GNSS/INS system, cameras and a keyboard to record events manually by an operator.

The road sections have been selected in collaboration with the Italian Road Agency (ANAS) to validate the detection accuracy of LSS, considering also the marking data available in their database. ANAS collected data on the retroreflectivity index (RL) [33], [138] and GNSS position using the DELPHI Delineation photometric instrument, with measurements statistically aggregated (mean, max, min, standard deviation) every 50 meters on the right side of the lane. Data on the road infrastructure are derived from Open Street map (OSM). Figure 5 illustrate the data acquisition systems and Figure 6 shows the diverse datasets and sources used in this project.

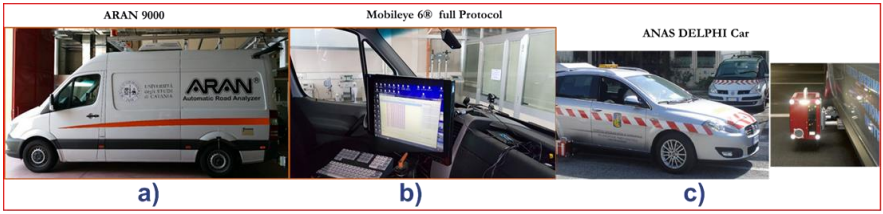


**Figure 5 Data acquisition; a) University of Catania Aran 9000 Car, b) Mobileye 6 full protocol, c) ANAS DELPHI Car** [139]

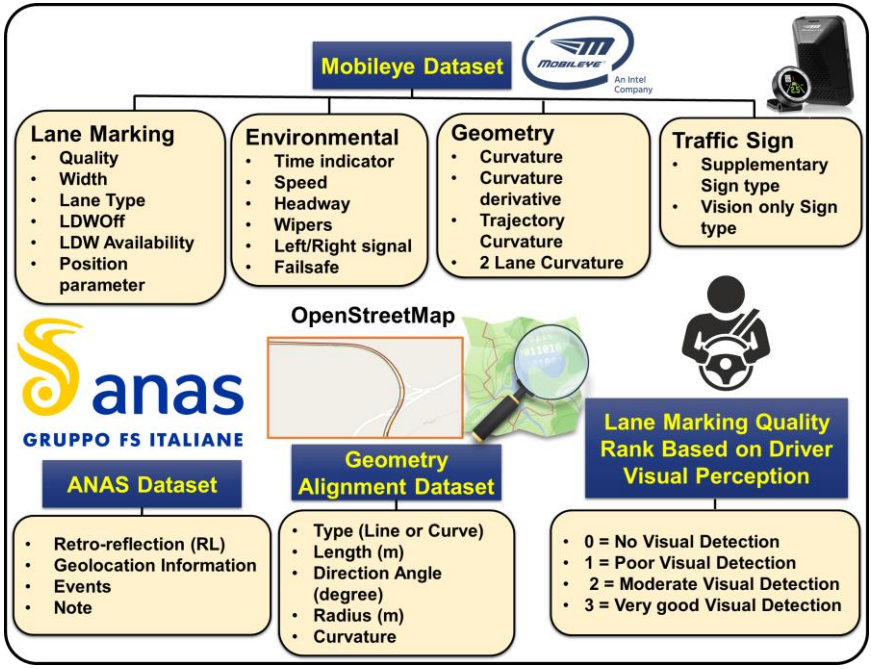


**Figure 6 Schematic of data collection from different sources**

### *2.1.1 Mobileye 6.0 Data*

Mobileye 6.0, developed by Intel®, is an advanced driver assistance system (ADAS) that enables the collection of a wide range of road, vehicle, and environmental data through its full protocol Lane Keeping Assist (LKA) system. This system is particularly useful for applications involving roadway analysis, sensor performance evaluation, and intelligent transportation research.

In terms of lane-related data, Mobileye 6.0 can detect and recording several critical parameters. These include the lane marking quality score, which reflects the clarity and detectability of road markings, as well as the lane marking width, type (e.g., solid, dashed,

double), and curvature. This information can be used to assess road marking conditions and their influence on LKA system performance. Furthermore, the system can determine the vehicle's position relative to the lane, providing data on lane offset and supporting lane departure studies.

Vehicle dynamics are also captured through parameters such as vehicle speed, steering angle, yaw rate, and heading direction. These values are essential for evaluating vehicle behaviour, system responsiveness, and the accuracy of lane-keeping functionalities under real-world conditions.

Environmental factors can also be analyzed through Mobileye's data. The system records light conditions such as daylight, dusk, and nighttime allowing researchers to assess sensor performance in various visibility scenarios.

In addition to lane and environmental data, Mobileye 6.0 supports several ADAS features, including Forward Collision Warning (FCW), vehicle and pedestrian detection, and Traffic Sign Recognition (TSR). These features not only enhance driving safety but also provide valuable data points for traffic environment characterization and driver behaviour analysis.

When integrated with GPS or external data loggers, Mobileye 6.0 can also offer geolocation information, enabling spatial mapping of detected features and facilitating the analysis of road infrastructure across different segments. Table 11 present some Mobileye CAN message parameters with their description for LKA system.

**Table 11 Mobileye® CAN messages parameters and definitions for LKA system**

| Feature Parameter | Description |
|---|---|
| Quality (Left – Centre (2) Right) | 0 -1- 2 - 3 from low quality to high quality marking detection |
| Lane type (Left – Centre (2) Right) | Dashed, Solid, Undecided, Road edge, Double lane mark (including dashed on one side), Botts' dots, Invalid |
| Position Parameter C0 (Left – Centre (2) Right ABS) | physical distance between lane mark and camera on the lateral position. |
| Curvature Parameter C2 (Left – Centre (2) Right) | parameter C2 of polynomial to calculate curvature from this parameter. |
| Curvature Derivative Parameter C3 | parameter C3 of polynomial model to calculate curvature derivative from this parameter |
| Width Right\Left Marking (Left – Centre (2) Right) | Right\Left Lane marking width |
| LDW OFF (Left – Centre (2) Right) | Lane Departure Warnings are disabled (due to low speed or configuration). |
| Time Indicator | Day, Dusk, Night indicator |
| Speed | Speed (Km/h) |
| Headway | Headway Measurement |
| Wipers | Passage of wiper on the windshield |
| Right\Left signal | Right\Left turn signal is on |
| Failsafe | Bitwise signal, which indicates failsafe situation in this scene. (0,1 & 2) |
| Vision only Sign Type | Traffic Sign (speed sign) Numerical Values for each speed sign (km/h or mph). |
| Supplementary Signs Types | Rain, Snow, Trailer, Time, Arrow left\right, Bend arrow left\right, Truck, Distance arrow, Weight, Distance in, Tractor, Snow rain, School, Rain cloud, Fog, Hazardous material, Night. |

### *2.1.2 Road Geometry*

The geometric characteristics of the road, including curvature and radius, were extracted using a combination of OpenStreetMap (OSM) road centerline data and Autodesk Civil 3D software. The centerline geometry was first obtained from OSM and then imported into Civil 3D, where it was processed for geometric analysis.

The layout was generated by applying polygonal interpolation to the point-based axis extracted from the OSM centerline. This process allowed for the creation of a continuous alignment that accurately represents the road geometry. Civil 3D was then used to calculate key alignment parameters, including curvature, radius, and direction angle, which are critical for understanding road design and vehicle dynamics.

Table 12 summarizes the alignment parameters derived from this process. Each segment of the road is classified as either a straight line or a curve, and the corresponding geometric properties were calculated accordingly.

**Table 12 Alignment parameters**

| Feature Parameter | Description |
|---|---|
| Type | Line or Curve |
| Length | Length (m) |
| Direction Angle | Direction Angle (degree) |
| Radius | Radius (m) |
| Curvature | Curvature (1/m) |

### *2.1.3 Driver perception of lane marking quality*

In addition to sensor-based data, this study also uses information on the driver's perception of lane marking quality. This parameter provides insight into how well lane markings are perceived by a human driver under real-world conditions and allows for a comparison with machine-based detection performance, particularly that of the Mobileye system.

The driver assessment was performed during road surveys, where the ARAN vehicle operator rated the visibility and quality of the lane markings based on their visual perception. A Likert scale from 0 to 3 was used to record this perception, where:

0 = No visual detection
1 = Poor visual detection
2 = Moderate visual detection
3 = Very good visual detection

This subjective evaluation was captured in real time using a keyboard, where the driver manually entered the corresponding score for each road segment. These human perception scores were then used to assess the correlation between subjective human perception, objective sensor detection (Mobileye), and retroreflectivity measurements provided in the ANAS dataset. Retroreflectivity, as a physical and measurable property of the road markings, served as the main benchmark for quality comparison.

This dual approach combining human perception with sensor data and physical measurements enables a comprehensive understanding of how lane marking quality influences both human driving behaviour and ADAS system performance, particularly under varying environmental and lighting conditions.

## 2.2 Data fusion

ADAS data was collected and provided by Department of Civil Engineering and Architecture (DICAR) [140]. The ADAS outputs were collected via the Mobileye Standard CAN protocol and synchronized with ARAN data High-resolution GNSS RTK/IMU systems ensured precise georeferencing (Figure 7). Moreover, the geometric curvature parameters were derived from the OpenStreetMap road centerline using CIVIL 3D (Figure 8 a & b). ANAS data were imported to open street map and buffers created for ANAS points (Figure 9). Since all the data were accurately geo-localized, various spatial data fusion techniques in GIS including

intersection and aggregation (QGIS, Ver 3.28.0) were employed to merge ADAS, MAP, and ANAS datasets [141], [142]. Figure 10 illustrates the ANAS database buffer and Mobileye parameters in QGIS OpenStreetMap during the data fusion stage.

**Figure 7 Mobileye survey for right and left lane**

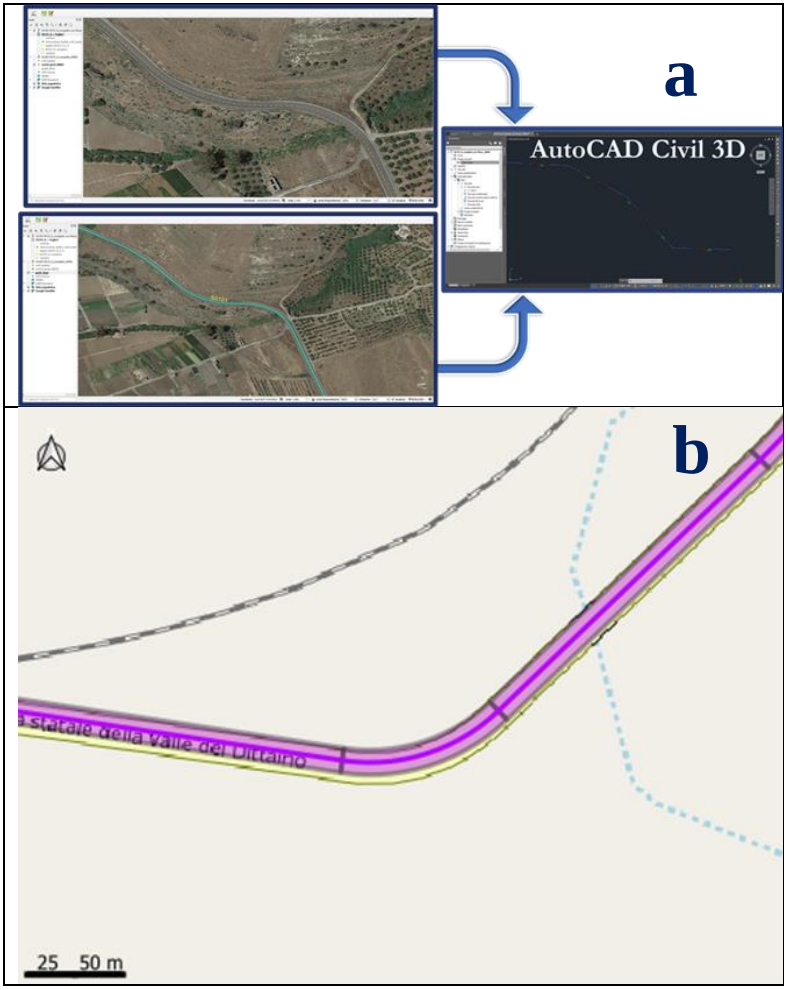


**Figure 8 a) Geometric parameters extraction in GIS environment and geometric curvature from Civil 3D, b) Road Track construction**

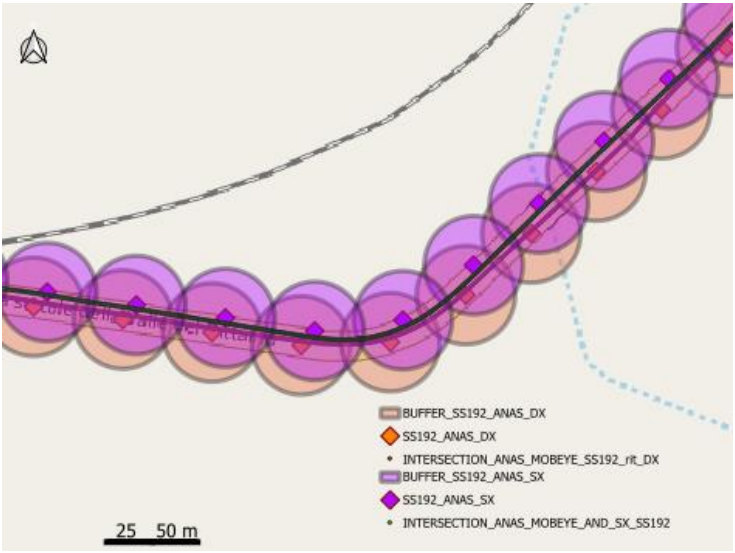


**Figure 9 ANAS points and buffering**

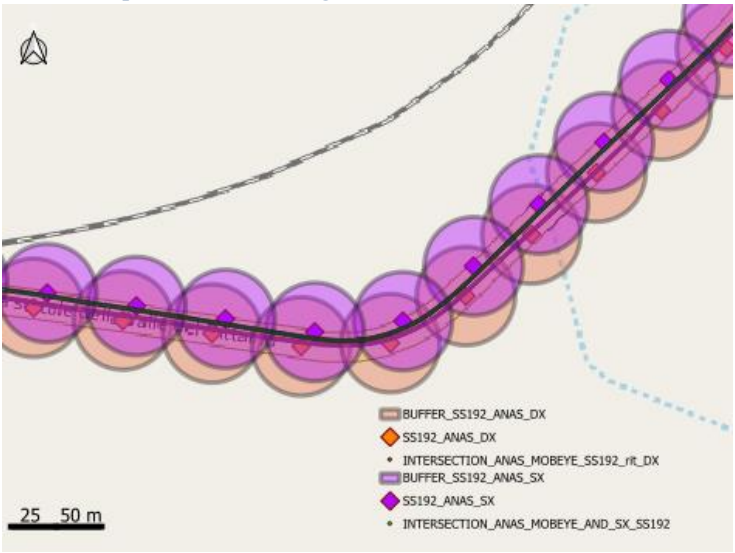


**Figure 10 Intersection and aggregation of ANAS buffers, Mobileye data and geometry for right and left lane**

1194 kilometers of running data were collected under various weather and light conditions, creating a robust dataset to evaluate the ODD of the LSS (Table 13). This dataset is essential for investigating correlations among road features (e.g., lane marking quality, cross-section width, horizontal alignment, section type), driving conditions (speed, vehicle headway), and environmental conditions (day, night, wet, rain, glare, lighting) with the LSS detection capability.

**Table 13 Surveyed Road Sections under different environmental conditions**

| Road Section | Light Condition | Weather Condition | Length (km) |
|---|---|---|---|
| SS121 | Day | Dry | 26 |
| SS121 | Night | Dry | 26 |
| SS121 | Day | Wet/Rain | 26 |
| SS121 | Night | Wet/Rain | 26 |
| SS284 | Day | Dry | 50 |
| SS284 | Night | Dry | 50 |
| SS284 | Day | Wet/Rain | 50 |
| SS284 | Night | Wet/Rain | 50 |
| RA15-A01-SS114 | Day | Dry | 120 |
| RA15-A01-SS114 | Night | Dry | 140 |
| RA15-A01-SS114 | Day | Rain | 70 |
| RA15-A01-SS114 | Night | Rain | 70 |
| SS192 | Day | Dry | 50 |
| SS192 | Night | Dry | 50 |
| SS192 | Day | Rain/Wet | 100 |
| SS192 | Night | Rain | 50 |
| SS194 | Day | Dry | 45 |
| SS194 | Night | Dry | 45 |
| SS194 | Day | Rain/Wet | 45 |
| SS194 | Night | Rain | 45 |
| SS514 | Day | Dry | 40 |
| SS514 | Night | Dry | 40 |
| SS514 | Day | Wet/Rain | 40 |
| SS514 | Night | Wet/Rain | 40 |

## 2.3 Aggregation Datasets

As ANAS and Mobileye data are collected with different frequencies and intervals, aggregation procedures were applied on datasets to synchronize both with the same sample size (Figure 10). Then these datasets were merged and created a unique dataset for further analysis. A step after this is to label data based on ground truth. All datasets were imported to open street Qgis environment and intersections and some especial road geometry condition that are effective on lane marking and its detection by our vision-base system were labelled to filter and analyze the possible noise in the data. Figure 11 shows this procedure for data labelling based on road geometry.

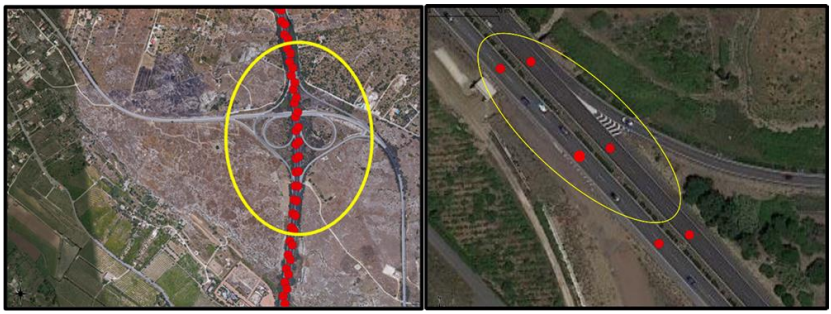

**Figure 11 Data labeling based on road geometry**

With this dataset we have curvature and lane marking information on the map, Figure 12 shows right and left turn actual geometric curvatures and the effect of this geometric feature on detected curvature parameters by Mobileye. Based on the direction of travel, positive curvature values indicate a right-hand side curve and vice versa. In this figure the quality scores are shown based on a color scale where the dark green is the highest quality and red is the lowest score by Mobileye system. Also, this detected curvature parameter by Mobileye can be evaluated by curvature parameter from road

geometry (Figure 13).

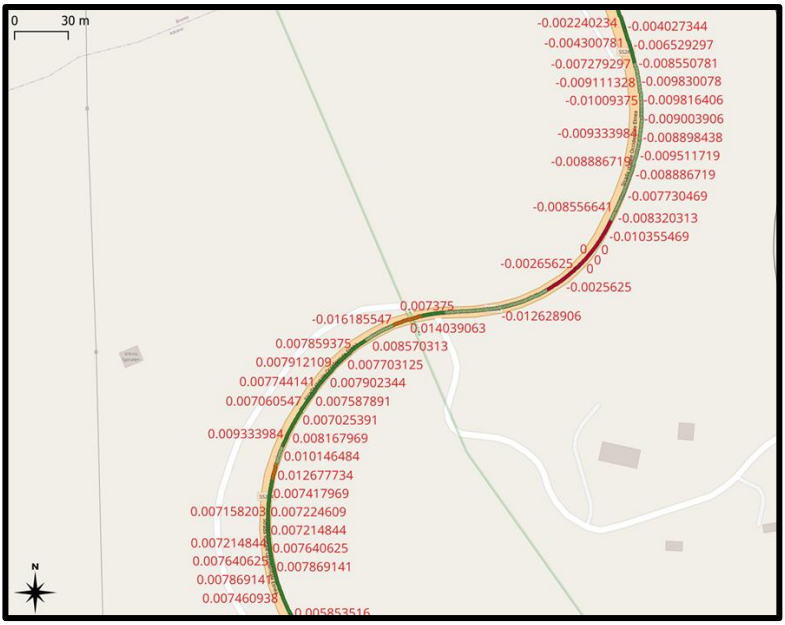


**Figure 12 The effect of Right (+) and left (-) curvature on curvature parameter & quality scores (dark green is highest and red for lowest quality) by Mobileye.**

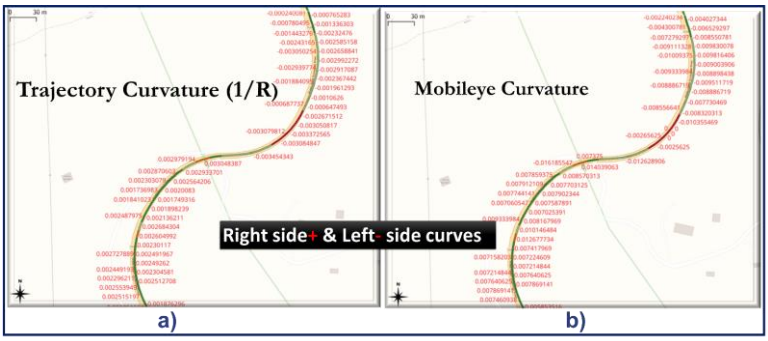


**Figure 13 Curvature parameter on open street map (QGis); a) Trajectory**

**Curvature (1/R), b) Mobileye Curvature**

## *2.4 Data stratification*

The aggregated dataset is for all conditions so for a more in-depth analysis several methods of data stratification need to be used to check the evaluation in different circumstances. For example, lane departure warning off (LDWoff) was recorded by Mobileye. The system turns LDW off based on special conditions like low vehicle speed. by filtering dataset based on this parameter and analysis a better perspective of operational design domain (ODD) will be achievable. Another important factor in detection of lane markings is width parameter that was recorded by LKA system, The dataset consisted of different road type with it regulation of lane marking and also in special cases for some part of the road we have special lane marking that may affect the detection of feature parameters by this vision-base system so possible errors can be avoided by classifying data according to width of lane marking. Another factor that effects on operation of all Mobileye systems is vehicle speed, some systems turn off or on based on speed and in very high speeds the detection for lane markings features is harder. By filtration based on speed, the thresholds for different systems and faults in detection will be measurable. Figure 14 shows this data stratification based on these three factors.

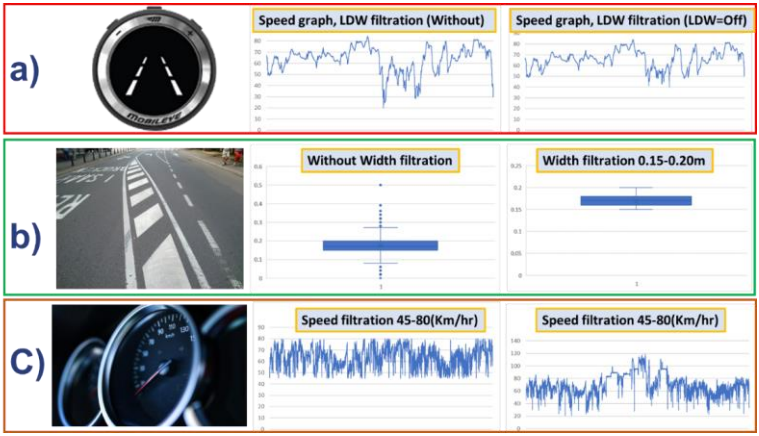


**Figure 14 Data stratification; a) LDWoff base; b) Lane marking width base; c) Speed base**

## 2.5 Data Cleaning

We excluded data marked by the Mobileye system as Failsafe due to blurred photos and glare, and omitted data with lane change signals, accounting for 6.43% of the total. After data fusion and cleaning, we created a comprehensive dataset encompassing the three main fields of the ODD's taxonomy: the physical infrastructure attributes of road geometry (horizontal alignment, cross-section width, intersection), lane marking quality (RL), the dynamic driving conditions (speed, headway), and the environmental factors (day/night, weather). The outcome variable is the lane detection quality rate, classified by Mobileye as Low (1), Medium (2), or High (3).

Table 14 provides summary statistics for the dataset, which includes 9,520 sections covering a total of 476 km. Pearson correlation analysis revealed correlations between the statistical parameters in the 50 m section of retroreflectivity (RL), Headway and Curvature. A correlation exists also between lane and shoulder width and speed and

lane width (Figure 15).

**Table 14 Summary statistic parameters**

| Numerical | | | | | | | | | | | |
|---|---|---|---|---|---|---|---|---|---|---|---|
| | RL Mean | RL Min | RL Max | Mean speed | Headway Max | Headway Min | Headway Mean | Curvature Min | Curvature Max | Lane | Shoulder |
| Count | 9520 | 9520 | 9520 | 9520 | 9520 | 9520 | 9520 | 9520 | 9520 | 9520 | 9520 |
| Average | 192.843 | 106.033 | 205.389 | 67.2329 | 3.33696 | 3.29036 | 3.31593 | 0.00076161753 | 0.00173191 | 3.46525 | 0.520609 |
| Standard Deviation | 96.1916 | 67.1364 | 101.331 | 12.8105 | 0.551012 | 0.626678 | 0.578179 | 0.00217547 | 0.00333271 | 0.224647 | 0.377686 |
| Coeff. of Variation | 49.8807% | 63.3166% | 49.3364% | 19.0538% | 16.5124% | 19.0459% | 17.4364% | 285.625% | 192.429% | 6.48286% | 72.5469% |
| Minimum | 42.0 | 40.0 | 42.0 | 3.76 | 0.6 | 0.1 | 0.56 | 1.E-10 | 1.E-10 | 3.15 | 0.1 |
| Maximum | 614.0 | 423.0 | 786.0 | 99.7 | 3.5 | 3.5 | 3.5 | 0.033624 | 0.063451 | 3.9 | 1.6 |

| Categorical | | | |
|---|---|---|---|
| Light | 1= Day (66.78%) | 0= Night (33.22%) | |
| Weather | 1= Dry (49.12%) | 2= Rain (34.97%) | 3= Wet (15.91%) |
| Section Type | Bridge (1.3%) Tunnel (0.1%) | Junction (4.1%) | Other (94.5%) |

| Lane Marking Quality (Categorical) | | | |
|---|---|---|---|
| Class | Class 1 | Class 2 | Class 3 |
| Qmax | 7.46% | 14.66% | 77.68% |
| Qmin | 22.61% | 16.57% | 60.82% |
| Qmode | 12.99% | 16.84% | 70.16% |

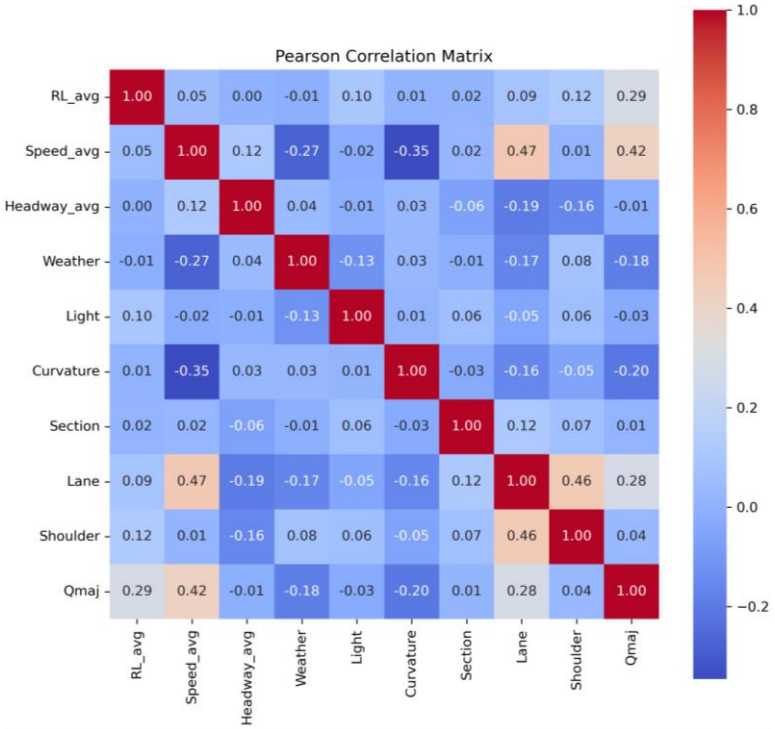


**Figure 15 Pearson Correlation of Features**

As previously mentioned, the LSS classifies lane marking detection with three scores: Low (1), Medium (2), and High (3). Figure 16 clearly indicates that for class 1, there is the highest probability of LSS failure to detect lane markings, which is close to 100% when Qmax or Qmode are in class 1.

.

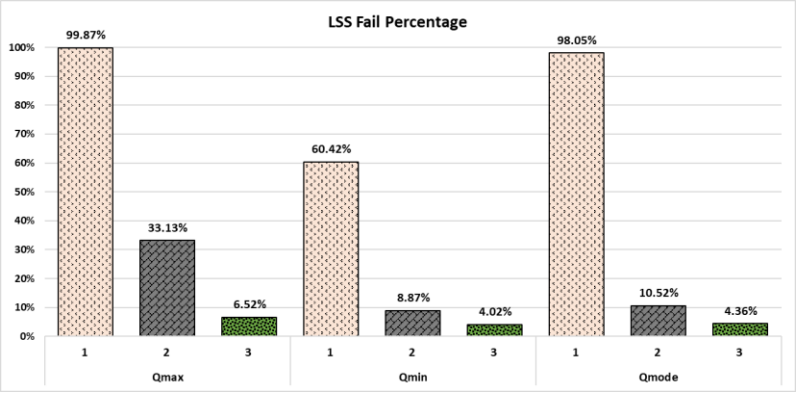


**Figure 16 Percentages of LSS fail for different marking detection scores**

## 2.6 Project 1: Lane marking quality assessment

This section presents the methodological approach for assessing lane marking quality as detected by the Mobileye Lane Support System (LSS) and evaluating the corresponding Operational Design Domain (ODD). The goal is to determine under what physical, geometric, and environmental conditions the LSS operates reliably and where its detection capabilities degrade. Feature selection, dataset balancing using SMOTE, and the application of various classification models including ordinal statistical, machine learning, and deep learning approaches are detailed in this section. The results are used to derive interpretability insights and infrastructure recommendations aimed at enhancing LSS robustness under real-world scenarios.

### 2.6.1 Features selection

Data summaries reveal a broad distribution of values with high coefficients of variation and notable correlations among RL, headway, and curvature statistics within the 50 m road sections, necessitating a

preliminary features' selection. Initially, feature importance analysis identified key parameters for the model. These parameters will be further used in advanced machine learning and deep learning models for classification and prediction of quality classes.

To analyze the impact of each feature on lane marking quality detection by LSS, various machine learning algorithms were evaluated, including Voting classifiers which combines Random Forest (RF) and Support Vector Machines (SVM), Gradient Boosting Machines (GBM), and CatBoost. These algorithms consistently ranked feature relevance similarly. Ultimately, CatBoost was chosen for its reliable performance, superior accuracy, and ability to handle categorical data effectively.

CatBoost is a gradient boosting algorithm designed for decision trees, capable of efficiently handling both numerical and categorical features without extensive preprocessing. It uses a permutation-driven process to minimize data leakage and reduce overfitting, thereby enhancing model performance [143], [144]. CatBoost employs binary decision trees as base predictors and iteratively minimizes expected loss, making it suitable for both classification and regression tasks. By applying the same split criteria across an entire level, it prevents overfitting and speeds up computation[145], [146], [147]. In summary, CatBoost's ability to handle both numerical and categorical features, its novel permutation techniques, and robust performance make it a powerful tool for the fast and easy interpretation of feature scores by implementing a recursive feature elimination algorithm. Based on CatBoost results (Figure 17), we selected the nine variables from Table 14, which account for the highest feature importance in the model.

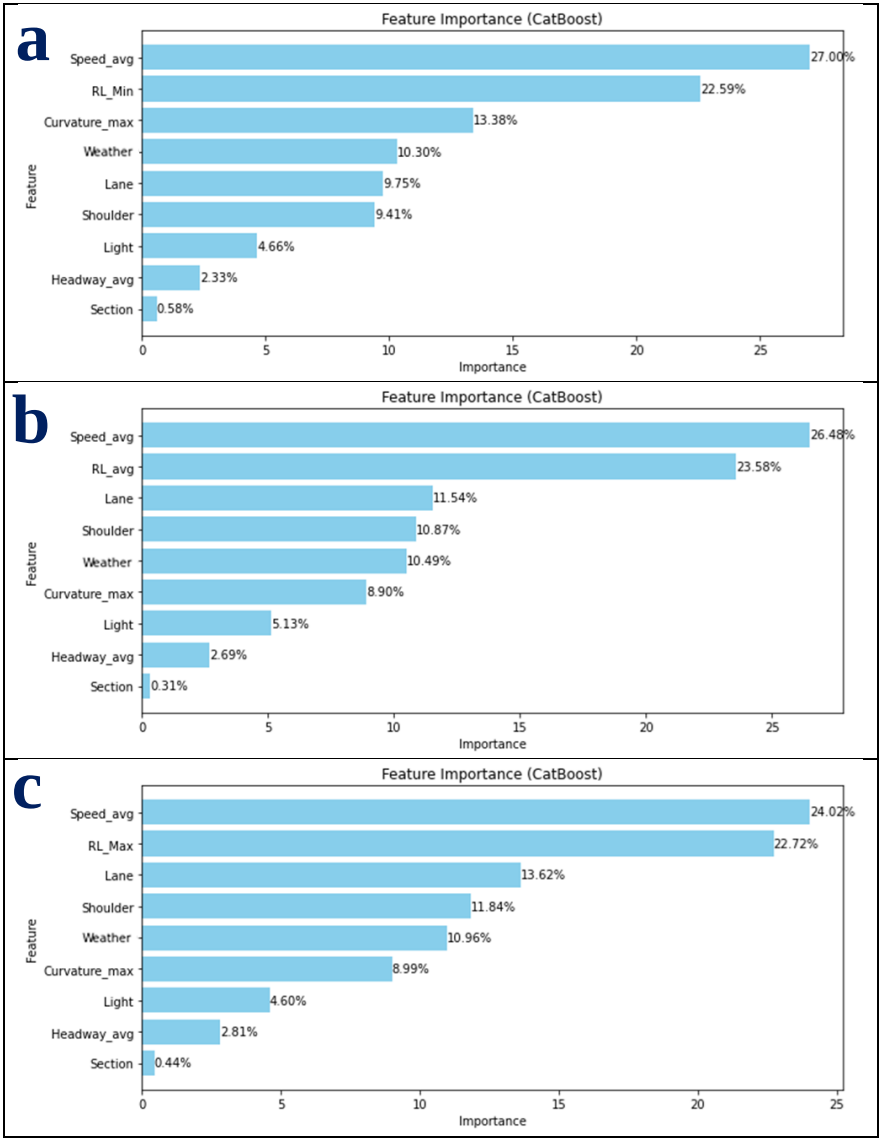


**Figure 17 Catboost Feature Importance Analysis for different outcomes: a) Qmin, b) Qmode, c) Qmax**

### *2.6.2 Database Balancing*

After the selection of the most relevant features as inputs and outcome, to create a robust model for the predictive classification of lane marking quality scores, we defined an articulated modelling approach based on following steps:

- Data balancing (SMOTE)
- Identification of most appropriate model form (Ordinal)
- Identification of alternative modelling algorithms (GLM, ML, DL)
- Validation of the best model (LightGBM)
- Analysis of features relevance and interactions (SHAP)

#### *2.6.2.1 Synthetic Minority Over-sampling Technique (SMOTE)*

Table 14 shows the frequency of the three quality classes of lane marking detection in the data sample, highlighting that class 1 (12.99%) and class 2 (16.84%) are underrepresented compared to class 3 (70.16%) that is predominant, resulting in an unbalanced dataset. To prevent the model from being biased towards the most frequent class and to ensure accurate classification of the critical class 1, we employed different techniques like as weighting and balancing and choose the Synthetic Minority Over-sampling Technique (SMOTE) due to good performance.

SMOTE generates synthetic samples of the minority classes to balance the class distribution, enhancing the model's performance across these less-represented classes without compromising the natural distribution of data. The procedure involves: **1.** Identify minority class instances. **2.** Select a minority class instance. **3.** Find the k-nearest neighbours of the selected minority class instance using Euclidean distance. **4.** Randomly select a neighbour. 5. Generate a synthetic sample by choosing a random point along the line segment joining the selected minority class instance and its randomly chosen

neighbour. This procedure is repeated until the desired number of samples is reached.

Instead of equalizing the class distributions, which could distort real-world proportions and potentially introduce bias, we opted for a more nuanced strategy: adjusting the samples of classes 1 and 2 to be half of class 3's size. This rate for SMOTE was selected to generate synthetic samples amounting to 50% of the major class (Class 3) for the minority classes so the class 3 remained majority class with a high quantity difference than two other classes that is a realistic choice (Figure 18).

This custom resampling strategy aims to increase the statistical power of minority classes by enhancing the model's learning capabilities and generalizing across such underrepresented classes without entirely overwriting the data's original structure. Therefore, with enhanced classes 1 and 2, it is expected that the model will have better sensitivity for these classes, hence leading to much more balanced performance under different class conditions, a very important factor in those applications where the detection of less frequent classes is just as crucial as the more common ones. The imbalance in the dataset is handled in a very methodologically sound manner, which gives the study good reliability and validity of the outputs; hence, the robustness of the analytical framework amid challenges that class-skewed data distributions present.

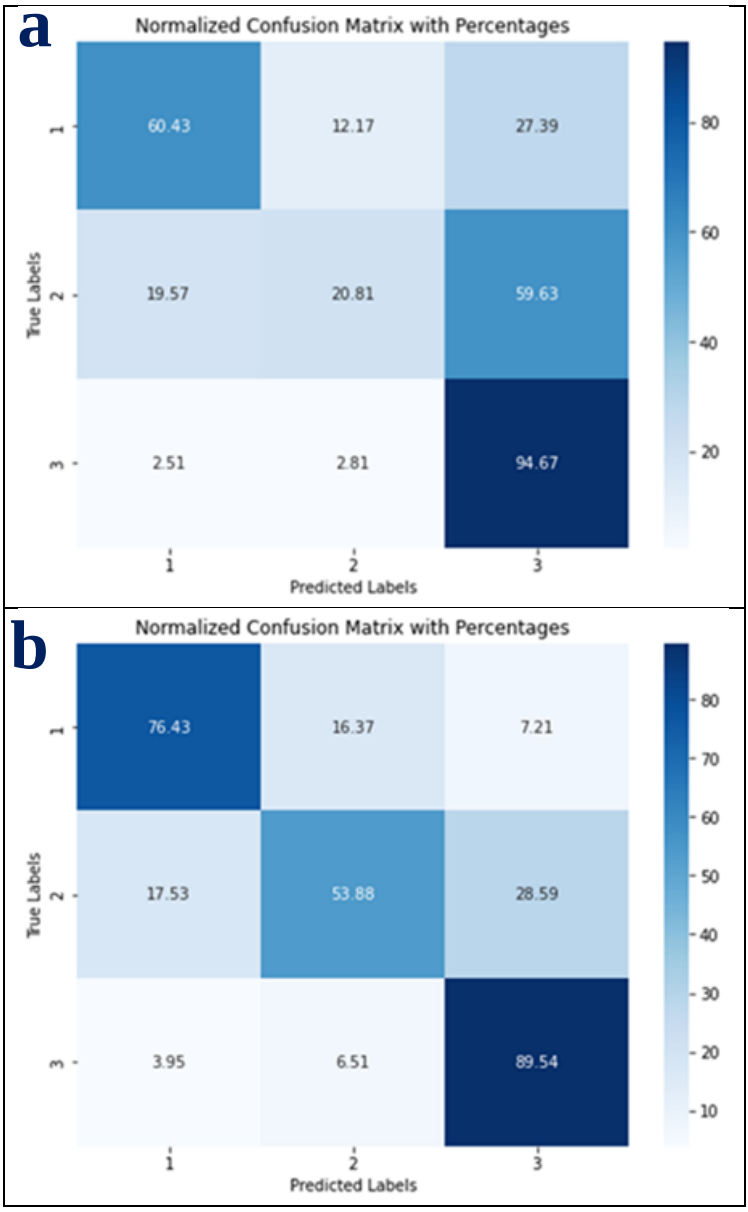
a
Normalized Confusion Matrix with Percentages
60.43
12.17
27.39
19.57
20.81
59.63
2.51
2.81
94.67
True Labels
Predicted Labels
b
Normalized Confusion Matrix with Percentages
76.43
16.37
7.21
17.53
53.88
28.59
3.95
6.51
89.54
True Labels
Predicted Labels

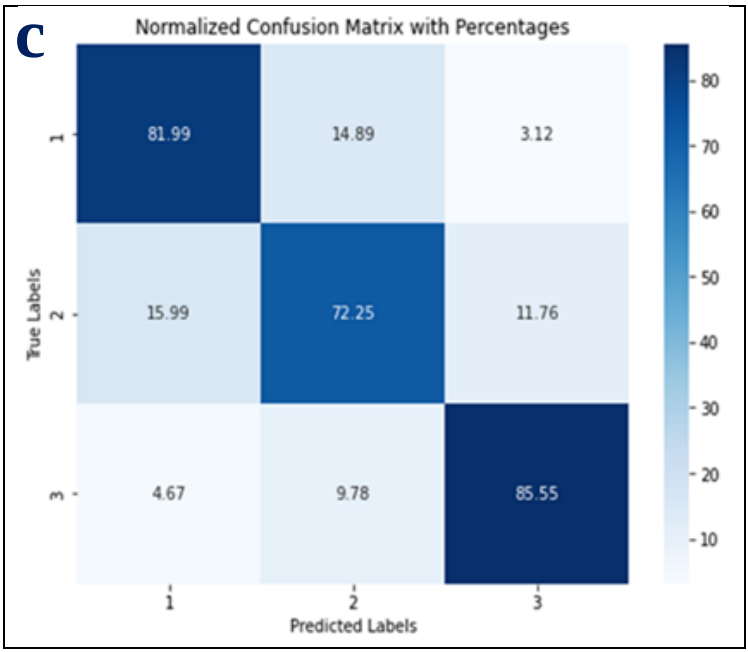


**Figure 18 Resampling Strategy, a) Normalized confusion matrix before resampling. b) Normalized confusion matrix after resampling with 50% SMOTE. c) Normalized confusion matrix after resampling with 100% SMOTE.**

### *2.6.3 Model Selection*

As we discussed previously, the lane marking quality is categorized into three classes: class 1 (lowest quality), class 2 (medium quality), and class 3 (highest quality). These classes are ordinal, meaning they have a meaningful order but no precise numerical difference between them. Thus, using ordinal classification methods is more suitable than standard classification techniques. General models like Random Forest or Logistic Regression treat each class independently, ignoring the inherent order, which can lead to overfitting as they fail to leverage the ordinal relationships, resulting

in poorer generalization to unseen data.

In contrast, ordinal classification methods like Ordinal Logistic Regression (Proportional Odds Model) and Ordinal Random Forest (ORF), along with other ordinal techniques, utilize the natural order present in the data to improve predictive accuracy. In conclusion, ordinal methods perform better because they consider the target variable's natural order during the modelling process. This strategy helps to minimize overfitting, boosts generalization, and increases accuracy, making these methods especially useful for classification tasks that involve ordered categories. This study explores different methods, including statistical models, machine learning (ML), and deep learning (DL) techniques, to handle the challenges regarding the ordinal and imbalanced nature of the dataset. Each method was selected to balance interpretability and predictive power, to reach an optimized model with less sensitivity to these two problems. By comprehensively analyzing the performance of lane support systems (LSS) in identifying lane markings using accuracy and F-score metrics, this study benchmarks statistical regression models while exploring the potential of ML and DL classifiers. The following sections are details of these models' analysis, reflecting a comprehensive research strategy aimed at enhancing understanding and performance in ordinal classification tasks.

### *2.6.4 Statistical Classification Models*

Statistical models are grounded in statistical theory and are typically used for inference or prediction, relying on assumptions about the data's distribution. These models are highly interpretable and can provide insights into the relationships between variables.

#### 2.6.4.1 Ordinal Logistic Regression (Proportional Odds Model)

The benchmark method selected for this study was the cumulative standard Ordinal Logistic Regression. This well-known linear regression technique models the relationship between an ordinal dependent variable and one or more independent variables. It assumes proportional odds ratios between all pairs of outcome categories, estimating a single set of coefficients for the log odds. This model is suitable when the response variable is ordinal, and the proportional odds assumption is valid [148].

#### 2.6.4.2 Ordinal Gaussian Process Regression

In statistical literature, most approaches are based on generalized linear models. Ordinal Gaussian Process Regression extends Gaussian process regression to ordinal data, offering a non-parametric, flexible method to model underlying relationships within a probabilistic framework. This approach effectively handles complex, non-linear relationships, providing better accuracy and interpretability than traditional linear models [149], [150].

Statistical models provide the idea of interpretable baselines for classification problems and conceptually explain the relationships among variables. However, their dependence on assumptions about linearity and proportional odds often constrains performance in response to complicated nonlinear relationships or high-dimensional data, requiring more flexible methods. Therefore, machine learning models are reassuring for the future of the field due to their adaptability in handling such challenges.

### 2.6.5 Machine Learning Models

Linear regression is widely used for modelling and analysis.

However, most of the time, it does not work very well on data with highly nonlinear relationships, high-dimensional datasets, and noisy data. The issues can be handled by machine learning methods, deep learning models in particular, but they require a large number of labelled data. When data is limited, ensemble methods can be more effective by leveraging multiple models trained on different data subsets. In the machine learning field, ordinal regression models have been developed by extending classification algorithms to utilize multiple binary classification tasks. In this study, two deep-learning models and two ensemble models were selected for ordinal classification.

#### *2.6.5.1 Ordinal Random Forest tuned by Genetic Algorithm*

In the area of parallel ensemble machine learning, Ordinal Random Forest extends the traditional random forest algorithm to handle ordinal target variables adjusting the impurity measure to better reflect the target variable's order, improving both accuracy and interpretability [151], [152]. This method modifies the splitting criteria in decision trees to respect the ordinal nature of the target variable, thereby enhancing predictive performance and interpretability compared to treating the ordinal variable as either continuous or nominal [153], [154]. This ORF model was further optimized using a genetic algorithm for hyperparameter tuning in the R environment.

#### *2.6.5.2 Automated Machine Learning-Light Gradient Boosting Machine (AutoML-LGBM)*

LightGBM, or Light Gradient Boosting Machine, is a highly efficient gradient boosting ensemble model developed by Microsoft. It is designed for speed and performance, especially with large

datasets. LightGBM offers several advantages over traditional gradient boosting methods due to its efficiency, accuracy, scalability, and advanced features. Unlike other boosting algorithms, it uses a leaf-wise strategy for tree growth rather than the traditional depth-wise approach, making it effective for both regression and classification tasks [155].

LightGBM settings were optimized using TPOT (Tree-based Pipeline Optimization Tool) through a custom configuration dictionary specifying ranges for hyperparameters such as the number of leaves, tree depth, learning rate, number of boosting rounds, minimum child samples, subsample fraction, fraction of features used to build each tree, regularization terms (alpha and lambda), and minimum gain required to make a split. Genetic programming within TPOT evolves machine learning pipelines by starting with a population of random pipelines and iteratively selecting, mutating, and recombining them based on performance. This evolutionary process is guided by a fitness function, in this case, model accuracy. TPOT runs multiple generations of LightGBM models with these hyperparameters, evolving and selecting the best configurations based on the fitness function [156].

#### *2.6.5.3 Catboost*

As discussed in the "Feature Selection" section, we chose the CatBoost classifier over other methods due to its strong performance in handling categorical data and its robustness across varied data distributions. After applying SMOTE to balance the dataset, we optimized CatBoost's hyperparameters using TPOT (Tree-based Pipeline Optimization Tool). TPOT uses a genetic algorithm to streamline the selection and setup of the best machine learning pipeline. It emphasizes fine-tuning hyperparameters like the number

of iterations, learning rates, tree depths, and border counts. It also uses L2 regularization to penalize large coefficients; thus, avoiding overfitting and giving preference to simpler models, which may generalize well to a wider array of data sets. The resultant technique explores not only the ordinal nature of target classes but also boosts up the predictive accuracy and robustness of several operational scenarios.

Machine learning models effectively address the limitations of statistical approaches through their flexibility, ensemble techniques, and ability to handle complex, nonlinear relationships between features. These models are particularly suitable for this research datasets, which exhibit complex interdependencies but lack the scale typically required for deep-learning methods. Machine learning techniques can achieve strong performance with computational efficiency by optimizing hyperparameters and leveraging ensemble techniques. Although deep learning models offer additional flexibility, their dependency on large datasets poses challenges in this subject, as described in the next section.

### *2.6.6 Deep Learning Models*

Deep learning models are a subset of machine learning models that use multi-layer neural networks. These models are known for their high level of complexity that can model extremely nonlinear patterns.

#### *2.6.6.1 Fully Connected Neural Network (FCNN)*

In this study, a Fully Connected Neural Network (FCNN) was employed as a deep learning method to predict lane marking quality. FCNNs, where each neuron in one layer is connected to every neuron in the subsequent layer, are a quintessential example of deep learning models due to their layered architecture and the complex

transformations they apply to input data. Deep learning methods, such as FCNNs, are characterized by their ability to automatically learn and extract features from raw data through multiple layers of abstraction, which enables them to model complex, non-linear relationships within the data [157], [158].

FCNNs utilize specialized loss functions in ordinal classification, including ordinal cross-entropy, which penalizes misclassifications regarding the ordinal nature of the data. The architecture consists of several neuronal layers, each followed by batch normalization and dropout to avoid overfitting, thus ensuring good generalization. Efficient Adam optimization was used in combination with the categorical cross-entropy loss. Other hyperparameters, like the number of units, dropout rate, and learning rate, were optimized by a genetic algorithm. In that evolutionary approach, model configurations are selected, and mutation and recombination aim to enhance their performances toward better efficiency. This has shown the capability of FCNN in handling high-dimensional complex data for classification problems.

#### *2.6.6.2 Ordinal MLP Network (OMLP-N)*

A Multi-Layer Perceptron (MLP) is a sophisticated type of Feedforward Neural Network (FFNN), consisting of multiple layers of nodes arranged in a directed graph [159]. This architecture allows the MLP to model information flow from the input layer, through one or more hidden layers, to the output layer without cycles or feedback loops. Each neuron in these layers applies a nonlinear activation function, such as sigmoid or ReLU, enhancing the network's nonlinear capability to learn complex patterns and relationships in data. MLPs are trained using the backpropagation algorithm, which efficiently computes the gradients for every neuron to minimize the error in

output by iteratively adjusting the weights. This makes MLPs very powerful for a wide range of applications, including classification, regression, and even feature learning in unsupervised settings. The flexibility in adapting the network architecture by modifying the number of hidden layers and neurons enables MLPs to be designed for specific complexities of data. However, the same flexibility results in a difficult tuning of hyperparameters since the learning rate, number of epochs, and configuration of the layer have to be optimally chosen in order to avoid the problems of underfitting and overfitting, especially with diverse and large datasets. The general applicability and robust performance of MLPs in broad areas of artificial intelligence and machine learning are thus underpinned by the ability of MLPs to approximate any continuous function, notwithstanding the very challenges.

In our study, we employed a Multilayer Perceptron (MLP) classifier. The MLP model was integrated within a machine learning pipeline that included preprocessing steps such as feature scaling with StandardScaler, crucial for neural network effectiveness. We used the SMOTE technique to balance the dataset by generating synthetic samples, ensuring that our model was trained on a representative distribution of classes. The MLP architecture was configured with 100 hidden neurons, using the ReLU activation function and the Adam solver, with an emphasis on regularization through an L2 penalty to prevent overfitting.

Deep learning methods adapt loss functions like ordinal cross-entropy to penalize misclassifications in a way that respects ordinal relationships. Deep learning models extend the capabilities of machine learning by leveraging multi-layered architectures to automatically extract features and handle highly complex, nonlinear data relationships. However, their effectiveness is often dependent on the availability of large-scale datasets. The following chapter evaluates

the performance of all selected models to identify the most effective approach for ordinal classification of lane marking quality.

## 2.7 Project 2: Monitoring Lane Marking Retroreflectivity Using ADAS Sensor Data

This section introduces the methodology developed to monitor lane marking retroreflectivity (RL) using Mobileye sensor outputs in conjunction with certified photometric measurements from the ANAS vehicle. The focus is on deriving RL estimations based on ADAS marking quality assessment contextual with geometric and environmental features, aiming to create a cost-effective alternative to conventional RL surveys. Following exploratory correlation and feature importance analyses, both regression and classification modelling techniques are applied. The study further explores how lighting and road curvature influence the predictive performance under different thresholding and filtering strategies.

### 2.7.1 Data Preparation and Dataset Derivation

Data were compiled from Mobileye sensor outputs and ANAS RL measurements. Three datasets were derived from the spatial buffering of road segments:

- **RL Average (RLavg):** The mean RL within the 50 m section.
- **RL Minimum (RLmin):** The lowest RL value within the 50 m section, emphasizing worst-case conditions.
- **RL3:** RLavg minus 3 standard deviations (i.e. 99.7%) to get minimum values of RL excluding outliers.

### 2.7.2 Exploratory Analysis

Segments with rain condition were removed due to noise on system detection. Before diving into the modelling, exploratory analyses were performed to understand the relationships among features and to identify the most influential predictors (Table 25 to Table 30 of appendix).

#### *2.7.2.1 Correlation Analysis*

A correlation heatmap was generated to examine the pairwise linear relationships among the explanatory features such as Marking quality (Qmaj), speed, lane width, shoulder width, curvature, headway (Figure 19). Key findings include:

- **Speed** showed the highest correlations with **lane width** and **curvature**.
- **RLavg outcome showed the best correlation with Qmaj**.

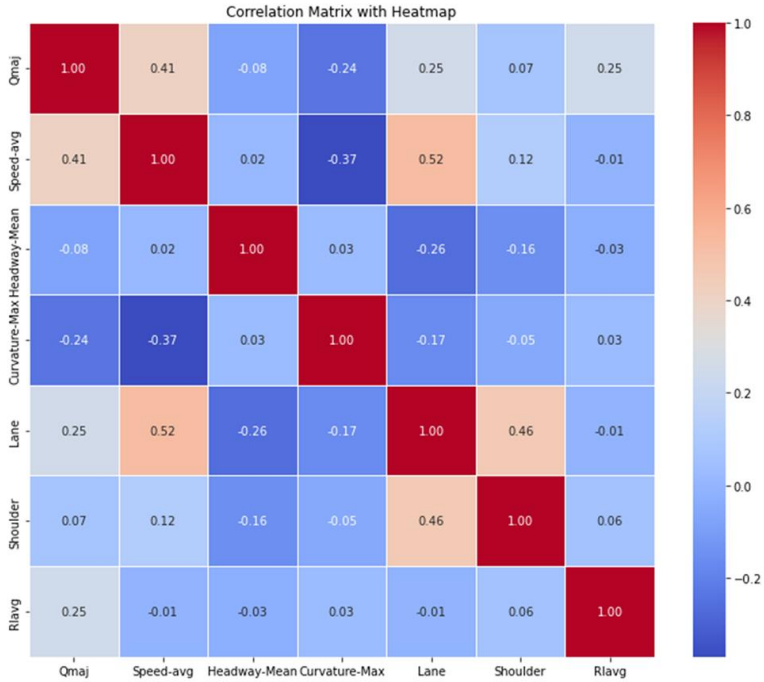


**Figure 19 Correlation heatmap**

### *2.7.2.2 Network Graph Analysis*

A network graph was constructed using a correlation threshold (e.g., r > 0.3) to capture more complex, multi-variable relationships. In the network graph (Figure 20), speed emerged as a key "hub" node, with edges to lane width, shoulder width, and curvature. Lane detection quality formed links to curvature and speed as well. This visualization reinforced our earlier conclusion that speed affects multiple geometric parameters simultaneously, which is directly correlated to, though its importance as explanatory variable might depend on the other correlated factors (i.e. lane width, shoulder width and curvature).

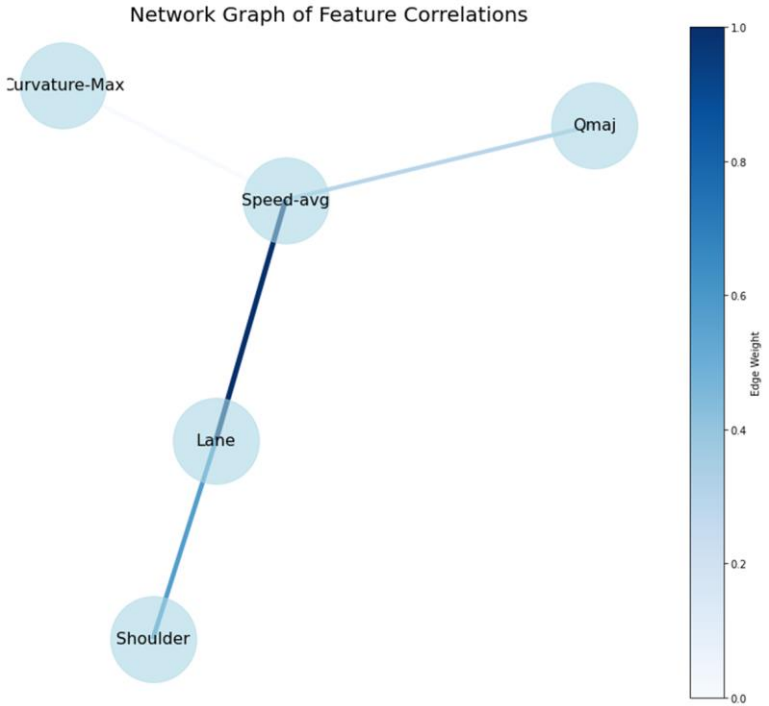


**Figure 20 Network graph (TR=0.3)**

### *2.7.2.3 Feature Importance Analysis*

An XGBoost model was applied to the full (non-rainy) dataset to compute feature importance scores (Figure 21). The analysis revealed that:

- **Shoulder width** is the most influential variable.
- **Lane detection quality** and **lane width** also rank highly.
- **Speed**, **curvature**, and **headway** have secondary contributions.

These findings confirmed that geometric attributes and quality score have meaningful roles in RL assessment. The pavement edge,

and the camera's own perception of lane clarity are critical for estimating marking retroreflectivity. In particular, shoulder width may play a large role because it influences how the marking stands out from the pavement boundary, potentially affecting the camera's view of marking brightness and contrast. Meanwhile, the system's own lane detection quality class can signal whether the marking is generally well-defined or fading.

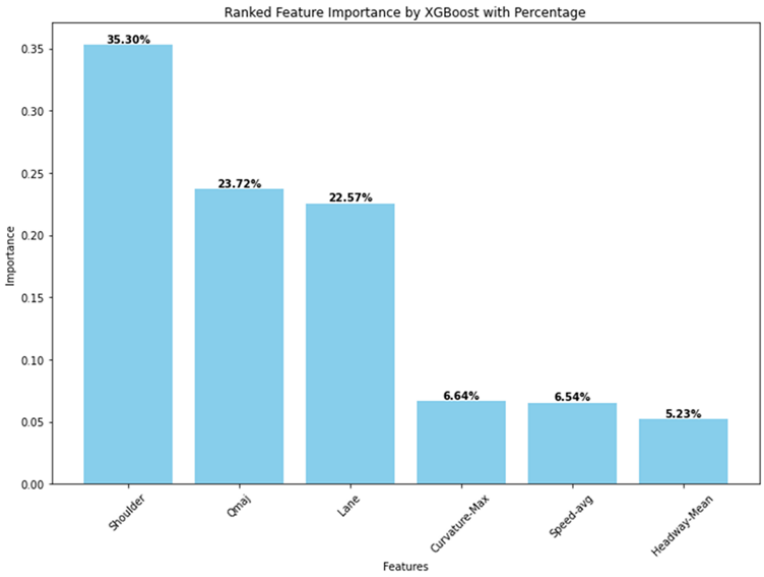


**Figure 21 XGBoost feature importance analysis for general dataset (Removed rain)**

### *2.7.2.4 Feature Importance under Day and Night Conditions*

To delve deeper, we repeated the feature importance analysis separately for daytime and nighttime data (Figure 22a & b). During daytime, the top three factors were lane width, lane detection quality, and shoulder width, followed by speed, curvature, and headway. In

contrast, at night, shoulder width and lane width switched places in importance, with quality ranking third. Speed dropped to last in the nighttime subset, implying that while velocity matters in daylight (possibly due to motion blur or changing camera angles), reduced visibility at night may overshadow any speed-related effects. These differences highlight that lighting conditions alter how certain features drive RL prediction, likely because low ambient light places greater emphasis on road-edge definition (i.e., shoulder and lane boundaries).

It is worthily to mention that the marking quality is more relevant in daytime conditions.

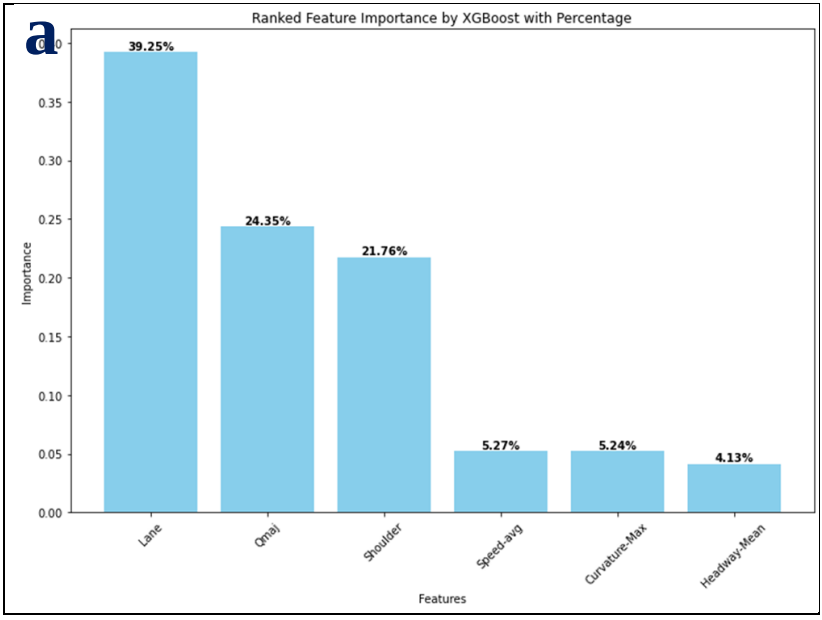

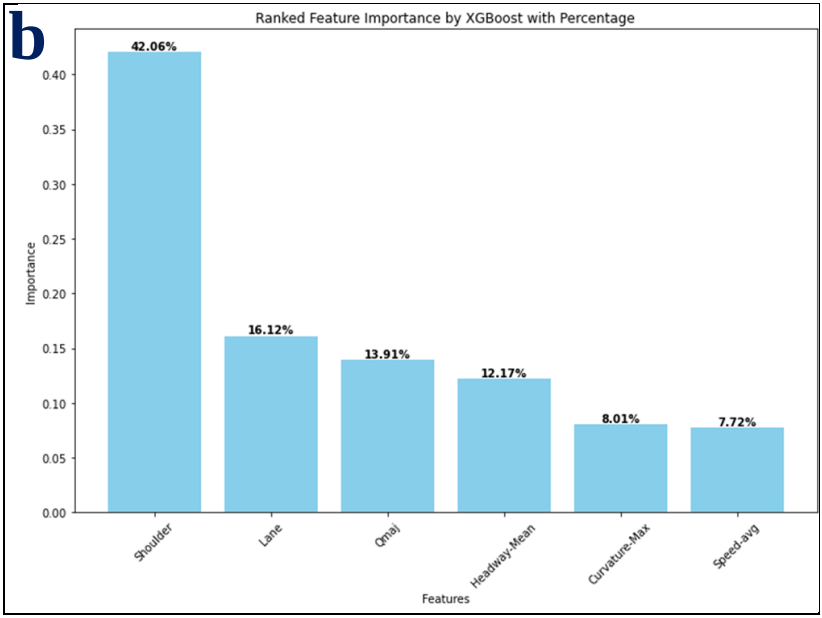


**Figure 22 XGBoost feature importance. a) Daytime. b) Nighttime**

### *2.7.3 Regression Modelling*

Regression models were first applied using different modelling and among them Random Forest, XGBoost, and LightGBM were selected based on their performance and stable results. Feature importance analysis indicated that geometric characteristics such as shoulder width, lane marking quality, and lane width play a dominant role in RL estimation. Environmental segmentation (day versus night) revealed that sensor performance is enhanced under natural lighting.

### *2.7.4 Classification Modelling*

Due to the challenges of continuous RL prediction that returned R2 values lower than 0.48 a classification framework was adopted:

**RL Thresholding:** RL was categorized into three classes (poor, acceptable, and excellent) using two threshold schemes:

- **Threshold A:** Class 1 (C1) Poor (RL < 80), Class 2 (C2) Acceptable ($80 \leq RL \leq 150$), Class 3 (C3) Excellent (RL > 150)
- **Threshold B:** Class 1 (C1) Poor (RL < 100), Class 2 (C2) Acceptable ($100 \leq RL \leq 200$), Class 3 (C3) Excellent (RL > 200)

Threshold B generally offered a more balanced class distribution, especially for the lower, maintenance-critical class.

**Segmentation:** Six conditions were implemented:

- General (No filtering: all data no-rain)
- Curvature Filtering: CU≥0.005 and CU≥ 0.006
- CV Filtering: CV thresholds of 0.6, 0.2, and 0.1

These filters were applied to each of the three datasets (RLavg, RL3, RLmin) to assess their influence on F1-scores and overall accuracy for each class.

### *2.7.5 Environmental Conditions Integration*

Both parts incorporated environmental analyses:

- **Lighting Conditions:** Daytime versus nighttime data were examined, as sufficient illumination significantly affects sensor performance.
- **Weather Conditions:** Although rain-affected segments were largely removed to reduce noise, comparisons between dry–wet and dry-only conditions were performed. Comparing these environmental checks allows for a comprehensive understanding of how external conditions influence both regression and classification results. Moreover, for practical routine applications, the identification of data collected in wet pavement conditions could be challenging and less reliable.

## 2.8 Project 3: Human–ADAS Lane Marking Quality assessment

The visibility and recognizability of lane markings are fundamental elements for ensuring safe and efficient vehicular guidance. In recent years, the integration of Advanced Driver Assistance Systems (ADAS), such as Lane Keeping Assistance (LKA), has heightened the need for reliable detection of road infrastructure features, particularly lane boundaries, by both ADAS and humans. While ADAS technologies employ sensor-based systems to assess the quality and continuity of lane markings, it remains essential to evaluate how these automated detections align with human perception under real-world driving conditions.

This study focuses on the subjective evaluation of lane marking quality as perceived by drivers and investigates its relationship with both ADAS-based detection (specifically the Mobileye Lane Support System) and objective physical measurements of retroreflectivity in different road geometries and environmental conditions. By incorporating driver perception into the analysis, the research aims to provide a more comprehensive understanding of the usability of lane markings from a human-centric perspective, complementing sensor-based assessments with experiential data.

It is important to clarify that the human perception ratings in this study were collected from a single trained driver during dynamic surveys. The aim was not to conduct a subjective assessment across a sample population of drivers, but rather to capture a representative human interpretation of lane marking visibility under real-world driving conditions. This approach allows for a consistent and controlled reference point when comparing human perception with automated detection and physical retroreflectivity values. As such, the

term "human assessment" throughout this study specifically refers to the evaluations provided by this designated driver and should not be interpreted as the result of a broader subjective study involving multiple participants.

The driver's perception was recorded during dynamic road surveys, in which the driver assigned quality ratings to lane markings using a four-point Likert scale ranging from 0 (no visual detection) to 3 (very good visual detection). For the analysis, 0-1 ranks have been associated with class 1 (Poor visual detection). These ratings were then systematically compared with the outputs of the Mobileye system and with retroreflectivity values derived from the ANAS dataset, which served as the benchmark for the physical condition of the markings.

By correlating these three perspectives—human, machine, and physical measurement—the present study seeks to identify patterns of agreement and discrepancy under varying environmental conditions (e.g., lighting, weather) and geometric features (e.g., curvature, cross section, road segment type). Such analysis contributes to the broader objective of enhancing ADAS calibration and improving the alignment between automated systems and human driving experience, particularly in scenarios where the visibility of road markings may be compromised.

### *2.8.1 Analytical Framework*

This section outlines the analytical framework developed to examine the agreement between human driver perception and the Mobileye Lane Support System (LSS) in evaluating lane marking quality. The approach integrates subjective assessments, sensor-based classifications, and physical retroreflectivity data, progressing through multiple stages of statistical and discriminant modelling. This

structure ensures the robustness of findings under varying road and environmental conditions.

**Step 1: Descriptive and Visual Analysis through Frequency Distributions**

The first phase of analysis focused on gaining an initial understanding of the classification behaviour of both human perception and the Mobileye system. To this end, frequency distribution graphs were generated to visualize the proportion of lane marking segments categorized into quality classes (1 = Poor, 2 = Moderate, 3 = Good) by each source.

These distributions were stratified by contextual conditions, including lighting (day/night), weather (dry/wet/rain), and road geometry (straight vs. curved). The objective was to:

- Detect overarching trends in detection behaviour,
- Observe conditions under which divergence in classification emerges, and
- Provide an empirical basis for deciding where further correlation and modelling analysis were required.

This stage served as the foundation for evaluating the consistency or discrepancy between human and system perception patterns under real-world driving scenarios.

**Step 2: Rank-Based Association Using Spearman's Correlation**

To formally quantify the degree of agreement between the ordinal ratings provided by the driver and the ADAS, Spearman's Rank Correlation Coefficient ($\rho$) was applied. This non-parametric statistic is appropriate for assessing monotonic relationships between ranked variables, without the limitation of normality and linearity assumptions of the parametric tests.

Spearman's correlation was chosen over Pearson's because the

lane marking quality scores are ordinal in nature and do not fulfil the assumptions necessary for parametric correlation. A moderate or strong ρ would indicate that as the driver's perception of quality increases or decreases, when the Mobileye scores shift in the same direction, thereby we can confirm some level of perceptual alignment.

Moreover, the correlation analysis was also stratified by environmental and geometric contexts to identify the influence of external conditions on perception agreement.

**Step 3: Data Simplification via Binary Classification and Agreement Factor (AF) Definition**

While a three-class system provides granularity, it introduces complexity in statistical modelling and interpretation. To enhance model clarity and focus on meaningful differences, lane marking quality scores were recoded into two categories:

- Poor Quality (Class 1): Not usable for vehicle alignment
- Acceptable Quality (Classes 2 and 3): Usable by both human and system

This binary classification aligns with practical ADAS safety applications where the key question is whether lane markings are sufficient for guidance for both human and automated driving.

Based on this simplification, an Agreement Factor (AF) was introduced:

$$AF = |ADAS\ Score - Human\ Score|$$

- AF = 0: Agreement in classification
- AF = 1: Disagreement between human and ADAS scores

This derived variable became a suitable outcome for the statistical Discriminant Analysis.

**Step 4: Statistical Testing of Group Differences**

To explore the environmental and geometric characteristics associated with agreement or disagreement, descriptive statistics were first computed separately for each AF group. These include variables such as:

- Retroreflectivity (RL)
- Curvature (1/R)
- Lane and shoulder width
- Headway
- Lighting and weather conditions

Following the descriptive phase, one-way Analysis of Variance (ANOVA) was applied to determine whether the observed differences in means between the agreement and disagreement groups were statistically significant. A significance level of 0.05 was used as the threshold.

These tests provided empirical justification for including specific features in the subsequent modelling stage, allowing for a data-driven variable selection process.

**Step 5: Discriminant Function Analysis for Agreement Classification**

To assess the extent to which environmental and geometric variables can affect agreement (AF = 0) or disagreement (AF = 1), a Stepwise Linear Discriminant Function Analysis (DFA) was conducted. DFA is a statistical technique used to create linear combinations of predictor variables that best discriminate between groups defined by a categorical dependent variable.

This method was selected due to:

- Its capability to determine which variables are most effective at separating groups, providing a multivariate test of differences between them
- Its ability to handle multivariate classification with categorical grouping,
- Its interpretability compared to black-box machine learning approaches, and

A stepwise approach ensured that only statistically significant and non-collinear predictors were retained in the model. Key assumptions including multivariate normality and equality of group covariance matrices were verified using Box's M test.

Equal prior probabilities were also imposed due to the imbalanced class sizes (AF = 0 being the dominant case). This choice prevents the model from being biased toward the majority class.

The resulting canonical discriminant function was then evaluated using:

- **Eigenvalues and canonical correlation** (model explanatory power),
- **Wilks' Lambda and Chi-square test** (statistical significance),
- **Group centroids** (degree of separation), and
- **Classification matrix** (model accuracy).

Finally, both standardized discriminant coefficients and structure matrix loadings were interpreted to assess the relative contribution and directional influence of each predictor.

By adopting this structured analytical pipeline from exploratory visualizations to statistical testing and multivariate classification this methodology offers a comprehensive framework for understanding

the perceptual alignment between human drivers and ADAS systems. It also provides a foundation for identifying context-specific factors where disagreement is most pronounced, offering practical implications for future ADAS calibration and infrastructure design.

In summary, this chapter detailed the comprehensive methodological framework adopted to investigate three interrelated aspects of lane marking quality and ADAS performance. **Project 1** focused on assessing lane marking quality and the Operational Design Domain (ODD) of the Lane Support System under varying roadway and environmental conditions. **Project 2** explored the potential of estimating lane marking retroreflectivity (RL) from ADAS sensor data as a cost-effective monitoring alternative. **Project 3** examined the agreement between human driver perception and system detection to evaluate perceptual alignment. Together, these methodologies establish a robust foundation for analyzing ADAS for Lane Support Systems, infrastructure quality, and their intersection under real-world conditions. The following chapter presents the results and insights derived from these analyses.

# Chapter 3: Results

# 3 Chapter 3: Results

This chapter presents the results obtained from the three core projects of this dissertation, each targeting a distinct aspect of lane marking quality and its relationship with ADAS performance. Project 1 focuses on evaluating the lane marking quality and operational performance (ODD) of the Lane Support System (LSS) under varying road, environmental, and infrastructure conditions using advanced classification techniques. Project 2 investigates the potential of assessment of lane marking retroreflectivity (RL) through ADAS sensor data, using both regression and classification frameworks. Project 3 examines the agreement and divergence between human driver and ADAS-based lane marking perception under real-world scenarios. The findings from each project are presented in dedicated sections, including performance evaluations, validation tests, and feature importance or interpretability analyses, which collectively contribute to understanding the operational limitations and enhancement potential of tested LSS technology.

## *3.1 Analysis and Results of Project 1: Lane marking quality assessment*

This section evaluates the performance of the seven classification methodologies employed in this study, focusing on their ability to classify lane marking quality accurately. Among the statistical, machine learning, and deep learning approaches, machine learning models, especially AutoML-LGBM and CatBoost, showed the best performance due to their robustness in handling the dataset's complexity and imbalances. Statistical models provided useful benchmarks, while deep learning models showed promise but with limitations due to the dataset's size and noise.

In this study we compared seven different methodologies for classification to select the best method. Figure 23 shows the overall accuracy obtained using these seven selected classification models, while Figure 24 compares the F-scores for the three classes using these models. As we can see, the AutoML-LGBM method has the highest accuracy and the highest F-scores. These scores are particularly high for classes 1 and 2, which represent critical conditions for the system compared to other methods that the score for different classes is high. Additionally, Figure 25 & Figure 26 presents the precision and recall for these seven models.

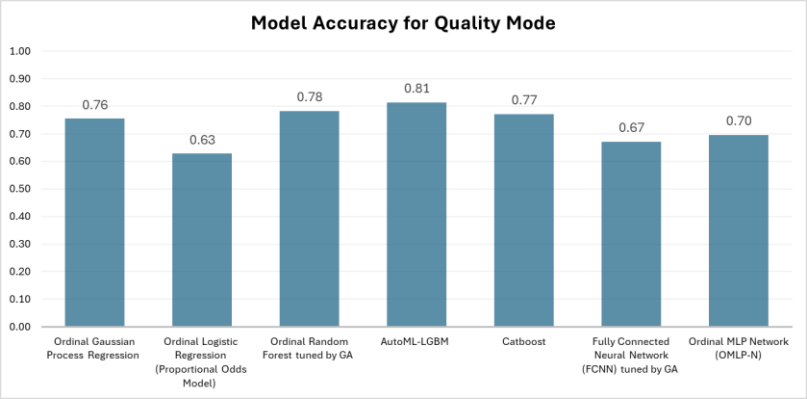


**Figure 23 Overall model accuracy**

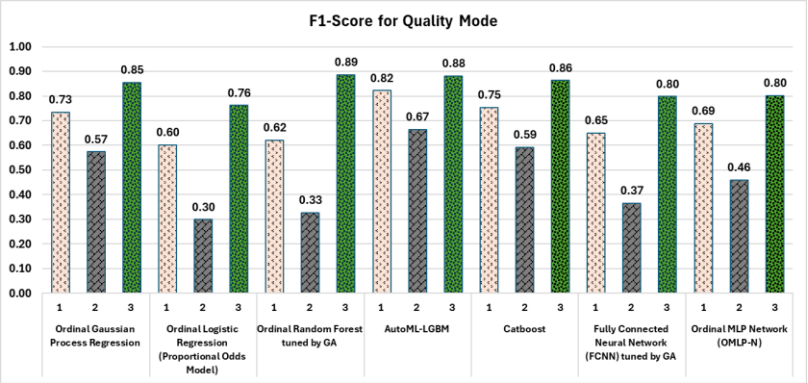


**Figure 24 Comparison of classes F1-Scores by different models**

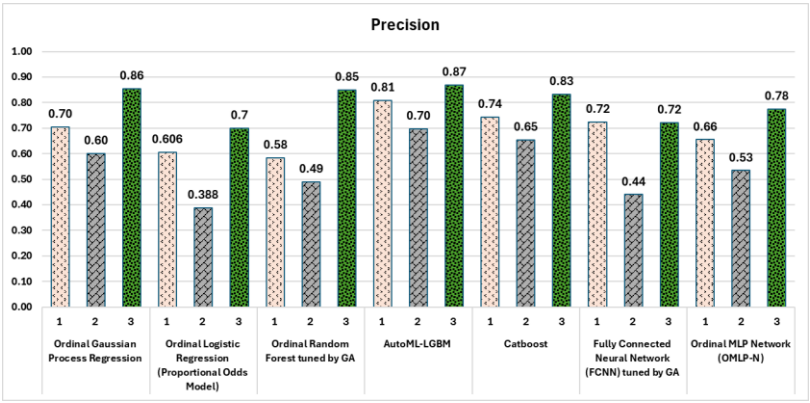


**Figure 25 Comparison of classes precision by different models**

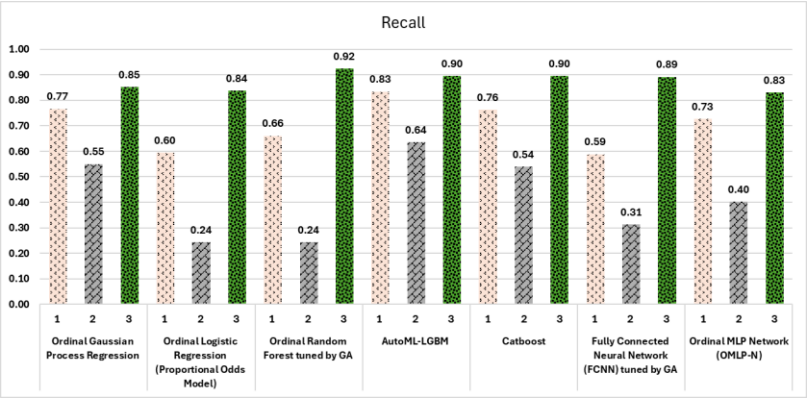


**Figure 26 Comparison of classes recall by different models**

In the current study, we explored a variety of statistical and machine-learning models. Firstly, we used Ordinal Logistic Regression and Gaussian Process Regression, which gave us some basic insights. However, these models have limitations due to their assumptions about linearity and scalability, making it hard to capture complex and nonlinear patterns. Among the different approaches we applied, machine learning models like AutoML-LGBM and CatBoost outperformed. These ML models use ensemble techniques and advanced optimization strategies, which helped them perform exceptionally well. They have been properly set and resulted capable of handling high dimensionality, ordinal nature, and imbalances in datasets very effectively and achieving high accuracy and F-scores across all classes.

We also experimented with deep learning models, which, thanks to their multi-layered architectures, excel at handling complex, nonlinear relationships. However, the size and noisy nature of our dataset limited their performance. LightGBM and CatBoost, both advanced implementations of the gradient boosting framework using

decision trees, showed remarkable capabilities. They managed large datasets efficiently and handled categorical features without much preprocessing. The core idea of boosting, where new models iteratively correct the errors of previous ones, is central to their design.

LightGBM uses a leaf-wise growth strategy, selecting the leaf that minimizes loss, which helps manage complex decision boundaries and reduces overfitting. On the other hand, CatBoost uses ordered boosting and symmetric tree structures to mitigate overfitting. It also has innovative feature encoding techniques for handling categorical data. The superior performance of AutoML-LGBM and CatBoost can be attributed to their ability to handle the dataset's ordinal nature, high dimensionality, and imbalances. Their iterative learning approach ensured a balanced representation of all classes, avoiding overfitting to highly frequent classes. These models are capable of capturing complex, nonlinear relationships within the data while maintaining computational efficiency and scalability. These models are augmented with sophisticated strategies such as LightGBM's Gradient-based One-Side Sampling (GOSS), which prioritizes informative instances during training, and CatBoost's Exclusive Feature Bundling (EFB), which efficiently reduces feature dimensionality. This combination of strategies makes these models particularly adept at navigating challenges posed by high dimensionality, class imbalances, and the diverse nature of feature types within the dataset, ensuring high predictive accuracy under various operational conditions.

For comparison, other classic ones are Gaussian Process Regression (GPR) and Ordinal Logistic Regression, which model the problem in a more naive but bounded way of handling regression and classification tasks. GPR, on the one side, offers an elegant probabilistic view that masterfully captures the uncertainties within ordinal data but does not scale into larger, noisier environments. Finally, Ordinal Logistic Regression finds its perfect application in

datasets with more linear feature relationships, yet it is constrained in complex ones where interactions are nonlinear.

Deep learning models such as the Fully Connected Neural Network (FCNN) and the Ordinal MLP Network (OMLP-N) bring the capacity to discern intricate patterns through their deep architectural designs and multi-level feature abstraction capabilities. However, their performance hinges significantly on the availability of substantial data volumes to avoid overfitting and effectively learn the underlying data structure. Despite efforts toward the augmentation of this dataset using techniques like SMOTE, the inherent complexity, together with noisy conditions prevalent in this data, may impede these models from performing optimally and have shown the limitations of deep learning when conditions are not ideal.

The significant differences in the performance of these models highlight the need for model capabilities to match the unique characteristics and requirements of the dataset. The success seen with LightGBM and CatBoost can be largely credited to their customized strategies for tackling specific challenges in this dataset, such as high dimensionality, a large number of categorical features, and class imbalances. Their approach of progressively correcting errors helps ensure that no single class has an outsized impact on the learning process, which is vital for achieving consistent accuracy across various operational scenarios a key factor for the reliability of lane support systems.

The findings of this research highlight the importance of model selection based on dataset characteristics and ordinal classification tasks. AutoML-LGBM showed as the most effective model due to its ability to handle complex relationships, classes imbalancies, and high-dimensional features while maintaining computational efficiency. Future work could focus on augmenting the dataset or exploring hybrid approaches to enhance model performance further.

### *3.1.1 Model Validation*

One key challenge in machine learning is overfitting, where a model performs exceptionally well on training data but poorly on unseen data due to capturing noise and random fluctuations. To evaluate our best model (AutoML-LGBM) and check for overfitting, we used K-Fold cross-validation, training curves, and learning curves.

Cross-validation estimates a model's generalization performance. In k-fold cross-validation, the dataset is divided into k equal-sized folds. Each fold takes a turn as the validation set while the remaining k-1 folds are used for training. This process is repeated k times, resulting in k models and performance estimates. If a model performs well across all folds, it is likely to perform well on unseen data. In this study, k was set to 5, and the overall performance was calculated as the mean of these k metrics, providing a robust estimate of the model's generalization ability. Figure 27 shows the cross-validation with 5 folds. As we can see, the training accuracy is high (0.98) and higher than the validation accuracy (0.81). The small difference between training and testing accuracies indicates that the model was created well and there is no overfitting.

Learning curves are used to understand how the model's performance changes as the size of the training dataset increases by plotting training and validation accuracy (or error) against the size of the training set. In Figure 28, the training and validation curves are very close together with high accuracy, indicating that the model performs well on unseen data.

Validation curves illustrate how the model's performance changes as a function of a hyperparameter (in our analysis, the L1 regularization term on weights). As seen in Figure 29, the small distance between the training and validation curves indicates no

overfitting. Both curves converging shows the optimal range of hyperparameter values where the model performs well on both training and validation data.

To determine how much other classes are effective on prediction of each class a normalized confusion matrix was used as presented in Figure 30. As we can see for class 1, 83.43% is predicted by class 1 and 11.88% and 4.69% are predicted by class 2 and 3.

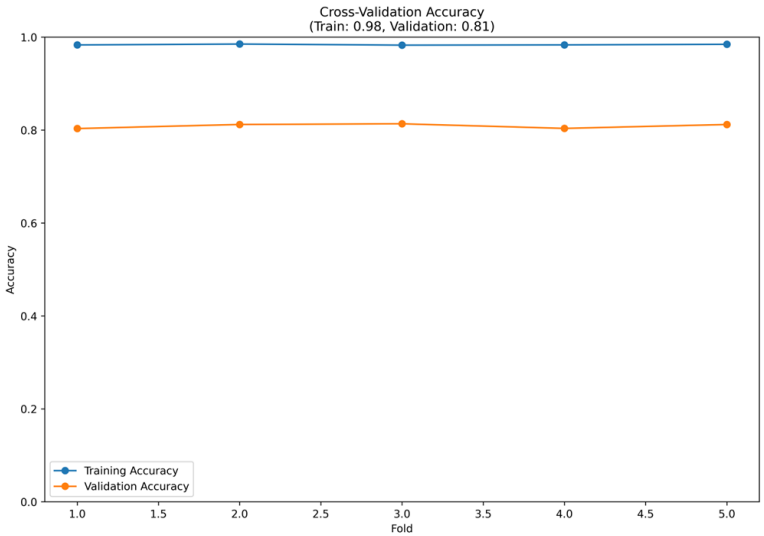


**Figure 27 K-Fold cross validation**

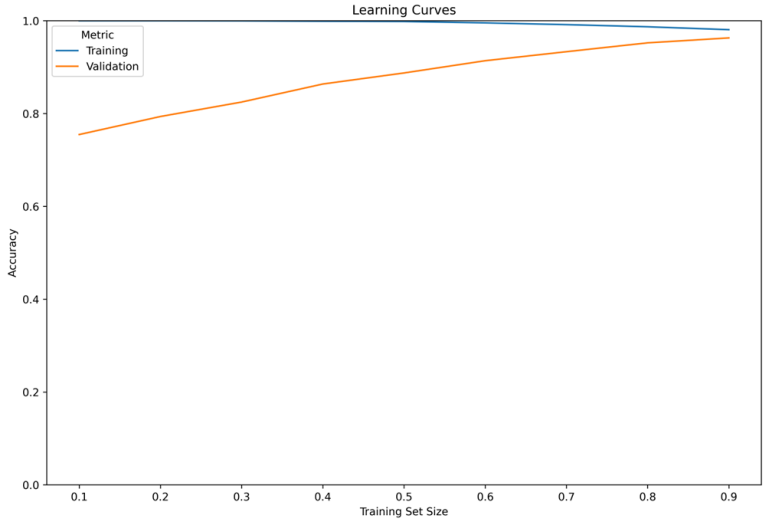


**Figure 28 Learning curves**

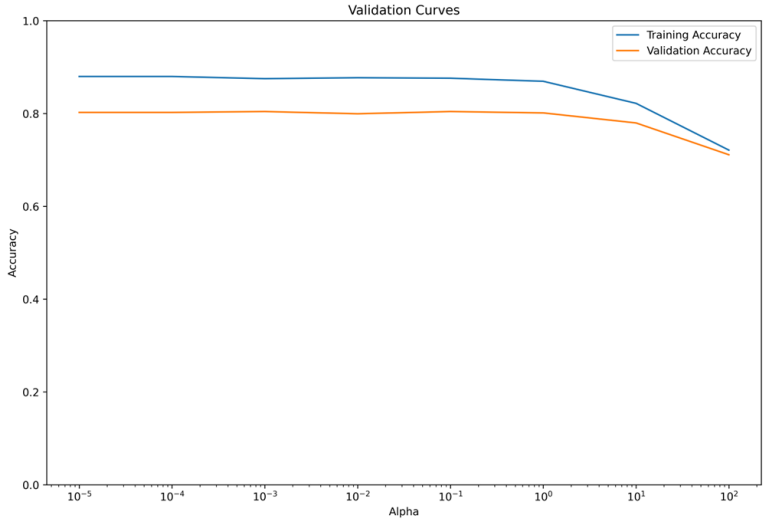


**Figure 29 Validation Curves**

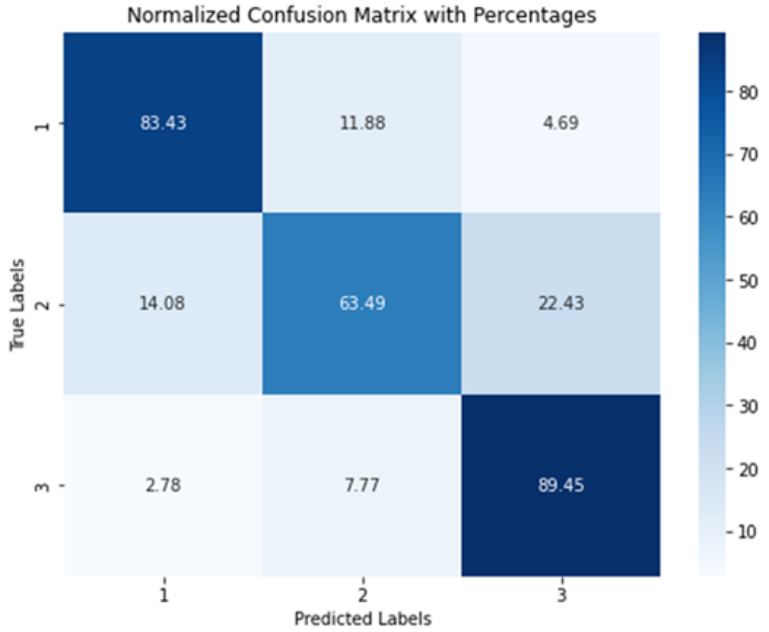


**Figure 30 Normalized confusion matrix for AutoML-LGBM**

### *3.1.1.1 Validation of SMOTE strategies based on LightGBM model*

As discussed in Section 2.6.2.1, the frequency distribution of the three lane marking quality classes reveals a significant imbalance, with Class 3 comprising 70.16% of the dataset. This imbalance can lead to biased classification results, favoring the majority class. To mitigate this issue and ensure accurate classification of the critical minority class (Class 1), we employed the Synthetic Minority Over-sampling Technique (SMOTE) due to its proven effectiveness.

SMOTE generates synthetic samples for the minority classes to balance the class distribution, thereby enhancing model performance without distorting the natural structure of the data.

We tested two SMOTE strategies:

- Equalizing the class frequencies by generating synthetic samples to match the majority class.
- Resampling based on a fixed percentage, in which Classes 1 and 2 were increased to 50% of Class 3's size.

In the second, more nuanced strategy, we deliberately avoided fully equalizing the class frequencies, as doing so could distort real-world proportions and introduce bias. Instead, by adjusting Classes 1 and 2 to half the size of Class 3, we preserved the original dataset with a more limited dominance of the majority class while improving the representation of the minority classes. This approach reflects a more realistic class distribution and data reliability.

This custom resampling strategy aims to boost the statistical power of the minority classes by enhancing the model's ability to learn from underrepresented examples without overwriting the original structure of the data. As a result, the model is expected to demonstrate improved sensitivity to Classes 1 and 2, leading to a more balanced performance across all classes. This is particularly important in applications where detecting the less frequent classes is just as critical as identifying the majority class.

To assess the impact of these resampling strategies, we applied classification modelling using our best-performing model (LightGBM) across three scenarios. Figure 31 & Figure 32 show the model accuracy and F1-scores under each condition.

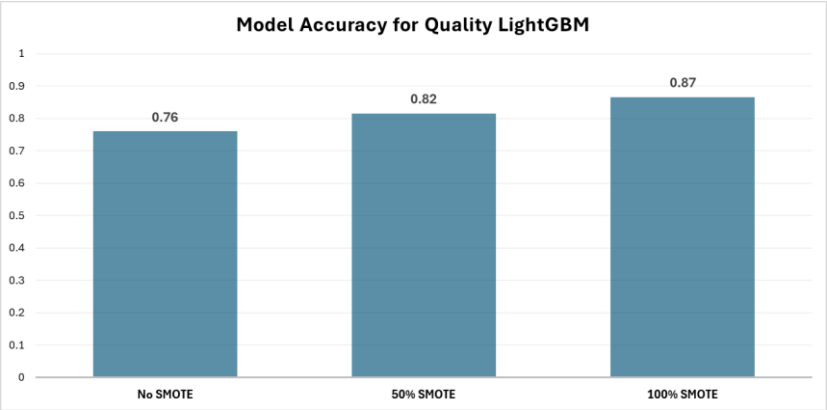


**Figure 31 LightGBM model accuracy for three SMOTE strategies**

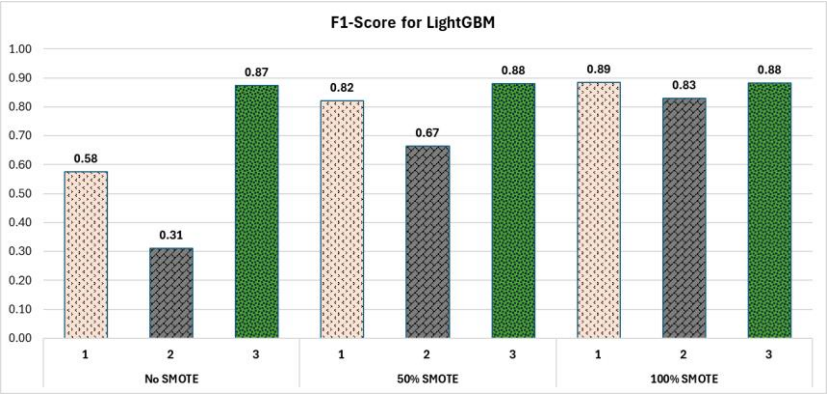


**Figure 32 LightGBM model F1-score for different classes based on three SMOTE strategies**

The results demonstrate that classification without resampling is heavily biased toward the majority class, with 87% predictions falling into Class 3 and an F1-score of only 31% for Class 2. The 100% SMOTE strategy yielded highly balanced scores but loses realism. In contrast, the 50% SMOTE strategy—our chosen approach—achieved

high accuracy while maintaining an acceptable level of class balance, making it both effective and practically acceptable.

### *3.1.2 SHAP (SHapley Additive exPlanations) analysis (class 1):*

Understanding why a model makes a certain prediction is as crucial as the prediction's accuracy for any practical application. Statistical Generalized Linear Models (GLM), for example, can use their coefficients as a metric for the overall importance of each feature, but the coefficient cannot account for the local importance of the feature or their interactions. The same can be said for the feature importance of machine learning models, which is why SHapley Additive exPlanations (SHAP) is used for interpreting models. SHAP is based on Shapley values from cooperative game theory and can be applied to machine learning models to produce consistent explanations. It helps understand how different features affect the model prediction, especially when features interact with each other. SHAP values quantify the contribution of each feature to the difference between the model's prediction for a given instance and the average prediction across all instances. Positive SHAP values indicate that the feature contributes to increasing the prediction, while negative SHAP values indicate a contribution to decreasing the prediction.

In this research, we performed SHAP analysis on the output of AutoML-LGBM, our best model, to explain the effect of features on the prediction of the lower class Q1 by the model. In the plot, the SHAP value indicates how much a particular feature has influenced the model: negative values indicate the feature decreases the model output, while positive values indicate an increase. The red color indicates high feature values, and blue indicates low feature values compared to the average for the entire population. Each value is plotted as a dot on the chart.

### *3.1.2.1 SHAP Summary Plots*

To display a summary of how each feature in a dataset impacts the model's output, Figure 33a shows the SHAP Beeswarm Chart for class 1. The features are sorted by their importance. The highest SHAP positive effect on class 1 prediction is observed for lower values of Speed, RL, and lane width, and for higher curvature. A clear separation of positive effects is observed for Daylight and Rain conditions. Meanwhile, Headways, shoulder width, and section typology don't show a clear trend in their relationship with the outcome. Also, by using the mean SHAP values e can plot SHAP summary plot to know general features influences on the model (Figure 33b).

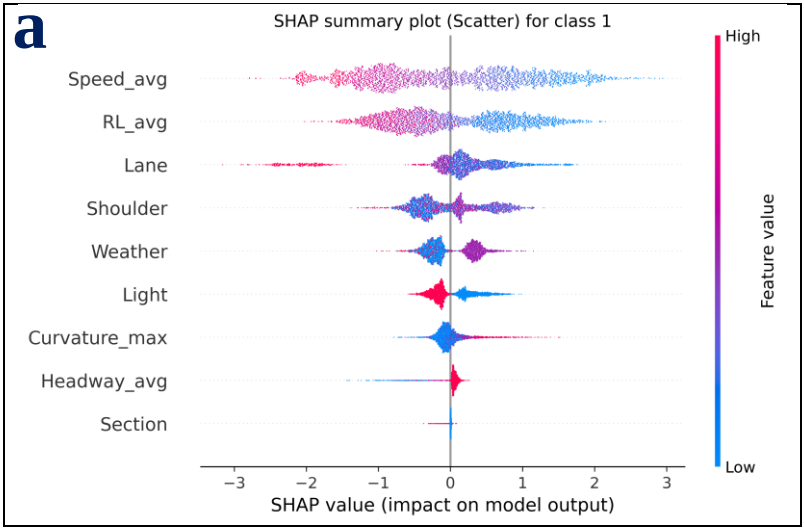

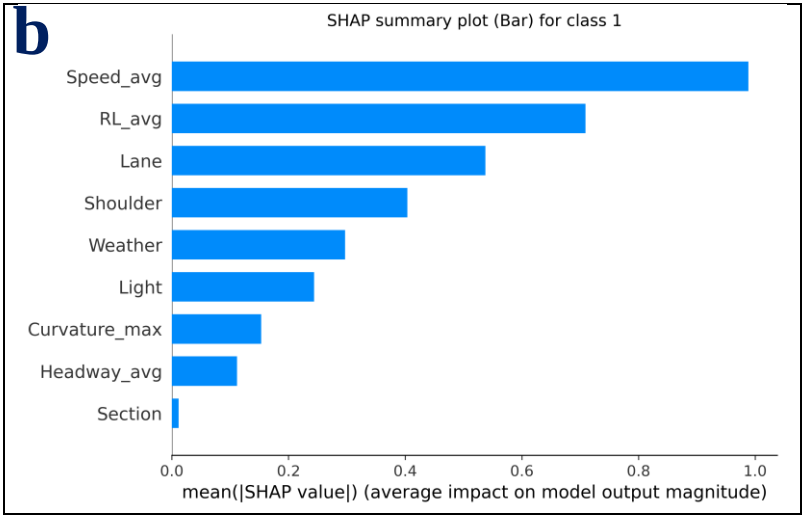


**Figure 33 a) SHAP Summary Plot (Beeswarm) for Critical Condition (Class 1) (Light: Day=1, Night=0; Env.: Dry=1, Rain=2; Wet=3) b) Shap summary bar plot (with mean SHAP value)**

### *3.1.2.2 SHAP Dependence Plots*

The SHAP dependence plot is a powerful visualization tool that shows the relationship between SHAP values and feature values, with the option to include interactions with another feature. Unlike partial dependence plots, which only illustrate mean effects, SHAP dependence plots capture both mean effects and variations, indicating interactions. These plots visualize how changes in a feature's value affect the model's predictions. The x-axis represents the feature of interest, while the y-axis shows the SHAP values. Point colors represent the values of another feature, highlighting feature interactions. We selected the features most representative of the ODD factors in the road scene field that can be improved by both the design (i.e., horizontal alignment, lane and shoulder width) and the maintenance of the road (i.e., Marking RL). The mutual interaction of

these features and their interaction with other features in the dynamic (i.e., speed, headway) or environmental (i.e., light, weather) fields of ODD are also of interest because they could be considered for mitigation actions taken by the vehicle's driving control system.

The SHAP dependence plots shows the mean effect variation and interaction of the following features for class 1 (Figure 34): RL-avg & Speed (a); Curvature & RL (b); Lane width & RL (c); Shoulder width & RL (d); RL & Weather (e); RL & Light (f); Weather & RL-avg (g); Light & RL-avg (h); Lane & Speed (i); Speed & Headway (j); Speed & Curvature (k); Speed & Lane Width (l).

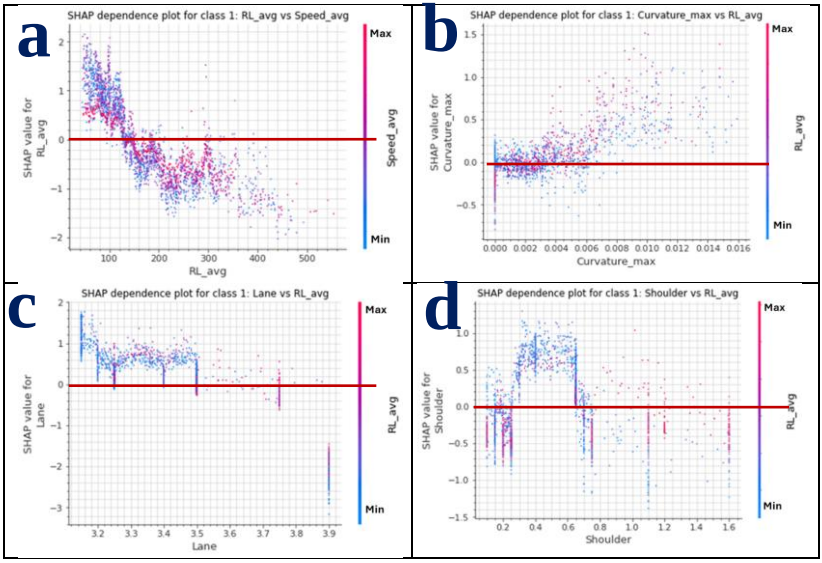

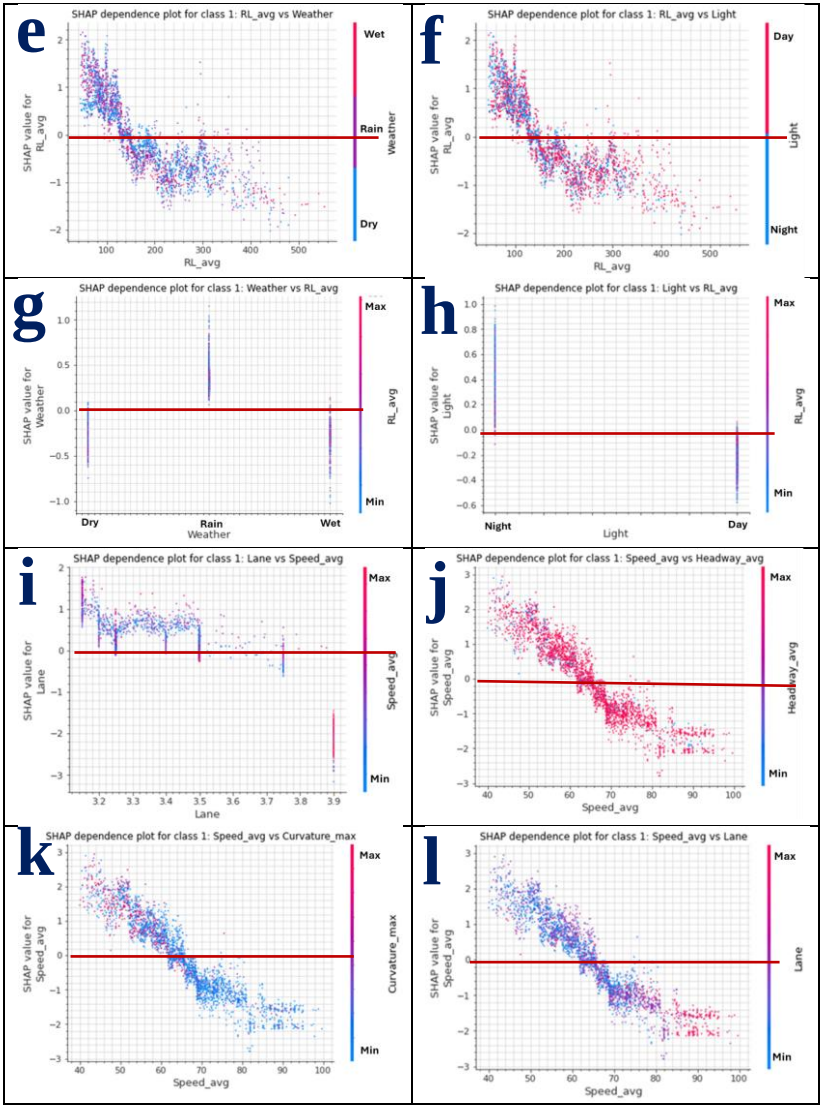


**Figure 34 SHAP Dependence Plots for critical system condition (class 1)**

The main results observed in the SHAP dependence plot are

reported below:

**RL-avg & Speed:** The plot shows the main positive effect (i.e. increase in class 1 prediction) reducing RL, values less than 120 (mcd/m²/lux) increase the probability of positive effects (Figure 34a). Speed variability doesn't influence the role of RL. It is worthily to mention that the value of 120 (mcd/m²/lux) is higher than the critical threshold of 80 assume in the UK standards [160] for human perception. It must be considered that human perception is more flexible and resilient to lane keeping with lower values of marking quality than the LSSs.

**Curvature & RL:** There is a clear positive effect of curvature for values higher than 0.006÷0.007 (i.e., radius less than 150 m) (Figure 34b). Increasing RL doesn't mitigate the effect of curvature. In curves with a sharp radius, the lane marking exits from the lateral field of view of the camera, which is limited to avoid optical distortion. Multi-camera and sensor fusion is adopted in the most advanced AVs to solve this issue.

**Lane width & RL:** Lane widths narrower than 3.5 m have a small positive effect on class 1 prediction, which becomes particularly significant for widths lower than 3.2 m (Figure 34c). Additionally, the plot shows that in this area, there are often lower RL values, probably because narrower lane widths are often associated with minor road classes with lower marking maintenance and higher probability of marking abrasion by the tires.

**Shoulder width & RL:** For very narrow shoulders with a width of less than 0.3 m, the role of RL is revealed to be important in guaranteeing good system performance, as high class 1 predictions are always associated with lower RL values. Shoulder widths in the range of 0.25 - 0.65 m showed the highest impact, not affected by RL (Figure 34d). For higher shoulder widths, lane edge detection is dependent only on RL. For shoulder widths less than 0.25 m, the pavement edge

is very close to the marking border, which could help LSS performance because the detection is based on the variation of pixel intensity over the pavement surface (contrast). Similarly, the most critical condition for widths between 0.25 and 0.62 m can be related to the lack of uniform contrast between the marking and pavement on the external side.

**RL & Weather:** Values of RL < 120 (mcd/m²/lux) are confirmed to be critical for marking detection in any weather condition. However, RL > 150 (mcd/m²/lux) can mitigate the effects for even the worst rain conditions (violet dots in Figure 34e).

**RL & Light:** Similar to the environmental factor, RL < 120 (mcd/m²/lux) always increase the chance to have class 1 detection (Figure 34f). RL values effect mainly the night detection, Increasing the value of RL (e.g. RL>300), can improve the night detection, but is of limited support to other critical conditions in day light.

**Lane & Speed:** Lane width and speed have not shown any significant mutual interaction (Figure 34i). The effect of lane width, like other road features, cannot be mitigated by driving actions on speed as typically done by human drivers.

**Speed & Headway:** headway does not affect LSS performance at any speed (Figure 34j).

## *3.2 Analysis and Results of Project 2: Monitoring Lane Marking Retroreflectivity Using ADAS Sensor Data*

The exploratory analyses (2.7.2) provided foundational insights into the relationships and relative importance of features relevant to RL prediction. The correlation analysis indicated moderate linear relationships among geometric features (particularly speed, lane width, and shoulder width), highlighting the interdependency between road geometry and vehicle dynamics. The network graph further

emphasized the role of speed with its complex connections to other geometric and detection-quality features, revealing multidimensional interactions not fully captured by pairwise correlations alone. Feature importance analysis using XGBoost reinforced these findings, clearly identifying lane detection quality strongly correlated to lane marking retroreflectivity with shoulder and lane width as the most influential road factors. Notably, differences between lighting and weather conditions altered the relative importance of these predictors, underscoring the necessity of considering environmental factors in modelling approaches and operative monitoring conditions. Collectively, these exploratory results informed the subsequent modelling efforts described below, guiding both feature selection and methodological decisions.

### *3.2.1 Regression Analysis*

We tested three selected models for estimation of RL values: Random Forest, XGBoost, and LightGBM to see how accurately each predicted RL under distinct subsets of data. For full Dataset (Excluding Rain) Initially, correlation between predicted and actual RL was around 0.48 and by removing the rain condition the correlation dropped. Another modelling was for removing sharp curves, by eliminating data points with curvature $\geq 0.006$ had little impact on correlation or overall performance. Although extreme curves hamper lane detection, they apparently do not strongly influence how features like lane/shoulder widths, speed, and headway track real-world RL. Lastly the analysis was done for day and night lighting condition to see the performance of the model. Separate evaluations of daytime and nighttime data showed that daytime predictions typically achieved a higher correlation (~0.45) than nighttime (~0.40). This is likely because the camera has more ambient light to distinguish markings,

allowing stronger alignment between observed lane clarity and the true reflectivity. At night, extrinsic factors (headlight positioning, glare, or local lighting conditions) may reduce the direct link between the system's detection parameters and actual RL readings.

Across all scenarios, Random Forest, XGBoost, and LightGBM performed similarly once hyperparameters were tuned, with slight performance gains favoring the boosting methods (XGBoost, LightGBM). The day-night gap in accuracy, and the relatively moderate correlations overall, underscore that while Mobileye-based data do carry information about RL, they only capture it indirectly through contrast, geometry, and the camera's detection confidence. Figure 35 & Figure 36 are showing the models R squares and mean absolute percentage error (MAPE) under different conditions.

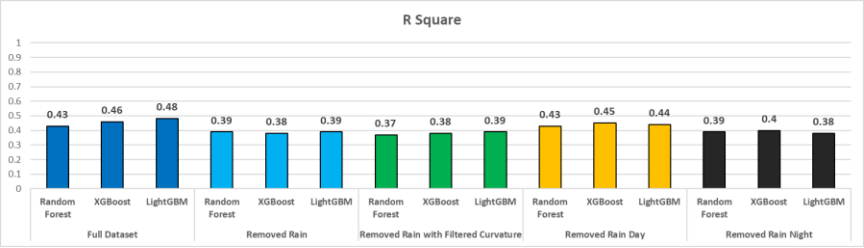


**Figure 35 Model's R Square for different conditions**

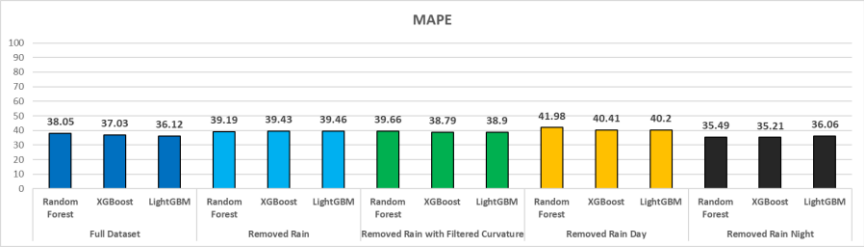


**Figure 36 Model's MAPE for different conditions**

The regression models confirmed that features such as shoulder

width and lane marking quality are central to RL prediction. Daytime conditions generally yielded higher correlations than nighttime and removing rain-affected segments modestly improved performance. However, the regression goodness of fitting was only moderate ($R^2$<0.48) to provide a reliable assessment of RL especially at its lower and critical values.

### *3.2.2 Classification Analysis*

#### *3.2.2.1 Performance Across Segmentation Conditions and Datasets*

The classification analysis aimed to estimate RL quality using three derived datasets: RLavg (mean RL), RLmin (minimum RL), and RL3 (mean minus 3 standard deviations) based on 50-meter segments. To categorize RL into three quality levels (poor, acceptable, excellent), two thresholding schemes were applied: Threshold A (80–150) and Threshold B (100–200), with the latter offering a more balanced class distribution. Additionally, six segmentation conditions: covering general data, curvature filters (CU ≥ 0.005 and CU ≥ 0.006), and coefficient of variation (CV ≤ 0.6, 0.2, and 0.1) were used to evaluate model performance under various geometric and consistency scenarios. Figure 37Figure 38Figure 39 are the F1-scores of different classification models for various conditions of three datasets. Also Figure 40 is the total modelling accuracies for different classification models.

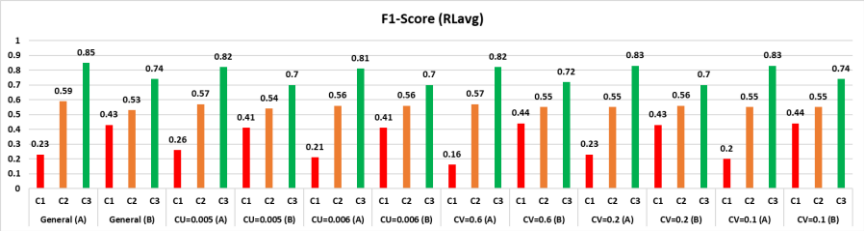


**Figure 37 RLavg F1-Scores for RL Classes under Each Filtering Condition (for Thresholds A and B)**

*Note: General is Full dataset without rain; CU is the thresholding based on curvature; CV is thresholding based on Coefficient of Variation of RL values; C1, C2, and C3 are three RL classes defined by thresholds A & B.*

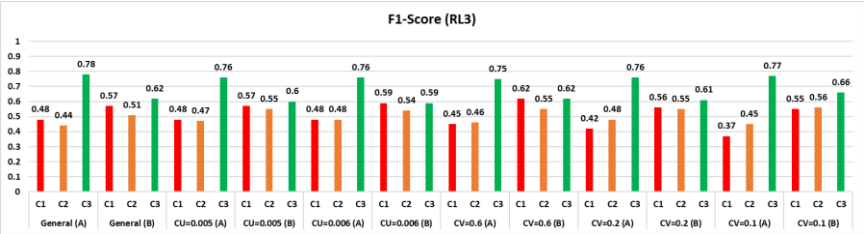


**Figure 38 RL3 F1-Scores for RL Classes under Each Filtering Condition (for Thresholds A and B)**

*Note: General is Full dataset without rain; CU is the thresholding based on curvature; CV is thresholding based on Coefficient of Variation of RL values; C1, C2, and C3 are three RL classes defined by thresholds A & B.*

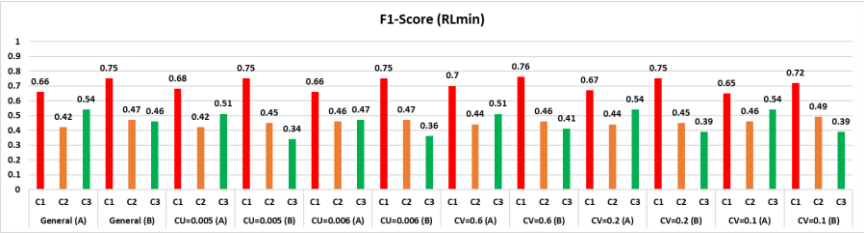


**Figure 39 RLmin F1-Scores for RL Classes under Each Filtering Condition (for**

**Thresholds A and B)**

*Note: General is Full dataset without rain; CU is the thresholding based on curvature; CV is thresholding based on Coefficient of Variation of RL values; C1, C2, and C3 are three RL classes defined by thresholds A & B.*

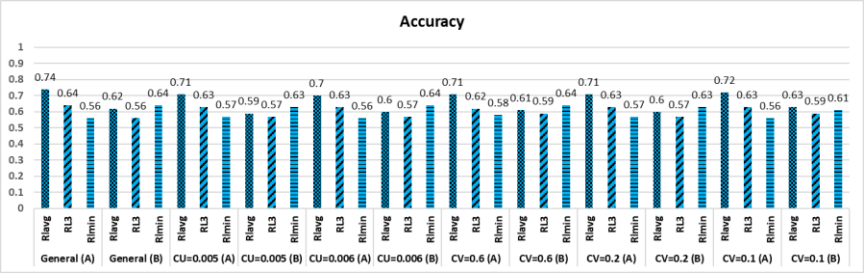


**Figure 40 Overall Accuracy for RLavg, RL3, and RLmin under Each Filtering Condition for thresholds A& B.**

*Note: General is Full dataset without rain; CU is the thresholding based on curvature; CV is thresholding based on Coefficient of Variation of RL values.*

The classification analysis strongly improved model accuracy yielding varied results based on the target outcome, class thresholds and segmentation conditions:

- **RLavg:**

  Under the general condition, RLavg exhibited moderate F1-scores across classes. When curvature filtering was applied (CU = 0.005 and CU = 0.006), minor improvements were observed in specific classes particularly when using threshold B, where the "poor" class (Class 1) improved significantly. However, the differences between CU = 0.005 and CU = 0.006 were subtle, suggesting that the sensor's readings are not overly sensitive to slight variations in curvature filtering. In contrast, applying CV filtering had a mixed impact: while a CV threshold of 0.1 sometimes improved the detection of critical low-RL segments, it occasionally led to a reduction in performance for classes 2 and 3. For RLavg, the

overall balance appears optimal when a moderate curvature filter (CU = 0.006) is applied, which reduces noise without eliminating too much valid data.

- **RL3:**
  The RL3 dataset, which captures both central tendency and variability excluding outliers, generally provides more balanced F1-scores across all classes. Here, the general condition performed robustly; however, moderate CV filtering (CV = 0.2) tended to further refine the predictions, especially for Class 1. The benefits of curvature filtering were less pronounced in this dataset, likely because the variability component in RL3 already captures some of the dispersion introduced by road geometry. In this case, the general condition or light CV filtering (CV = 0.6) preserved the inherent variability, whereas too strict filtering (CV = 0.1) risked discarding critical fluctuations.
- **RLmin:**
  As expected, the RLmin dataset, designed to capture the worst-case conditions, showed the highest F1-scores for Class 1 across several filtering conditions. Notably, applying a strict CV filter (CV = 0.1) often resulted in the best performance for Class 1 in RLmin, as it effectively removed outlier noise while preserving the extreme low values. Conversely, for RLmin, the general condition or a curvature filter (CU = 0.005 or 0.006) sometimes diluted the critical signal by including too much variability, thereby reducing F1-scores for the lowest class.

#### *3.2.2.2 Overall Environmental Analysis*

As we discussed before, one aspect of this analysis was to determine the effect of different environmental conditions on RL modelling performance. For this analysis the best model with highest

accuracy for each of three datasets were selected as the base to analyze the impact of environmental conditions. Also based on observations in the last section we choose thresholding B because of its balanced and high scores among different classes.

Followings are the results of classification modelling under different conditions for these three datasets using different environmental scenarios (Figure 41, Figure 42 & Figure 43).

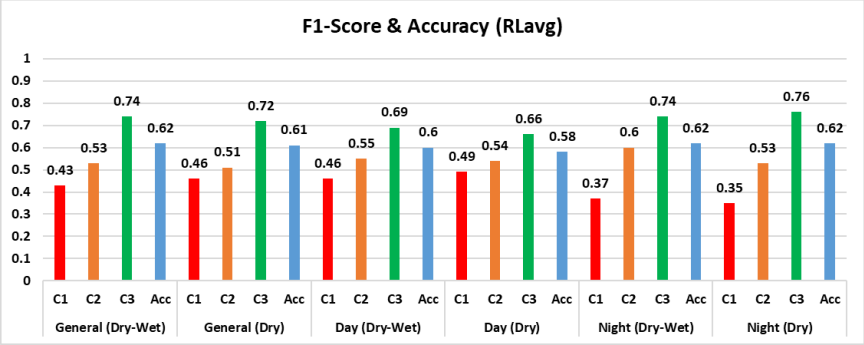


**Figure 41 Environmental Analysis – F1-Scores and general model accuracy for RLavg dataset for Day/Night and Dry–Wet vs. Dry Conditions.**

*Note: General is the full dataset without rain; Day and Night are the dataset filtered for day and night (rain is deleted); Dry, Wet, or Dry-Wet is the environmental condition that is present in that dataset. In this figure the red, orange and green bars are f-1scores for three classes and blue bar is the general model accuracy for that dataset.*

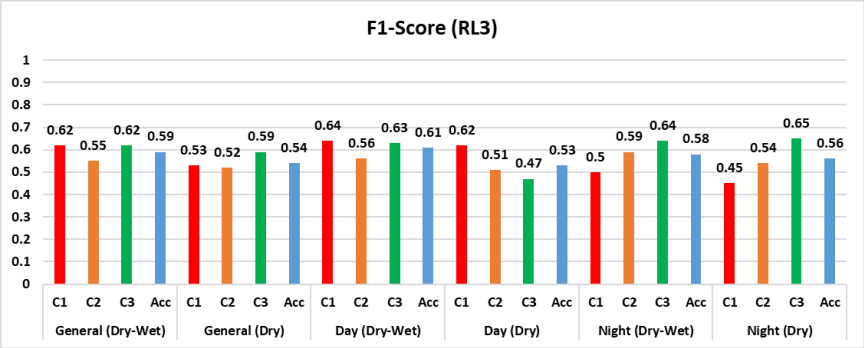


**Figure 42 Environmental Analysis – F1-Scores and general model accuracy for RL3 dataset for Day/Night and Dry–Wet vs. Dry Conditions.**

*Note: General is the full dataset without rain; Day and Night are the dataset filtered for day and night (rain is deleted); Dry, Wet, or Dry-Wet is the environmental condition that is present in that dataset. In this figure the red, orange and green bars are f-1scores for three classes and blue bar is the general model accuracy for that dataset.*

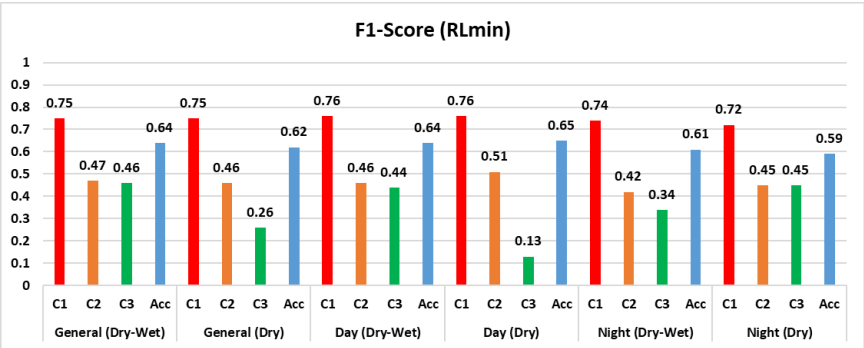


**Figure 43 Environmental Analysis – F1-Scores and general model accuracy for RLmin dataset for Day/Night and Dry–Wet vs. Dry Conditions.**

*Note: General is the full dataset without rain; Day and Night are the dataset filtered for day and night (rain is deleted); Dry, Wet, or Dry-Wet is the environmental condition that is present in that dataset. In this figure the red, orange and green bars are f-1scores for three classes and blue bar is the general model accuracy for that dataset.*

Environmental analysis showed that:

- **Lighting:** Daytime data improved F1-scores for critical classes in RLavg and RL3, while nighttime models tended to favour the higher quality (Class 3) segments.
- **Weather:** Models using exclusively dry conditions showed a slight lower performance that those using combined dry–wet datasets, anyway wet pavement conditions are more difficult to identify in a cloud data collection approach.

## *3.3 Analysis and Results of Project 3: Lane Marking perception and assessment by Human vs. ADAS*

This chapter presents the results obtained from the analysis of driver versus ADAS (Mobileye LSS) perception of lane marking quality under real-world driving conditions. Building upon the analytical framework outlined in Chapter 2, the results are structured around the core stages of the analysis: (1) comparative frequency distribution of classification outcomes, (2) correlation analysis using Spearman's rank coefficient, (3) evaluation of binary classification agreement, and (4) discriminant analysis to identify the factors influencing agreement and disagreement.

The outputs include graphical summaries, correlation coefficients, and statistical tests which collectively highlight the patterns of alignment and discrepancy between human and system perception across varying environmental and geometric conditions. These results provide the empirical foundation for the interpretation and discussion that follows in Chapter 4.

### *3.3.1 Frequency Analysis of Lane Marking Quality under Varying Environmental Conditions*

To illustrate how lane marking quality is perceived across different environmental and geometric contexts, frequency distribution analyses were conducted separately for the Lane Support System (LSS) and for the driver-based assessment. It is important to clarify that the human evaluation was not based on subjective personal perception, but rather followed structured visual inspection criteria aligned with established standards, specifically the UK TD 26/17 – Inspection and Assessment of Road Markings and Road Studs [35]. The assessments were made by a single experienced driver trained to apply these guidelines, which define quality classes based on marking visibility under various conditions such as lighting (day vs. night), surface condition (dry, wet, rainy), and roadway geometry (curved vs. straight segments). These structured criteria allowed the driver to perform a rule-based evaluation of lane marking quality comparable to system classification, despite the absence of a sample group of drivers. The aim of this analysis was to visually compare the classification tendencies of both observers—human (standard-based) and system (ADAS)—and to identify consistent patterns or notable discrepancies in their assessments.

While numerical correlation metrics offer a single measure of association, frequency-based visualizations provide a richer context. They help uncover trends such as whether the LSS consistently rates a higher proportion of markings as high-quality (Class 3), or whether drivers more frequently classify markings as moderate or poor (Classes 1 and 2), particularly in challenging conditions. These insights are valuable for identifying environmental scenarios in which discrepancies are more pronounced, potentially guiding future system calibration or enhancement efforts. Figure 44 presents the distribution of lane marking classes as detected by both the Mobileye Lane Keeping Assistance system (Quality) and by human perception (Mode).

Frequecy (General)
100%
90%
80%
70%
60%
50%
40%
30%
20%
10%
0%
14%
18%
68%
31%
51%
18%
Class1
Class2
Class3
Class1
Class2
Class3
Quality
Mode
Frequecy (Day Dry)
8%
15%
77%
24%
41%
35%
Frequecy (Day Rain)
18%
28%
54%
40%
54%
6%
Frequecy (Day Wet)
9%
17%
75%
13%
46%
41%
Frequecy (Night Dry)
2%
4%
95%
6%
79%
14%
Frequecy (Night Rain)
47%
18%
35%
74%
25%
0%
Frequecy (Night Wet)
17%
10%
72%
36%
56%
9%

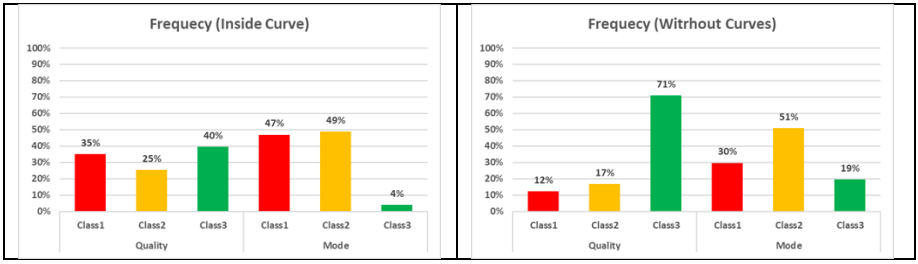


**Figure 44 Frequency distribution of lane marking quality classes under different conditions: LSS (Quality) vs. Human (Mode) perception.**

#### *3.3.1.1 Observed Patterns Across Conditions*

Across the full dataset, the LSS consistently assigned a substantially greater proportion of lane sections to the highest RL category (Class 3) compared to human drivers. Conversely, drivers were more likely to assign lower or moderate quality ratings, indicating a general trend of the system being more "positive" in its assessment.

Under daytime conditions, this optimism is particularly apparent: the LSS frequently categorizes the majority of markings as high quality, while drivers remain more reserved in their evaluations, especially in rainy environments, where their ratings shift significantly toward lower classes. This indicates that precipitation notably reduces perceived marking visibility for human drivers, even when the system still performs effectively.

The divergence between system and human assessments is even more pronounced during nighttime driving. In dry night conditions, the LSS still classifies most markings as high quality, whereas the driver infrequently assigns the top rating, suggesting reduced visual clarity of markings under low-light conditions. In contrast, nighttime rain causes both human and system assessments to drop into lower classes, although the driver remains distinctly more critical. This

demonstrates that visibility loss under compounded conditions darkness and precipitation is reflected in both detection systems, albeit with different sensitivities.

Road geometry also influences the quality ratings. On curved segments, both the LSS and the driver reduce their use of high-quality ratings; however, the driver again proves more conservative, with Class 3 being rarely assigned. On straight segments, the LSS tends to return to optimistic classifications, while the driver continues to show restraint, favoring moderate or lower classifications more frequently.

These frequency distributions collectively suggest that the LSS is generally more lenient across most conditions, but certain environments particularly nighttime rain and curves highlight more alignment between the system and human difficulties in marking perception. Recognizing these areas of agreement and divergence is essential for identifying where both ADAS ODD and lane marking management could be refined to make roads ready for ADAS and Human.

### *3.3.2 Spearman's Rank Correlation Between Human and System Assessments*

To quantify the association between human perception and ADAS-based evaluation of lane marking quality, Spearman's Rank Correlation Coefficient (denoted as $\rho$) was estimated. This nonparametric statistical measure is particularly appropriate for ordinal data, such as the quality ratings used in this study, which are based on discrete ranks ranging from 1 to 3.

Spearman's correlation assesses the strength and direction of a monotonic relationship between two ranked variables. The coefficient $\rho$ ranges from $-1$ to $+1$, where $\rho = +1$ indicates a perfect positive monotonic relationship, $\rho = -1$ indicates a perfect negative monotonic

relationship, and $\rho = 0$ signifies no monotonic association. In practical interpretation, absolute values below 0.3 are typically considered weak, values between 0.3 and 0.5 moderate, and those exceeding 0.5 strong.

Unlike Pearson's correlation, Spearman's does not require assumptions of linearity or normal distribution, making it well-suited to the nature of the human and system-derived quality scores in this analysis.

Applying Spearman's correlation to the full dataset yielded a coefficient of $\rho = 0.460$ with a p-value $< 0.001$, indicating a high-moderate and statistically significant monotonic relationship between the two sets of quality assessments. This result suggests a general trend of agreement in the ranking of lane marking quality between the human observer and the Mobileye Lane Support System, though with notable variation. Table 15 presents the correlation matrix for the full dataset.

**Table 15 Correlation matrix**

Correlations

| | | | Qmaj | Mode |
|---|---|---|---|---|
| Spearman's rho | Qmaj | Correlation Coefficient | 1.000 | .460** |
| | | Sig. (2-tailed) | . | <.001 |
| | | N | 8923 | 8923 |

**. Correlation is significant at the 0.01 level (2-tailed).

Further analysis examined the variability of the Spearman correlation coefficient across different environmental and geometric contexts. These subgroup analyses revealed that the degree of correlation fluctuates depending on factors such as lighting conditions, pavement wetness, and road geometry, as visualized in Figure 45.

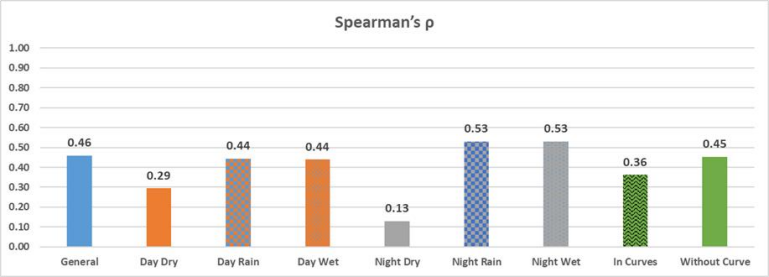


**Figure 45 Spearman's Rank Correlation for different conditions**

This stratified analysis supports the observation that while a general agreement exists between the ADAS and human assessments, this agreement is condition-dependent. For instance, higher consistency may occur under unfavourable visibility conditions (e.g., night Wet/rai), while larger discrepancies emerge under dry conditions. These findings underscore the necessity of context-aware system tuning to improve alignment with human visual perception.

### *3.3.3 Descriptive Statistics and Group Comparison*

To further investigate the contextual factors influencing the agreement between human perception and ADAS-based lane marking classification, a statistical analysis was conducted using the Agreement Factor (AF) as the grouping variable. The analysis aimed to identify which environmental, geometric, and traffic-related variables are associated with divergence (AF = 1) or agreement (AF = 0) between the two assessments.

The analysis proceeded in two stages. First, descriptive statistics and a one-way ANOVA were used to evaluate the differences in key variables across the two AF groups. Next, a discriminant function analysis (DFA) was employed to examine whether a combination of variables could effectively classify road segments

based on agreement status, and to quantify the relative influence of each variable in the different classification.

The statistical assumptions for the application of DFA, including equality of covariance matrices and multivariate normality, were tested and met. The results provide insight into the specific road and environmental conditions most strongly associated with disagreement/agreement between human and system evaluations of lane marking quality.

To explore how geometric, environmental, and traffic-related parameters differ between segments with and without agreement between human and ADAS assessments, descriptive statistics were computed separately for each AF group. Table 16 presents the means and standard deviations for key variables such as retroreflectivity (RL), road curvature, headway distance, lighting, and lane geometry across AF = 0 (agreement) and AF = 1 (disagreement). These descriptive summaries provide an initial understanding of how specific features may be associated with higher levels of agreement or misalignment between the two classification sources, thereby supporting the subsequent inferential and discriminant analyses.

**Table 16 summary statistics of Groups means**

| AF | variable | Mean | Std. Deviation | N |
|---|---|---|---|---|
| 0 | RL | 199.915 | 95.673 | 6718 |
| | Curvature(1/R) | .001157 | 0.00270 | 6718 |
| | Min_Headway | 3.248 | .6863 | 6718 |
| | environment | 1.733 | .7547 | 6718 |
| | Light | 1.31 | .4641 | 6718 |
| | LANE | 3.514 | .2229 | 6718 |
| | SHOULDER | .5602 | .3845 | 6718 |
| 1 | RL | 171.425 | 92.969 | 2076 |
| | Curvature(1/R) | .001551 | .00378 | 2076 |
| | Min_Headway | 3.299 | .60727 | 2076 |
| | Environment | 1.838 | .6762 | 2076 |
| | Light | 1.24 | .4288 | 2076 |
| | LANE | 3.383 | .1693 | 2076 |
| | SHOULDER | .5228 | .4197 | 2076 |
| Total | RL | 193.190 | 95.80 | 8794 |
| | Curvature(1/R) | .00125 | .002998 | 8794 |
| | Min_Headway | 3.260 | .6688 | 8794 |
| | environment | 1.758 | .7382 | 8794 |
| | Light | 1.297 | .4570 | 8794 |
| | LANE | 3.483 | .2187 | 8794 |
| | SHOULDER | .5514 | .3934 | 8794 |

### *3.3.4 One-Way ANOVA and Box's M Test*

To statistically assess whether the observed difference in variable means between the agreement groups (AF = 0 and AF = 1) are significant, a one-way Analysis of Variance (ANOVA) was conducted for each independent variable. This test evaluates whether group membership exerts a statistically significant effect on the distribution of each variable. As shown in Table 17, all variables showing a p-values less than 0.05 are considered to contribute meaningfully to distinguishing between agreement and disagreement groups, thus justifying their inclusion in the discriminant analysis.

**Table 17 Equality of Group Means test**

| | Wilks' Lambda | F | df1 | df2 | Sig. |
|---|---|---|---|---|---|
| RL | .984 | 142.510 | 1 | 8792 | <.001 |
| Curvature(1/R) | .997 | 27.404 | 1 | 8792 | <.001 |
| Min_Headway | .999 | 9.226 | 1 | 8792 | .002 |
| Environment | .996 | 32.427 | 1 | 8792 | <.001 |
| Light | .996 | 38.765 | 1 | 8792 | <.001 |
| LANE | .935 | 611.203 | 1 | 8792 | <.001 |
| SHOULDER | .998 | 14.357 | 1 | 8792 | <.001 |

Discriminant analysis aims to identify a function of linear combination of variables that best separates predefined groups, in this case, agreement (AF = 0) and disagreement (AF = 1) between human and ADAS assessments. As this method considers multiple predictors simultaneously, it requires the assumption of multivariate normality and homogeneity of covariance matrices across groups. To verify the latter, Box's M test was performed, as shown in Table 18. A significant result indicates that the covariance matrices differ across groups. Additionally, to mitigate the imbalance between class sizes, equal prior probabilities were assigned to both AF groups, ensuring that the model does not favour the majority class during classification.

**Table 18 Tests null hypothesis of equal population covariance matrices**

| | | |
|---|---|---|
| Box's M | | 1203.068 |
| F | Approx. | 42.912 |
| | df1 | 28 |
| | df2 | 53801992.004 |
| | Sig. | <.001 |

### *3.3.5 Discriminant Function Analysis*

Following the preliminary statistical analysis, a stepwise discriminant function analysis was performed to identify the most relevant variables for classifying road segments based on the Agreement Factor (AF). The model began with the full set of candidate predictors, and variables were iteratively selected based on their discriminatory power.

Given the binary nature of the AF variable, only a single canonical discriminant function was derived. This function represents a linear combination of the selected predictors that maximizes the separation between the two groups (AF = 0 and AF = 1).

To interpret the discriminant function, several metrics were considered. The standardized canonical discriminant function coefficients indicate the unique contribution of each variable, while the structure matrix reveals the overall correlation between each variable and the discriminant function. Additionally, examining the group means for the function allows for interpretation of how the function separates the groups.

The effectiveness of the discriminant function is first evaluated through its eigenvalue and canonical correlation (Table 19), which represent the amount of variance explained and the strength of association with the group classification, respectively. Wilks' Lambda and the associated Chi-square test (Table 20) are then used to assess the statistical significance of the function. A Lambda value closer to 1 implies a weak discriminatory power; however, a statistically significant Chi-square result ($p < 0.001$) confirms that the function nonetheless significantly differentiates between the two groups.

**Table 19 Summary of Canonical Discriminant Functions**

| Function | Eigenvalue | % of Variance | Canonical Correlation |
|---|---|---|---|
| 1 | .094 | 100.0 | .293 |

**Table 20 Wilks' Lambda estimates**

| Test of Function(s) | Wilks' Lambda | Chi-square | df | Sig. |
|---|---|---|---|---|
| 1 | .914 | 788.447 | 7 | <.001 |

To further evaluate the discriminative power of the canonical function, group centroids representing the mean discriminant scores for each AF group were examined. These centroids reflect how well the function separates the groups: greater distance between them indicates stronger differentiation. As shown in Table 21, the centroids offer insight into the direction and extent to which the discriminant function distinguishes between agreement (AF = 0) and disagreement (AF = 1) cases.

**Table 21 Functions at Group Centroids**

| | Function |
|---|---|
| AF | 1 |
| 0 | .170 |
| 1 | -.551 |

The classification results derived from the discriminant analysis provide insight into the model's predictive performance. As shown in Table 22, the overall accuracy of the model is 64.0%, indicating the percentage of cases correctly classified into agreement (AF = 0) and disagreement (AF = 1) groups. However, the accuracy is notably lower for the minority class (AF = 1), reflecting a tendency of the model to misclassify some disagreement cases as agreement. This imbalance highlights a limitation in the discriminant function's ability to capture the full complexity of disagreement scenarios.

**Table 22 Classification Results**

| | | | Predicted Group Membership | | Total |
|---|---|---|---|---|---|
| | | ModeQm) | 0 | 1 | |
| Original | Count | 0 | 4272 | 2446 | 6718 |
| | | 1 | 724 | 1352 | 2076 |
| | % | 0 | 63.6 | 36.4 | 100.0 |
| | | 1 | 34.9 | 65.1 | 100.0 |

a. 64.0% of original grouped cases correctly classified.

Standardized Canonical Discriminant Coefficients in Table 23, indicate the relative importance of each predictor variable. Larger absolute values suggest that the variable has a greater impact on the discriminant function. Positive coefficients indicate that higher variable values are associated with higher discriminant scores, while negative coefficients indicate the opposite. While standardized canonical discriminant function coefficients show the unique contribution of each variable, the structure matrix coefficients in Table 24, show the overall correlation, including shared variance with other variables. However, these coefficients do not tell us between which of the groups the respective functions discriminate. Therefore, we can identify the nature of the discrimination for each discriminant (canonical) function by looking at the means for the functions across groups in Table 16.

**Table 23 Standardized Canonical Discriminant Function Coefficients**

| | Function 1 |
|---|---|
| RL | .406 |
| environment | .011 |
| Light | .207 |
| LANE | .952 |
| SHOULDER | -.339 |
| Curvature | -.082 |
| Min_Headway | .008 |

**Table 24 Structure Matrix**

| | Function 1 |
|---|---|
| LANE | .861 |
| RL | .416 |
| Light | .217 |
| environment | -.198 |
| Curvature | -.182 |
| SHOULDER | .132 |
| Min_Headway | -.106 |

*Variables ordered by absolute size of correlation within function.*

The results from Table 23 & Table 24 highlight key variables that contribute to the separation between agreement and disagreement groups. Among geometric features, lane width (LANE) exhibits the strongest discriminant power, with higher lane widths associated with greater agreement (positive coefficient in the discriminant function and higher mean in group 0), while shoulder width shows a negative coefficient with higher mean in group 0, indicating that narrower shoulders are linked to increased agreement. These patterns are supported by the group mean values reported in Table 16.

Retroreflectivity (RL) also plays a significant role, showing a positive coefficient in the discriminant function. Higher RL values are

associated with increased alignment between human and ADAS evaluations, while lower RL values more common in the disagreement group corresponding to reduced visibility and lower perceived quality.

Among environmental factors, lighting conditions emerge as the most discriminative. The positive loading in both the standardized coefficients and the structure matrix suggests that daylight conditions (coded as 1) are more frequently associated with disagreement, whereas night conditions (coded as 2) align more closely with agreement. This finding may indicate that the ADAS system performs relatively better in day-light than human drivers expect.

The discriminant analysis reveals that narrow lane and large shoulder widths, low retroreflectivity, and daytime conditions are the most influential factors contributing to disagreement between human and system assessments of lane marking visibility.

In summary, the results from the three projects provide a multifaceted view of the interaction between lane marking quality, ADAS detection capabilities, and human driver perception. Project 1 demonstrated that machine learning models particularly AutoML-LGBM and CatBoost can reliably classify lane marking quality based on infrastructure and environmental parameters, offering practical tools for assessing LSS performance boundaries. Project 2 confirmed that retroreflectivity assessment through ADAS sensor data is feasible with limitations, although environmental conditions and extreme values require careful data segmentation to ensure model stability. Project 3 revealed that while there is a moderate correlation between human and system assessments, other than RL, contextual factors such as cross section geometry and lighting conditions play a crucial role in shaping perceptual agreement. These findings collectively underscore the need for adaptive ADAS calibration strategies and updated infrastructure standards. The next chapter builds on these insights to

provide a deeper interpretation of the results and propose engineering and policy recommendations.

# Chapter 4: Discussion

# 4 Chapter 4: Discussion

Chapter 4 presents a comprehensive discussion of the findings across the three core research projects, linking model performance with real-world implications for lane support systems (LSS), infrastructure maintenance, and human–machine perception. The chapter begins with an overarching interpretation of how the dataset design, environmental segmentation, and modelling strategies align with the broader goals of improving ADAS reliability and safety.

While each project had distinct objectives—ranging from classifying lane marking quality, predicting retroreflectivity using sensor data, to comparing human versus machine perception—they collectively contribute to a deeper understanding of the operational limits and performance variation of modern LSS under real-world conditions.

This discussion explores how specific features such as retroreflectivity (RL), road geometry, and lighting interact across different systems and perception sources. It also delves into model interpretability through SHAP analysis, the role of filtering and data conditioning in improving performance, and the practical-level implications of the observed results.

## *4.1 Interpretation and Discussion of Project 1: Lane Marking Quality Assessment*

### *4.1.1 Overview of Predictive Performance*

In this experimental real-world research, the ODD of a lane support system based on camera vision was analyzed considering a wide set of factors representative of the three main areas of the ODD taxonomy (physical infrastructure, environmental conditions, and traffic conditions) and their interactions. We employed various

machine learning algorithms to select the most relevant features to include in the model, thereby improving prediction accuracy and reducing the risk of overfitting. CatBoost emerged as the best method for feature importance analysis due to its advanced gradient-boosting capabilities, high computational performance, and ability to handle numerical and categorical features. By utilizing CatBoost's robust analysis, we identified the most relevant and practical features while avoiding including highly correlated variables in the more complex models. This step was beneficial in optimizing model performance.

Our study compared the classification performance of various models, including statistical methods (GLMs), machine learning techniques, and deep learning algorithms. Among these approaches, a pipeline consisting of a stacking estimator incorporating an LGBMClassifier and another LGBMClassifier as the final estimator achieved the best performance. This AutoML-LGBM method demonstrated exceptional classification accuracy, leveraging a core LightGBM model optimized and tuned by the TPOT tool. TPOT not only fine-tuned hyperparameters but also identified the most effective pipeline configuration and model order, ensuring a comprehensive optimization process.

### *4.1.2 SHAP Interpretability and Feature Interactions*

Understanding why a model makes a certain prediction is as crucial as the prediction's accuracy for any practical application. In the experimental design and data analysis, we selected features most representative of the ODD factors in the road scene field that can be improved through both design (i.e., horizontal alignment, lane and shoulder width) and road maintenance (i.e., Marking RL). Their mutual interaction and interaction with other features falling in the Traffic (i.e., Speed, Headway) or Environmental (i.e., Light, Weather)

fields of ODD are also of interest because they could be considered for mitigation actions taken by the driving control of the vehicle. SHAP is a method used to interpret and explain the output of machine learning models. In this research, we performed SHAP analysis on the output of AutoML-LGBM, our best model, to explain the effect of features on the prediction of the lower class Q1.

The SHAP dependence plots showed the highest SHAP positive effect on class 1 prediction for lower values of Speed, RL, and lane width, and for higher horizontal curvature. A clear positive effect on class 1 is observed for Daylight and Rain conditions. However, Headways, shoulder width, and section typology don't show a clear trend in the relationship with the outcome.

Key observations from the SHAP dependence plots include:

- **RL-avg:** RL values below 120 mcd/(m²/lx) have a strong positive effect, with speed variability showing minimal influence on the prediction.
- **Curvature & RL:** Higher curvature (R<150 m) exhibits a clear positive effect on lower class prediction. Increasing RL does not mitigate the curvature effect.
- **Lane Width & RL:** Narrow lanes (particularly < 3.2 m) have a positive effect on class 1 prediction. RL values below 120 mcd/(m²/lx), reduced lane and shoulder widths are particularly frequent in this road category, increasing the chance of class 1 prediction.
- **Shoulder Width & RL:** Shoulder widths between 0.25 - 0.65 m show the highest impact, emphasized by the lower values of RL.
- **RL & Weather:** RL values above 150 mcd/(m²/lx) can mitigate adverse rain conditions.

- **RL & Light:** RL values below 120 mcd/(m²/lx) negatively impact predictions under both day and night lighting conditions. Day light detection is not supported by higher values of RL.
- **Headway:** headway having no significant impact.

### *4.1.3 Implications for Road Design and Maintenance*

The features analyzed in this study are representative of Operational Design Domain (ODD) factors in road scenes that can be improved through design and maintenance. Horizontal alignment with curve radius higher than 150 m doesn't affect marking detection, but curvature effects cannot be mitigated by increasing RL. Narrow lanes width shoulder widths in the range 0.25-0.65 m showed the worst results, but proper maintenance of road markings (RL) can significantly influence LSS performance. The minimum RL value of 150 mcd/(m²/lx) suggested for LSS is higher than the critical threshold used for human vision.

Interaction with road and dynamic or environmental factors

Results showed that the deficiencies in the physical factors of road design and maintenance that limit the ODD of LSS can't be mitigated by changing the driving task (e.g. speed and headway). Vice versa good marking maintenance improves marking detection also in the worst rain conditions. Therefore, proper road adaptation and maintenance, or system improvements, are practical needs that must be addressed by both road administrations and AV manufacturers to ensure the availability of the ODD across the road network.

The mutual interactions between static road design features and dynamic (speed, headway) or environmental (light, rain) conditions are of particular interest for mitigation strategies in vehicle control systems. For example:

- Higher RL values can mitigate adverse rain conditions, suggesting that road maintenance strategies could focus on enhancing RL to improve safety in critical weather areas.

## 4.2 Interpretation and Discussion of Project 2: Monitoring Lane Marking Retroreflectivity Using ADAS Sensor Data

### 4.2.1 Model Behaviour under Filtering Strategies

The six filtering conditions were introduced to tackle the inherent noise in sensor data and the variability introduced by different roadway and environmental conditions. The choice of filtering condition has real implications for how well the system can identify maintenance-critical segments.

**General Condition:** The baseline condition, without additional filtering, offers a complete picture but also includes more noise. For RLavg and RL3, this condition provides robust performance overall, though it tends to average out extreme cases. In contrast, for RLmin, the inclusion of all data points can sometimes obscure the worst-case readings, resulting in slightly lower F1-scores for the most critical class (C1). For this reason, filtration improve the 1-score for critical condition.

**Curvature Filtering (CU):** The rationale behind curvature filtering is that extreme curvature may distort the camera's view, leading to misclassification of lane marking quality. The two thresholds, CU = 0.005 and CU = 0.006, yielded relatively similar results, with CU = 0.006 sometimes providing a slightly better balance in RLavg. This suggests that a modest exclusion of high-curvature segments can help improve the sensor's consistency without removing too many valid cases. In RLmin, however, the impact of curvature filtering is less pronounced because extreme low values may be

inherent to road sections with sharp curves.

**Coefficient of Variation Filtering (CV):** The CV filtering strategy aims to exclude segments with high internal variability, which are often unreliable. The results shows that by filtration based on CV the performance not improved and sometimes the accuracy fall down pointing that their ML models can effectively handle noise and outliers in dataset.

### *4.2.2 Dataset-Specific Analysis and Use Case Relevance*

**RLavg:**

When using RLavg, the sensor data's inherent averaging can mask critical low-RL values. The improvement in performance under threshold B suggests that re-calibrating the thresholds is essential to reveal maintenance-relevant information. For operational deployment, RLavg under these conditions may serve well for general monitoring, provided that the threshold settings are adjusted to emphasize critical segments.

**RL3:**

The inclusion of variability in RL3 makes it particularly suited for real-world applications where uncertainty is inherent. This dataset shows consistent performance across all classes (specially thresholding B), indicating its potential for both routine monitoring and early-warning systems.

**RLmin:**

Designed to capture the worst-case scenarios, RLmin naturally emphasizes the need for urgent maintenance. However, the potential underperformance in classes representing acceptable and excellent conditions implies that RLmin should ideally be used in tandem with one of the other settings for a comprehensive assessment.

### 4.2.3 Environmental Conditions and General Model Reflections

Both the regression and classification approaches benefit from an integrated view of environmental effects:

- **Lighting Conditions:** Daytime conditions consistently yield higher performance in both models, reinforcing the importance of ambient light in sensor accuracy. When the models are recalibrated for nighttime data, they tend to shift emphasis toward higher RL classes, possibly because poor illumination makes it harder to distinguish subtle degradations in lane marking quality. At night, the reduced ambient light shifts the relative importance of features (see Figure 22), necessitating recalibration for optimal performance.
- **Weather Conditions:** Dry conditions do not significantly improve model reliability compared to mixed dry–wet scenarios.

When synthesizing the findings from both modelling phases, several key insights emerge:

- **Model Understanding:**

Regression analysis provided a clear view of which road features and environmental parameters strongly influence RL assessment. Classification, on the other hand, transformed these insights into more accurate classification accuracy. Together, they offer a complete picture of sensor performance and maintenance implications.

- **Practical Implications:**

For road maintenance operations, the choice of dataset and segmentation strategy must be aligned with specific objectives. If the primary aim is to flag the most critical road sections quickly, RLmin is more appropriate. For broader monitoring, RL3 provides a more

balanced assessment. RL threshold selection is highly important for the performance of classification models; a good distribution among different levels makes the classification results more balanced. Adapting the model parameters based on environmental conditions (daytime/dry versus nighttime/wet) will further enhance operational reliability. Still, the presence of wet pavement should be more difficult to monitor during data acquisition. Therefore, limiting the RL classification only to data collected on dry days should be more practical.

## 4.3 Interpretation and Discussion of Project 3: Human vs. ADAS Lane Marking Quality Perception

### 4.3.1 Perception Biases under Varying Environmental Conditions

This subsection discusses the findings of the comparative analysis between human and ADAS assessment of lane marking quality. It interprets the implications of the results presented in Chapter 3, explores condition-dependent behaviors, and highlights the critical factors driving misalignment between the two sources.

**Perception Bias and Environmental Influence**

The ADAS system (Mobileye LSS) generally demonstrated an optimistic bias in its classification of lane markings, consistently assigning higher quality scores compared to human observers. This tendency was most visible in daytime and dry conditions, possibly due to the system's optimization for high-contrast environments. In contrast, human raters were more conservative, particularly under rain or reduced visibility, revealing that perceived clarity may involve subtleties not captured by automated vision algorithms.

**Surprising Trends at Night**

An unexpected yet important observation was the narrower gap in perception during nighttime conditions. While it is often assumed that night vision limitations would degrade both human and ADAS performance, the closer alignment suggests that Mobileye may possess compensatory capabilities possibly enhanced sensor calibration that maintain stable detection in low-light conditions. This trend calls for further study but opens interesting possibilities for nighttime ADAS tuning.

### *4.3.2 Quantitative Agreement Analysis and Condition-Dependent Behavior*

A moderate correlation ($\rho = 0.460$) between human and ADAS scores indicates some degree of alignment, yet the Agreement Factor (AF) analysis revealed that disagreement (AF = 1) is condition-specific. Discriminant modelling showed that variables like lane width, retroreflectivity (RL), and lighting conditions are the most influential in explaining when the system and the driver disagree. Notably, narrow lanes and low RL were strongly associated with misalignment, underscoring the importance of geometric and maintenance-based factors.

**Design and Maintenance Implications**

The results reaffirm that infrastructure plays a critical role in harmonizing human and machine perception. Road segments with narrow geometry or degraded markings are more likely to generate disagreement. This supports prioritizing lane marking maintenance and widening in critical segments, particularly under conditions where driver reliance is high, and ADAS may misclassify.

### *4.3.3 Infrastructure and Design Recommendations*

**Practical Recommendations**

- **ADAS Calibration and sensor fusion:** Manufacturers should consider reweighting environmental and geometric features during model training to better match human perception, especially in ambiguous conditions like curves or glare. The fusion of data from multiple sensors (e.g. more cameras or LIDAR) can mitigate/solve the issues related to one camera field of vision and computer vision limitations.
- **Road Agency Actions:** For road operators, ensuring consistent RL levels above 150 mcd/(m²/lx) may significantly reduce both human and system-based errors.
- **Policy Considerations:** This study supports a co-adaptive approach where both ADAS and infrastructure are tuned in tandem to ensure reliability under real-world conditions.

## *4.4 Cross-Project Synthesis and Implications*

This section synthesizes key insights across the three projects presented in this dissertation to identify overarching patterns, complementary findings, and broader implications for both infrastructure policy and ADAS development. While each project focused on a distinct perspective system performance, physical retroreflectivity estimation, and driver vs. machine perception several common threads emerged that highlight critical design, maintenance, and integration challenges for modern lane support systems (LSS).

### *4.4.1 Converging Influences: Geometry, Retroreflectivity, and Environmental Factors*

Across all three projects, road geometry, retroreflectivity (RL), and environmental conditions consistently emerged as the most

influential factors affecting lane detection quality regardless of whether the data source was a vision-based ADAS, physical measurements, or human observation.

In Project 1, narrow lane width, tight curvature (R < 150 m), and low RL (< 120 mcd/m²/lx) significantly increased the likelihood of LSS failure. These same factors appeared again in Project 2 as strong predictors in both regression and classification models for RL estimation. In Project 3, they were the main contributors to perceptual misalignment between humans and ADAS, particularly in challenging conditions such as nighttime rain or curved segments. These repeated patterns reinforce the centrality of geometric design and maintenance standards in supporting robust, reliable ADAS functionality.

Moreover, environmental conditions played a mediating role across all projects. Daytime lighting consistently improved system detection and model accuracy, while rainy or mixed conditions degraded performance, particularly for lower-quality markings. Interestingly, nighttime performance in Project 3 showed better alignment between human and system perception, suggesting a potential compensatory mechanism in the ADAS sensor design.

### *4.4.2 Complementarity Between Measurement, Machine, and Human Perspectives*

Each project offered a unique lens into lane marking assessment, and together they provide a multi-source validation framework:

- **Project 1** focused on how machine learning and feature selection can model and classify ADAS ODD of lane marking quality under different road and environmental conditions.
- **Project 2** extended this by demonstrating that physical properties of lane markings, particularly RL can be classified with reasonable

accuracy using ADAS outputs and geometric data, providing a non-invasive monitoring alternative.

- **Project 3** added a subjective, human-centric perspective, revealing where and why discrepancies between human judgment and ADAS outputs occur and highlighting the limitations of vision-based systems in replicating real-world human interpretation.

Together, these studies demonstrate the value of integrating sensor-based detection, physical measurements, and driver perception for a more holistic understanding of road visibility and ADAS performance. This triangulation strengthens the case for combining multi-source data in both research and real-world applications, from system calibration to road asset management.

### *4.4.3 Implications for ADAS Development and Infrastructure Planning*

The findings from this multi-project thesis point toward a few key implications for both vehicle system designers and transportation infrastructure agencies:

1. **LSS performance is deeply tied to infrastructure quality.** Poor lane marking RL, narrow shoulders, and high curvature increase the risk of detection failure and perception mismatches. Infrastructure upgrades particularly increasing RL to >150 mcd/m²/lx can dramatically improve both system and human performance.
2. **ADAS systems must be calibrated with contextual awareness.** Perception biases, especially under optimistic system assumptions in clear conditions, may not reflect true safety margins in poor visibility scenarios. Machine learning models should be trained to consider road geometry, marking age, and lighting in a more granular way.

3. **Maintenance prioritization should consider sensor feedback.** Real-time detection metrics from LSS can be used to identify potential maintenance-critical segments even before physical RL measurements are taken. Project 2's RL3 approach, for instance, could support early-warning systems or automated inspection protocols.
4. **Human–ADAS harmonization requires co-adaptive design.** Disagreements between driver and system assessments highlighted in Project 3 show that a one-size-fits-all detection threshold may be insufficient. Tailoring ADAS responses based on environmental context or driver confidence levels could improve trust and usability.

Bringing together the findings from all three projects, this chapter demonstrates that the performance and reliability of Lane Support Systems (LSS) are critically influenced by road infrastructure quality, environmental conditions, and the contextual tuning of detection algorithms. While ADAS technologies have evolved significantly, their ability to consistently interpret and respond to complex roadway scenarios still faces challenges especially under adverse conditions or when lane markings are poorly maintained.

Interestingly, our comparison of human and machine perception revealed that in certain low-visibility conditions, such as nighttime driving, ADAS systems may offer more consistent detection than the human eye. Yet, they still lack adaptability, contextual judgment, and resilience of human drivers. This underscores the need for a co-adaptive approach where both ADAS development and infrastructure design evolve in tandem.

Closing this discussion, it is clear that bridging the gap between

intelligent systems and real-world driving environments will require interdisciplinary collaboration. Future research should explore more complex environments, multi-sensor fusion, and human–machine interaction modelling, while road agencies and ADAS developers must work together on regulatory, technological, and maintenance strategies to ensure safe and reliable autonomous driving.

# Chapter 5: Conclusions and Recommendations

# 5 Chapter 5: Conclusions and Recommendations

## 5.1 General Overview and Chapter Structure

This chapter synthesizes the key findings from the three core projects conducted in this dissertation, each addressing a distinct aspect of lane support system (LSS) performance, monitoring, and perception. The aim is to draw practical and theoretical conclusions that can guide future developments in road infrastructure, ADAS technologies, and system–human interaction.

Each section of this chapter presents conclusions and recommendations for one project: Project 1 evaluates LSS performance under varying ODD conditions; Project 2 focuses on the estimation of retroreflectivity using ADAS sensors; and Project 3 investigates the alignment between human and system-based lane marking assessments. The chapter concludes with a cross-project synthesis and suggestions for future research and practical implementation.

## 5.2 Lane Support System Performance under ODD Variability

This study has successfully demonstrated the critical role of Operational Design Domain (ODD) factors in enhancing the performance of lane support systems (LSS) through an extensive real-world experimental setup. Our research highlights the intricate balance between road design, maintenance, and environmental conditions, and their substantial impact on the accuracy and reliability of camera-based vision systems in vehicles.

We confirmed that strategic enhancements in physical infrastructure, particularly through focused interventions in road marking reflectivity (RL) and lane geometries, significantly bolster

the efficacy of LSS. Moreover, our findings advocate for the integration of advanced machine learning techniques, such as the AutoML-LGBM model, in the developmental stages of autonomous vehicle technologies to optimize feature selection and model performance dynamically.

The implications of our study extend beyond technical applications, offering actionable insights for policy makers and road safety authorities. By adopting targeted improvements in road maintenance and design, particularly in adverse weather conditions and challenging traffic scenarios, a safer and more reliable operational environment for autonomous driving technologies can be achieved.

In conclusion, this research not only furthers the understanding of LSS within varied ODD contexts but also underscores the necessity for a holistic approach to autonomous vehicle development and road safety enhancements. As autonomous technologies evolve, continuous research and adaptive strategies will be paramount in realizing the full potential of these systems in real-world settings.

Despite the promising results achieved in evaluating lane support system (LSS) performance using machine learning models under varying ODD conditions, this study is not without limitations. First, the analysis was conducted exclusively using Mobileye data, which, while representative of vision-based systems, may not generalize to other ADAS technologies incorporating radar, LiDAR, or sensor fusion. The road network sampled was limited to two-lane rural segments, excluding high-speed motorway environments and complex urban contexts with frequent junctions, faded or temporary markings, and occlusions. Additionally, the absence of intersections and limited diversity in geometric configurations may underrepresent real-world ODD variability. For future developments, research should expand to cover urban, highway, and junction-rich networks and include multi-sensor ADAS platforms. Integration of vehicle-to-

infrastructure (V2I) communication systems could provide real-time updates on ODD limitations, enhancing the responsiveness and reliability of LSS. Furthermore, collaborations with OEMs could unlock access to larger, more diverse datasets that better capture the evolving complexity of automated driving contexts.

## 5.3 Monitoring Lane Marking Retroreflectivity Using ADAS Sensor Data

This study demonstrates that ADAS sensor data, when processed using a combined regression and classification framework, can effectively approximate direct RL measurements. The detailed analysis shows that:

- **Threshold calibration is crucial:** Threshold set B, in particular, improves the detection of maintenance-critical low-RL segments.
- **Dataset selection:** RLavg and RL offer a balanced view for general monitoring, while RLmin is optimal for identifying hazardous conditions.
- **Environmental factors significantly impact model performance:** Models are most reliable under daytime condition, underscoring the importance of adaptive calibration in operational settings.

Integrating insights from both regression and classification analyses, the study lays a solid foundation for a sensor-based monitoring system that can drive more efficient road maintenance. Future research may further refine these models under varying conditions and incorporate additional sensor modalities to enhance reliability.

While the study demonstrated that ADAS sensor outputs can be used to estimate lane marking retroreflectivity (RL) with reasonable accuracy, some limitations must be acknowledged. The models were

developed based on data from a single ADAS system, different visual systems and detection quality classification could provide different results. Furthermore, the analysis focused predominantly on dry conditions, whereas wet pavement scenarios, although acknowledged, remain underexplored due to their detection complexity. To enhance practical applicability, future work should explore the fusion of multiple sensor inputs, and longitudinal analysis of RL degradation over time. Additional efforts should also focus on refining model calibration for nighttime and adverse weather conditions, and on developing early-warning mechanisms for maintenance based on predictive RL classification models that account for environmental uncertainty.

## 5.4 Driver vs. ADAS Perception of Lane Marking Quality

This study investigated the agreement between human drivers and an Advanced Driver Assistance System (ADAS), specifically the Mobileye Lane Support System, in assessing the quality of lane markings under real-world driving conditions. Using a combination of subjective human perception scores, system-generated outputs, and physical retroreflectivity measurements, a comprehensive analysis was conducted to identify patterns of alignment and divergence across varying environmental and geometric conditions.

The frequency distribution analysis revealed that the ADAS consistently classified a higher proportion of lane markings as high quality compared to human drivers, particularly under daytime and dry conditions. In contrast, human perception was more conservative and especially critical in low-visibility scenarios such as nighttime rain or on curved road segments. This pattern indicates a general tendency of the system to overestimate marking quality under certain conditions.

Spearman's rank correlation demonstrated a statistically

significant, moderate positive relationship ($\rho = 0.460$, $p < 0.001$) between the two assessment sources. However, correlation strength varied across different contexts, with stronger agreement observed under specific environmental setups.

To further examine the conditions under which agreement deteriorates, the original quality ratings were transformed into a binary classification system, and an Agreement Factor (AF) was introduced. This allowed for the application of statistical and discriminant analyses to identify variables associated with disagreement.

The discriminant analysis showed that lane width, retroreflectivity, and lighting conditions were the most influential factors in separating agreement from disagreement cases. Narrower lanes and shoulders, lower retroreflectivity values, and daylight conditions were all associated with increased disagreement between human and system assessments. These findings suggest that both physical infrastructure features and environmental context significantly affect the perceptual alignment between ADAS and human drivers.

Overall, the results underscore the importance of contextual sensitivity in evaluating and calibrating ADAS systems. Systems that perform well in optimal conditions may still diverge significantly from human perception under complex or degraded environments. These insights can inform both system improvement and infrastructure planning, particularly in prioritizing maintenance for markings in areas where perception is likely to be inconsistent.

This study offers new insights into the perceptual alignment between human drivers and ADAS systems in evaluating lane marking quality, but its scope is constrained by some limitations. Human perception data were collected from a single experienced road inspector, offering consistency but limiting the generalizability of findings across a broader sample. The Mobileye system, while

effective, provides limited transparency into its internal confidence scoring or computer vision processes, reducing the ability to interpret discrepancies in depth. Moreover, the Likert-based scoring system, though practical, may not capture fine-grained perceptual subtleties or dynamic transitions in visibility perception. Future research should adopt a multi-driver approach and incorporate dynamic assessments that track agreement over time and across transitions in environmental and road conditions. There is also a need for adaptive ADAS calibration models that adjust to contextual cues and human feedback. Integrating ADAS and Human perception can help bridge the gap between human drivers and automated system interpretation, contributing to safer and more intuitive ADAS–driver roads.

## 5.5 Cross-Project Insights and Future Directions

Across all three projects, a consistent theme emerged: the performance and reliability of ADAS systems, particularly lane support systems, are fundamentally shaped by the condition of road infrastructure and the dynamic environmental context in which these systems operate.

While Project 1 confirmed that geometric design and retroreflectivity thresholds significantly influence LSS classification performance, Project 2 demonstrated that even without physical measurement tools, ADAS sensor data can be harnessed to predict RL levels through calibrated learning models. Project 3 revealed that discrepancies between ADAS and human perception are more pronounced in degraded visual environments and under suboptimal road conditions, with human judgment being especially cautious in these scenarios.

These findings point to the necessity of a co-adaptive approach

to intelligent transportation systems one that improves both the capabilities of sensing and classification algorithms and the quality and consistency of the infrastructure they depend on. Better integration of machine perception with human behavioral models, multi-sensor fusion, and real-time environmental awareness are essential next steps.

Future research should continue developing context-aware ADAS calibration techniques, explore more robust perception in complex environments, and investigate user trust and reliance patterns in shared control systems. From a practical standpoint, road agencies and policymakers should work alongside technology developers to align infrastructure standards with the evolving capabilities and limitations of modern ADAS technologies.

# References

[1] T. Geißler and E. Shi, “Taxonomies of connected, cooperative and automated mobility,” in *2022 IEEE Intelligent Vehicles Symposium (IV)*, IEEE, 2022, pp. 1517–1524.

[2] Society of Automotive Engineers (SAE), “Taxonomy and Definitions for Terms Related to Driving Automation Systems for On-Road Motor Vehicles,” 2018.

[3] International Organization for Standardization (ISO), “ISO 34503:2023 Road Vehicles — Test scenarios for automated driving systems — Specification for operational design domain,” Aug. 2023.

[4] FHWA, “Rumble Strips and Rumble Stripes: Design and Construction. ,” 2023.

[5] P. J. Carlson, E. S. Park, and C. K. Andersen, “Benefits of pavement markings: A renewed perspective based on recent and ongoing research,” *Transp Res Rec*, vol. 2107, no. 1, pp. 59–68, 2009.

[6] W. J. Rasdorf, J. E. Hummer, G. Zhang, and W. Sitzabee, “Pavement marking performance analysis,” 2009.

[7] H. Fu and C. G. Wilmot, “Evaluating alternative pavement marking materials,” *Public Works Management & Policy*, vol. 18, no. 3, pp. 279–297, 2013.

[8] M. Hussein, T. Sayed, K. El-Basyouny, and P. de Leur, “Investigating safety effects of wider longitudinal pavement markings,” *Accid Anal Prev*, vol. 142, p. 105527, 2020.

[9] H. T. Zwahlen and T. Schnell, “Visibility of new centerline and edge line pavement markings,” *Transp Res Rec*, vol. 1605, no. 1, pp. 49–61, 1997.

[10] W. N. Craig III, W. E. Sitzabee, W. J. Rasdorf, and J. E.

Hummer, “Statistical validation of the effect of lateral line location on pavement marking retroreflectivity degradation,” *Public Works Management & Policy*, vol. 12, no. 2, pp. 431–450, 2007.

[11] Y. Jiang, “Durability and retro-reflectivity of pavement markings (synthesis study),” 2008.

[12] N. A. Parker and M. S. J. Meja, “Evaluation of performance of permanent pavement markings,” *Transp Res Rec*, vol. 1824, no. 1, pp. 123–132, 2003.

[13] G. B. Thomas and C. Schloz, “Durable, cost-effective pavement markings phase I: synthesis of current research.,” Iowa State University. Center for Transportation Research and Education, 2001.

[14] N. Abboud and B. L. Bowman, “Cost-and longevity-based scheduling of paint and thermoplastic striping,” *Transp Res Rec*, vol. 1794, no. 1, pp. 55–62, 2002.

[15] F. Aktan and T. Schnell, “Performance evaluation of pavement markings under dry, wet, and rainy conditions in the field,” *Transp Res Rec*, vol. 1877, no. 1, pp. 38–49, 2004.

[16] O. Smadi, R. R. Souleyrette, D. J. Ormand, and N. Hawkins, “Pavement marking retroreflectivity: Analysis of safety effectiveness,” *Transp Res Rec*, vol. 2056, no. 1, pp. 17–24, 2008.

[17] Y. Zhang and D. Wu, “Methodologies to predict service lives of pavement marking materials,” in *Journal of the Transportation Research Forum*, 2006, pp. 5–18.

[18] W. E. Sitzabee, *A spatial asset management study through an analysis of pavement marking performance*. North Carolina State University, 2008.

[19] J. Kopf, “Reflectivity of pavement markings: Analysis of retroreflectivity degradation curves,” Washington State

Department of Transportation Olympia, 2004.

[20] A. Carlos and P. E. Lopez, "Pavement marking handbook," *Texas Department of Transportation", Texas, USA, http://onlinemanuals. txdot. gov/txdotmanuals/pm h/pmh. pdf*, 2004.

[21] Federal Highway Administration (FHWA), "Nighttime Visibility," 2017.

[22] R. J. Benz, A. M. Pike, S. P. Kuchangi, and Q. Brackett, "Serviceable pavement marking retroreflectivity levels: technical report.," Texas Transportation Institute, 2009.

[23] C. Satterfield, H. Hawkins, and G. Schertz, "Assessment of Economic Impacts of SNPA Proposed Minimum Levels of Pavement Marking Retroreflectivity," United States. Federal Highway Administration. Office of Safety, 2014.

[24] A. Oracheff, A. Shahin, C. Holzschuher, and J. H. Fletcher, "Raised pavement marker assessments using mobile retroreflectivity unit technology," *Transp Res Rec*, vol. 2676, no. 12, pp. 293–302, 2022.

[25] C.-P. Chou, Y.-X. Lee, and A.-C. Chen, "Applying Machine Vision Algorithm on Pavement Marking Retroreflectivity Measurement," *Journal of Infrastructure Systems*, vol. 29, no. 4, p. 04023027, 2023.

[26] G. L. Brinster *et al.*, "Evaluating Mobile LiDAR Intensity Data for Inventorying Durable Tape Pavement Markings," *Sensors*, vol. 24, no. 20, p. 6694, 2024.

[27] ASTM International, "ASTM E1710," 2018.

[28] ASTM International, "ASTM E2177," 2018.

[29] ASTM International, "ASTM E2832-12," 2017.

[30] Agenzia Nazionale Autonoma delle Strade (ANAS), "Carta dei Servizi," Rome, 2024. Accessed: Mar. 07, 2025. [Online]. Available:

https://www.stradeanas.it/sites/default/files/pdf/Carta-dei-Servizi-2024-Anas.pdf

[31] L. Sasidharan, V. Karwa, and E. T. Donnell, "Use of pavement marking degradation models to develop a pavement marking management system," *Public Works Management & Policy*, vol. 14, no. 2, pp. 148–173, 2009.

[32] Federal Highway Administration (FHWA), "National Standards for Traffic Control Devices; the Manual on Uniform Traffic Control Devices (MUTCD) for Streets and Highways; Maintaining Pavement Marking Retroreflectivity," 2022.

[33] "EN 1436. Road Marking Materials Road Marking Performance for Road Users and Test Methods," Milano, Italy, 2018. Accessed: Feb. 12, 2023. [Online]. Available: https://store.uni.com/uni-en-1436-2018

[34] Austroads, "ATS 4110 - Longitudinal Pavement Marking: Austroads Technical Specification," 2021.

[35] Highways England, "CS 126: Inspection and assessment of road markings and road studs. Design Manual for Roads and Bridges," Birmingham, 2020.

[36] Caltrans, "Use of Warranties and Retroreflectivity Values in Pavement Marking," 2016.

[37] V. K. Dravitzki, S. M. Wilkie, and T. J. Lester, *The safety benefits of brighter roadmarkings*, no. 310. 2006.

[38] E. T. Donnell, V. Karwa, and S. Sathyanarayanan, "Analysis of effects of pavement marking retroreflectivity on traffic crash frequency on highways in North Carolina: application of artificial neural networks and generalized estimating equations," *Transp Res Rec*, vol. 2103, no. 1, pp. 50–60, 2009.

[39] P. J. Carlson, E. S. Park, and D. H. Kang, "Investigation of longitudinal pavement marking retroreflectivity and safety," *Transp Res Rec*, vol. 2337, no. 1, pp. 59–66, 2013.

[40] R. E. Avelar and P. J. Carlson, "Link between pavement marking retroreflectivity and night crashes on Michigan two-lane highways," *Transp Res Rec*, vol. 2404, no. 1, pp. 59–67, 2014.

[41] A. Eskandarian, *Handbook of intelligent vehicles*, vol. 2. Springer London, 2012.

[42] J. Golias, G. Yannis, and C. Antoniou, "Classification of driver-assistance systems according to their impact on road safety and traffic efficiency," *Transp Rev*, vol. 22, no. 2, pp. 179–196, 2002.

[43] O. Gietelink, *Design and validation of advanced driver assistance systems*, no. Trail Thesis Series T2007/11. 2007.

[44] N. Ebinger, N. Neuhuber, J. Moser, S. Trösterer, and A. Stocker, "Which partially automated driving function do drivers prefer? Results from two field studies on public highways," *Transportation Engineering*, vol. 17, p. 100236, 2024.

[45] A. Knapp, M. Neumann, M. Brockmann, R. Walz, and T. Winkle, "Code of Practice for the Design and Evaluation of ADAS," *Preventive and Active Safety Applications, eSafety for road and air transport, European Commission Project, Brüssel*, 2009.

[46] European Road Safety Observatory (ERSO), "Advanced driver assistance systems. European Commission," 2021.

[47] The National Highway Traffic Safety Administration (NHTSA), "Early Estimate of Motor Vehicle Traffic Fatalities in 2022 DOT HS 813 428," 2023.

[48] SAE International, " Taxonomy and Definitions for Terms Related to Driving Automation Systems for On-Road Motor Vehicles, J3016_201609.," Warrendale PA., 2016.

[49] European Commission, "Road safety in the European Union:

Trends, statistics and main challenges.," 2015.

[50] D. Miller *et al.*, "Behavioral measurement of trust in automation: the trust fall," in *Proceedings of the human factors and ergonomics society annual meeting*, SAGE Publications Sage CA: Los Angeles, CA, 2016, pp. 1849–1853.

[51] J. D. Lee and K. A. See, "Trust in automation: Designing for appropriate reliance," *Hum Factors*, vol. 46, no. 1, pp. 50–80, 2004.

[52] W. H. Organization, *Global status report on road safety 2018*. World Health Organization, 2019.

[53] The European New Car Assessment Programme (Euro NCAP), "TEST PROTOCOL – Lane Support Systems," 2017.

[54] The European Parliament and the Council of the European Union, "EC) No. 1224/2009. Regulation (EU) 2019/2144 of the European Parliament and of the Council," 2019. Accessed: May 13, 2023. [Online]. Available: https://eur-lex.europa.eu/eli/reg/2019/2144/oj

[55] Z. H. Khattak, M. D. Fontaine, and B. L. Smith, "Exploratory Investigation of Disengagements and Crashes in Autonomous Vehicles Under Mixed Traffic: An Endogenous Switching Regime Framework," *IEEE Transactions on Intelligent Transportation Systems*, vol. 22, no. 12, pp. 7485–7495, 2021, doi: 10.1109/TITS.2020.3003527.

[56] R. Liu, Z. Yuan, T. Liu, and Z. Xiong, "End-to-end Lane Shape Prediction with Transformers," in *2021 IEEE Winter Conference on Applications of Computer Vision (WACV)*, 2021, pp. 3693–3701. doi: 10.1109/WACV48630.2021.00374.

[57] J. A. Khan *et al.*, "Smart Cities Connected and Autonomous Vehicles Readiness Index," in *Proceedings of the 2nd ACM/EIGSCC Symposium on Smart Cities and Communities*, in SCC '19. New York, NY, USA: Association for Computing

Machinery, 2019. doi: 10.1145/3357492.3358631.

[58] Austroads, "AP-T348-19 Infrastructure Changes to Support Automated Vehicles on Rural and Metropolitan Highways and Freeways: Road Audit (Module 2)," Oct. 2019.

[59] The British Standards Institution (BSI), "PAS 1883:2020 Operational Design Domain (ODD) taxonomy for an automated driving system (ADS)–Specification," London, Aug. 2020.

[60] S. A. E. Taxonomy, "Definitions for terms related to driving automation systems for on-road motor vehicles," *SAE: Warrendale, PA, USA*, vol. 3016, 2018.

[61] I. Colwell, B. Phan, S. Saleem, R. Salay, and K. Czarnecki, "An automated vehicle safety concept based on runtime restriction of the operational design domain," in *2018 IEEE Intelligent Vehicles Symposium (IV)*, IEEE, 2018, pp. 1910–1917.

[62] R. Bishop, *Intelligent vehicle technology and trends*. 2005.

[63] L. Eriksson *et al.*, "Driver acceptance and performance with LDW and rumble strips assistance in unintentional lane departures," 2013, *VTI*.

[64] The European New Car Assessment Programme (Euro NCAP), "Euro NCAP - Lane Support," Euro NCAP.

[65] C. J. Banta-Green and J. Williams, "AAA Foundation for Traffic Safety," *Washington, DC: AAA Foundation for Traffic Safety*, 2016.

[66] D. J. , H. D. L. , S. R. , B. J. , C. D. L. , and S. C. A. Torbic, "NCHRP Report 641: Guidance for the Design and Application of Shoulder and Centerline Rumble Strips," Washington, D.C., 2009.

[67] AASHTO, *Highway Safety Manual*. Washington, D.C.: American Association of State Highway and Transportation

Officials , 2024.

[68] A. Høye, *The Handbook of Road Safety Measures*. Norwegian Centre for Transport Research, 2015.

[69] S. Cafiso and G. Pappalardo, "Safety effectiveness and performance of lane support systems for driving assistance and automation – Experimental test and logistic regression for rare events," *Accid Anal Prev*, vol. 148, p. 105791, 2020, doi: https://doi.org/10.1016/j.aap.2020.105791.

[70] S. Cafiso and C. D'Agostino, "Reliability-based assessment of Benefits in roadway safety management," *Transp Res Rec*, vol. 2513, no. 1, pp. 1–10, 2015.

[71] G. Pappalardo, S. Cafiso, A. Di Graziano, and A. Severino, "Decision Tree Method to Analyze the Performance of Lane Support Systems," *Sustainability*, vol. 13, no. 2, 2021, doi: 10.3390/su13020846.

[72] T. Hummel, M. Kühn, J. Bende, and A. Lang, "Advanced driver assistance systems," *German Insurance Association Insurers Accident Research. Available on www. udv. de, accessed at*, vol. 6, no. 01, p. 2015, 2011.

[73] J. S. Jermakian, "Crash avoidance potential of four passenger vehicle technologies," *Accid Anal Prev*, vol. 43, no. 3, pp. 732–740, 2011.

[74] K. Kompass, "Accident Research 2.0: New methods for representative evaluation of integral safety in traffic," 2013.

[75] Murphy M. and Kahl M., "Technology roadmap, light vehicle safety. ," Hannover, Germany. , 2012.

[76] P.-Y. Hsiao, K.-C. Hung, S.-S. Huang, W.-C. Kao, C.-C. Hsu, and Y.-M. Yu, "An embedded lane departure warning system," in *2011 IEEE 15th International Symposium on Consumer Electronics (ISCE)*, IEEE, 2011, pp. 162–165.

[77] E. Salari and D. Ouyang, "Camera-based Forward Collision

and lane departure warning systems using SVM," in *2013 IEEE 56th International Midwest Symposium on Circuits and Systems (MWSCAS)*, IEEE, 2013, pp. 1278–1281.

[78] H. Takahashi, "Various perspectives for driver support systems in japan," in *The 6th International Conference on Soft Computing and Intelligent Systems, and The 13th International Symposium on Advanced Intelligence Systems*, IEEE, 2012, pp. 1627–1632.

[79] H. Farah *et al.*, "An Empirical Analysis to Assess the Operational Design Domain of Lane Keeping System Equipped Vehicles Combining Objective and Subjective Risk Measures," *IEEE Transactions on Intelligent Transportation Systems*, vol. 22, pp. 2589–2598, 2020, [Online]. Available: https://api.semanticscholar.org/CorpusID:263876355

[80] A. García and F. J. Camacho-Torregrosa, "Influence of lane width on semi-autonomous vehicle performance," *Transp Res Rec*, vol. 2674, no. 9, pp. 279–286, 2020.

[81] J. Marr, S. Benjamin, and A. Zhang, *Implications of pavement markings for machine vision*, no. AP-R633-20. 2020.

[82] A. García, F. J. Camacho-Torregrosa, and P. V. P. Baez, "Examining the effect of road horizontal alignment on the speed of semi-automated vehicles," *Accid Anal Prev*, vol. 146, p. 105732, 2020.

[83] C. Chai, T. Liu, J. Liu, X. Cao, Y. Hu, and Q. Li, "Surrogate evaluation model for assessing lane detection reliability of automated vehicles in complex road environments," *Transp Res Rec*, vol. 2677, no. 7, pp. 185–195, 2023.

[84] N. Reddy, H. Farah, Y. Huang, T. Dekker, and B. van Arem, "Operational Design Domain Requirements for Improved Performance of Lane Assistance Systems: A Field Test Study in The Netherlands," *IEEE Open Journal of Intelligent*

*Transportation Systems*, vol. 1, pp. 237–252, 2020, [Online]. Available: https://api.semanticscholar.org/CorpusID:228089891

[85] B. Seppelt, B. Reimer, L. Angell, and S. Seaman, "Considering the human across levels of automation: Implications for reliance," in *Driving assessment conference*, University of Iowa, 2017.

[86] Y. Xing *et al.*, "Advances in vision-based lane detection: Algorithms, integration, assessment, and perspectives on ACP-based parallel vision," *IEEE/CAA Journal of Automatica Sinica*, vol. 5, no. 3, pp. 645–661, 2018.

[87] A. Ziebinski, R. Cupek, D. Grzechca, and L. Chruszczyk, "Review of advanced driver assistance systems (ADAS)," in *AIP Conference Proceedings*, AIP Publishing, 2017.

[88] G. Pappalardo, R. Caponetto, R. Varrica, and S. D. Cafiso, "Assessing the operational design domain of lane support system for automated vehicles in different weather and road conditions," *Journal of Traffic and Transportation Engineering (English Edition)*, 2022, [Online]. Available: https://api.semanticscholar.org/CorpusID:248766235

[89] J. Jung, E. Che, M. J. Olsen, and C. Parrish, "Efficient and robust lane marking extraction from mobile lidar point clouds," *ISPRS journal of photogrammetry and remote sensing*, vol. 147, pp. 1–18, 2019.

[90] P. Rahnamayiezekavat, D. Wang, J. Chai, S. Moon, M. Rashidi, and X. Wang, "Automated pavement marking integrity assessment using a UAV platform–a test case of public parking," *Journal of Asian Architecture and Building Engineering*, pp. 1–12, 2024.

[91] R. Huggins *et al.*, "Assessment of key road operator actions to support automated vehicles," 2017.

[92] P. Nitsche, I. Mocanu, and M. Reinthaler, “Requirements on tomorrow’s road infrastructure for highly automated driving,” in *2014 International Conference on Connected Vehicles and Expo (ICCVE)*, IEEE, 2014, pp. 939–940.

[93] T. S. CATAPULT, “Future proofing infrastructure for connected and automated vehicles,” Milton Keynes: Transport Systems Catapult, 2017.

[94] S. Lawson, “Roads that Cars Can Read REPORT III: Tackling the Transition to Automated Vehicles,” 2018.

[95] A. M. Pike, T. P. Barrette, and P. J. Carlson, “Evaluation of the Effects of Pavement Marking Characteristics on Detectability by ADAS Machine Vision,” *National Cooperative Highway Research Program (NCHRP): Washington, DC, USA*, 2018.

[96] T. E. Burghardt *et al.*, “Visibility of various road markings for machine vision,” *Case Studies in Construction Materials*, vol. 15, p. e00579, 2021.

[97] M. Matowicki, O. Přibyl, and P. Přibyl, “Analysis of possibility to utilize road marking for the needs of autonomous vehicles,” in *2016 Smart Cities Symposium Prague (SCSP)*, IEEE, 2016, pp. 1–6.

[98] E. N. EuroRAP, “Roads That Cars Can Read—A Quality Standard for Road Markings and Traffic Signs on Major Rural Roads,” 2013.

[99] ERF, “Marking the way towards a safer future: an ERF position paper on how road markings can make our road safer. ,” Brussels, 2013.

[100] Y. Y. Ye, X. L. Hao, and H. J. Chen, “Lane detection method based on lane structural analysis and CNNs,” *IET Intelligent Transport Systems*, vol. 12, no. 6, pp. 513–520, 2018.

[101] F. Favarò, S. Eurich, and N. Nader, “Autonomous vehicles’ disengagements: Trends, triggers, and regulatory limitations,”

*Accid Anal Prev*, vol. 110, pp. 136–148, 2018.

[102] A. Eskandarian, C. Wu, and C. Sun, "Research advances and challenges of autonomous and connected ground vehicles," *IEEE Transactions on Intelligent Transportation Systems*, vol. 22, no. 2, pp. 683–711, 2019.

[103] D. Babić, D. Babić, M. Fiolić, A. Eichberger, and Z. F. Magosi, "A comparison of lane marking detection quality and view range between daytime and night-time conditions by machine vision," *Energies (Basel)*, vol. 14, no. 15, p. 4666, 2021.

[104] M. Hadi and P. Sinha, "Effect of pavement marking retroreflectivity on the performance of vision-based lane departure warning systems," *J Intell Transp Syst*, vol. 15, no. 1, pp. 42–51, 2011.

[105] C. Davies, "Effects of pavement marking characteristics on machine vision technology," 2017.

[106] S. Jeong *et al.*, "Optimizing lane departure warning system towards AI-centered autonomous vehicles," *Sensors*, vol. 24, no. 8, p. 2505, 2024.

[107] A. D. Storsæter, K. Pitera, and E. McCormack, "Camera-based lane detection—can yellow road markings facilitate automated driving in snow?," *Vehicles*, vol. 3, no. 4, pp. 661–690, 2021.

[108] A. Sapkal, Arti, D. Pawar, and P. Singh, "Lane detection techniques for self-driving vehicle: comprehensive review," *Multimed Tools Appl*, vol. 82, no. 22, pp. 33983–34004, 2023.

[109] J. Liu, "Learning full-reference quality-guided discriminative gradient cues for lane detection based on neural networks," *J Vis Commun Image Represent*, vol. 65, p. 102675, 2019.

[110] E. Pollard, D. Gruyer, J.-P. Tarel, S.-S. Ieng, and A. Cord, "Lane marking extraction with combination strategy and comparative evaluation on synthetic and camera images," in *2011 14th International IEEE Conference on Intelligent*

*Transportation Systems (ITSC)*, IEEE, 2011, pp. 1741–1746.

[111] D. K. Dewangan and S. P. Sahu, "Driving behavior analysis of intelligent vehicle system for lane detection using vision-sensor," *IEEE Sens J*, vol. 21, no. 5, pp. 6367–6375, 2020.

[112] D. Xiao, L. Zhuo, J. Li, and J. Li, "Structure-prior deep neural network for lane detection," *J Vis Commun Image Represent*, vol. 81, p. 103373, 2021.

[113] A. Al Mamun, P. P. Em, M. J. Hossen, A. Tahabilder, and B. Jahan, "Efficient lane marking detection using deep learning technique with differential and cross-entropy loss.," *International Journal of Electrical & Computer Engineering (2088-8708)*, vol. 12, no. 4, 2022.

[114] Y. Zhang, Z. Lu, X. Zhang, J.-H. Xue, and Q. Liao, "Deep learning in lane marking detection: A survey," *IEEE Transactions on Intelligent Transportation Systems*, vol. 23, no. 7, pp. 5976–5992, 2021.

[115] S. Sheng, N. Formosa, M. Hossain, and M. Quddus, "Advancements in lane marking detection: An extensive evaluation of current methods and future research direction," *IEEE Transactions on Intelligent Vehicles*, 2024.

[116] H.-Y. Lin and C.-K. Chang, "Lane detection networks based on deep neural networks and temporal information," *Alexandria Engineering Journal*, vol. 98, pp. 10–18, 2024.

[117] Y. Chai, S. Wang, and Z. Zhang, "A fast and accurate lane detection method based on row anchor and transformer structure," *Sensors*, vol. 24, no. 7, p. 2116, 2024.

[118] S. Srivastava and R. Maiti, "Advanced Lane Detection and Tracking Using Robust Thresholding and Frame Coherence," *IEEE Transactions on Intelligent Transportation Systems*, 2025.

[119] T. Getahun and A. Karimoddini, "An integrated vision-based

perception and control for lane keeping of autonomous vehicles," *IEEE Transactions on Intelligent Transportation Systems*, 2024.

[120] I. Fakhari and S. Anwar, "Computer vision model based robust lane detection using multiple model adaptive estimation methodology," *Front Mech Eng*, vol. 11, p. 1436338, 2025.

[121] T. Yuan, W. Cao, S. Zhang, K. Yang, M. Schoen, and B. Duraisamy, "Lane Detection and Estimation from Surround View Camera Sensing Systems," in *2023 IEEE SENSORS*, IEEE, 2023, pp. 1–4.

[122] Q. Zhang, J. Liu, and X. Jiang, "Lane detection algorithm in curves based on multi-sensor fusion," *Sensors*, vol. 23, no. 12, p. 5751, 2023.

[123] P. Jabłoński, J. Iwaniec, and M. Jabłoński, "Multisensory Testing Framework for Advanced Driver Assistant Systems Supported by High-Quality 3D Simulation," *Sensors*, vol. 21, no. 24, p. 8458, 2021.

[124] V. Sagar, "Revolutionary Enhanced Lane Departure Detection Techniques for Autonomous Vehicle Safety using ADAS".

[125] Y. Jeong, "Interactive lane keeping system for autonomous vehicles using LSTM-RNN considering driving environments," *Sensors*, vol. 22, no. 24, p. 9889, 2022.

[126] H. Alzraiee, A. Leal Ruiz, and R. Sprotte, "Detecting of pavement marking defects using faster R-CNN," *Journal of Performance of Constructed Facilities*, vol. 35, no. 4, p. 04021035, 2021.

[127] B. Li, D. Song, H. Li, A. Pike, and P. Carlson, "Lane marking quality assessment for autonomous driving," in *2018 IEEE/RSJ International Conference on Intelligent Robots and Systems (IROS)*, IEEE, 2018, pp. 1–9.

[128] W. Jang, J. Hyun, J. An, M. Cho, and E. Kim, "A lane-level

road marking map using a monocular camera," *IEEE/CAA Journal of Automatica Sinica*, vol. 9, no. 1, pp. 187–204, 2021.

[129] J. B. Martirena, M. N. Doncel, A. C. Vidal, O. O. Madurga, J. F. Esnal, and M. G. Romay, "Automated annotation of lane markings using lidar and odometry," *IEEE Transactions on Intelligent Transportation Systems*, vol. 23, no. 4, pp. 3115–3125, 2020.

[130] T. E. Burghardt, A. Pashkevich, D. Babić, H. Mosböck, D. Babić, and L. Żakowska, "Microplastics and road markings: the role of glass beads and loss estimation," *Transp Res D Transp Environ*, vol. 102, p. 103123, 2022.

[131] N. Formosa, M. Quddus, C. K. Man, M. K. Singh, C. Morton, and C. B. Masera, "Evaluating the impact of lane marking quality on the operation of autonomous vehicles," *J Transp Eng A Syst*, vol. 150, no. 1, p. 04023126, 2024.

[132] H. A. Ghani *et al.*, "Advances in lane marking detection algorithms for all-weather conditions.," *International Journal of Electrical & Computer Engineering (2088-8708)*, vol. 11, no. 4, 2021.

[133] A. D. Storsæter, K. Pitera, and E. McCormack, "Using ADAS to future-proof roads—Comparison of fog line detection from an in-vehicle camera and mobile retroreflectometer," *Sensors*, vol. 21, no. 5, p. 1737, 2021.

[134] T. Y. Teo, R. Sutopo, J. M.-Y. Lim, and K. Wong, "Innovative lane detection method to increase the accuracy of lane departure warning system," *Multimed Tools Appl*, vol. 80, pp. 2063–2080, 2021.

[135] S. S. Tikar and R. A. Patil, "A Novel Fast Responding Driver Assistance Technique with Efficient Lane Detection and Collision Avoidance Using Dynamic Feature Extraction in Any Environment.," *Traitement du Signal*, vol. 39, no. 2, 2022.

[136] S. Sultana, B. Ahmed, M. Paul, M. R. Islam, and S. Ahmad, "Vision-based robust lane detection and tracking in challenging conditions," *IEEE Access*, vol. 11, pp. 67938–67955, 2023.

[137] P. Lehoczký, M. Janeba, M. Galinski, and L. Šoltés, "Testing the readiness of slovak road infrastructure for the deployment of intelligent transportation," *Strojnícky časopis-Journal of Mechanical Engineering*, vol. 72, no. 2, pp. 103–112, 2022.

[138] the International Organization for Standardization (ISO), "ISO 17361-2017 (E) Intelligent transport systems — Lane departure warning systems — Performance requirements and test procedures," Geneva, Switzerland, 2017. Accessed: Feb. 08, 2023. [Online]. Available: https://www.iso.org/standard/72349.html

[139] ANAS, "Ricerca e Innovazione Report 2009-2010," Rome, 2010.

[140] D. of C. E. and A. (DICAR) University of Catania, "Mobileye 6.0 (Intel®) full protocol ADAS & human perception data," Catania, Italy., 2022.

[141] Giovanni Andrea Dimauro, "Modelli di decadimento per la valutazione della retroriflettenza della segnaletica orizzontale.," Master's thesis, Università di Catania, Catania, 2024.

[142] Daniele Bordonaro, "Integrazione di dati da mappe, sensori veicolari e sistemi di rilievo della segnaletica orizzontale per la definizione dell'Operational Design Domain del Lane Support System.," Master's thesis, Università di Catania, Catania, 2022.

[143] A. V. Dorogush, V. Ershov, and A. Gulin, "CatBoost: gradient boosting with categorical features support," *arXiv preprint arXiv:1810.11363*, 2018.

[144] L. Prokhorenkova, G. Gusev, A. Vorobev, A. V. Dorogush, and A. Gulin, "CatBoost: unbiased boosting with categorical features," *Adv Neural Inf Process Syst*, vol. 31, 2018.

[145] A. Gulin, I. Kuralenok, and D. Pavlov, "Winning the transfer learning track of yahoo!'s learning to rank challenge with yetirank," in *Proceedings of the Learning to Rank Challenge*, PMLR, 2011, pp. 63–76.

[146] M. Ferov and M. Modrý, "Enhancing lambdamart using oblivious trees," *arXiv preprint arXiv:1609.05610*, 2016.

[147] R. Kohavi and C.-H. Li, "Oblivious decision trees, graphs, and top-down pruning," in *IJCAI*, 1995, pp. 1071–1077.

[148] D. G. Kleinbaum and M. Klein, "Ordinal Logistic Regression," in *Logistic Regression: A Self-Learning Text*, D. G. Kleinbaum and M. Klein, Eds., New York, NY: Springer New York, 2010, pp. 463–488. doi: 10.1007/978-1-4419-1742-3_13.

[149] R. M. Neal, "Monte Carlo implementation of Gaussian process models for Bayesian regression and classification," *arXiv preprint physics/9701026*, 1997.

[150] W. Chu, Z. Ghahramani, and C. K. I. Williams, "Gaussian processes for ordinal regression.," *Journal of machine learning research*, vol. 6, no. 7, 2005.

[151] N. Japkowicz and M. Shah, *Evaluating learning algorithms: a classification perspective*. Cambridge University Press, 2011.

[152] A. Agresti, *Analysis of ordinal categorical data*, vol. 656. John Wiley & Sons, 2010.

[153] S. Janitza, G. Tutz, and A.-L. Boulesteix, "Random forest for ordinal responses: Prediction and variable selection," *Comput Stat Data Anal*, vol. 96, pp. 57–73, 2016, doi: https://doi.org/10.1016/j.csda.2015.10.005.

[154] R. Hornung, "Ordinal Forests," *J Classif*, vol. 37, no. 1, pp. 4–17, 2020, doi: 10.1007/s00357-018-9302-x.

[155] G. Ke *et al.*, "Lightgbm: A highly efficient gradient boosting decision tree," *Adv Neural Inf Process Syst*, vol. 30, 2017.

[156] F. Hutter, L. Kotthoff, and J. Vanschoren, *Automated machine learning: methods, systems, challenges*. Springer Nature, 2019.

[157] I. Goodfellow, Y. Bengio, and A. Courville, *Deep learning*. MIT press, 2016.

[158] C. M. Bishop and N. M. Nasrabadi, *Pattern recognition and machine learning*, vol. 4, no. 4. Springer, 2006.

[159] K. P. Murphy, *Machine learning: a probabilistic perspective*. MIT press, 2012.

[160] Highways England, "DMRB: Road Layout CS 126 Inspection and assessment of road markings and road studs (formerly TD 26/17)," Birmingham, 2020.

# Appendix

## Table 25 RLmin datasets summary statistics under different segmentation

| RLmin | | | Count | Mean | Std | Min | Max | CV |
|---|---|---|---|---|---|---|---|---|
| General | Speed-avg | | 6340 | 69.8144 | 12.79009 | 14.12 | 99.7 | 0.183201 |
| | Headway-Mean | | 6340 | 3.338737 | 0.563277 | 0.56 | 3.5 | 0.16871 |
| | Curvature-Max | | 6340 | 0.001666 | 0.003217 | 1.00E-10 | 0.063452 | 1.931031 |
| | Lane | | 6340 | 3.497808 | 0.243861 | 3.15 | 3.9 | 0.069718 |
| | Shoulder | | 6340 | 0.527058 | 0.341058 | 0.1 | 1.6 | 0.647097 |
| | RL | | 6340 | 107.6467 | 66.57054 | 40 | 415 | 0.618417 |
| | RL Class | A | C1: 45.43%, C2: 32.38%, C3: 22.19% | | | | | |
| | | B | C1: 57.18%, C2: 31.53%, C3: 11.29% | | | | | |
| | Quality | | Class 1: 15.50%, Class 2: 12.33%, Class 3: 72.16% | | | | | |
| CU=0.005 | Speed-avg | | 5642 | 71.54268 | 12.05978 | 14.12 | 99.7 | 0.168568 |
| | Headway-Mean | | 5642 | 3.327506 | 0.582181 | 0.56 | 3.5 | 0.17496 |
| | Curvature-Max | | 5642 | 0.000798 | 0.001381 | 1.00E-10 | 0.004963 | 1.730688 |
| | Lane | | 5642 | 3.517698 | 0.246272 | 3.15 | 3.9 | 0.070009 |
| | Shoulder | | 5642 | 0.539197 | 0.34068 | 0.1 | 1.6 | 0.631828 |
| | RL | | 5642 | 109.4727 | 67.29454 | 40 | 415 | 0.614715 |
| | RL Class | A | C1: 44.33%, C2: 32.35%, C3: 23.33% | | | | | |
| | | B | C1: 56.15%, C2: 31.97%, C3: 11.88% | | | | | |
| | Quality | | Class 1: 11.22%, Class 2: 11.31%, Class 3: 77.47% | | | | | |
| CU=0.006 | Speed-avg | | 5833 | 71.2264 | 12.0664 | 14.12 | 99.7 | 0.169409 |
| | Headway-Mean | | 5833 | 3.328347 | 0.581524 | 0.56 | 3.5 | 0.174719 |
| | Curvature-Max | | 5833 | 0.000953 | 0.0016 | 1.00E-10 | 0.005999 | 1.6782 |
| | Lane | | 5833 | 3.512909 | 0.245719 | 3.15 | 3.9 | 0.069947 |
| | Shoulder | | 5833 | 0.538136 | 0.341484 | 0.1 | 1.6 | 0.634569 |
| | RL | | 5833 | 109.3338 | 67.16424 | 40 | 415 | 0.614304 |
| | RL Class | A | C1: 44.33%, C2: 32.47%, C3: 23.2% | | | | | |
| | | B | C1: 56.11%, C2: 32.11%, C3: 11.78% | | | | | |
| | Quality | | Class 1: 11.78%, Class 2: 11.61%, Class 3: 76.62% | | | | | |
| CV=0.6 | Speed-avg | | 6329 | 69.84069 | 12.76933 | 14.12 | 99.7 | 0.182835 |
| | Headway-Mean | | 6329 | 3.339009 | 0.563127 | 0.56 | 3.5 | 0.168651 |
| | Curvature-Max | | 6329 | 0.001657 | 0.003191 | 1.00E-10 | 0.063452 | 1.925973 |
| | Lane | | 6329 | 3.497843 | 0.243802 | 3.15 | 3.9 | 0.069701 |
| | Shoulder | | 6329 | 0.526339 | 0.340306 | 0.1 | 1.6 | 0.646553 |
| | RL | | 6329 | 107.7538 | 66.57849 | 40 | 415 | 0.617876 |
| | RL Class | A | C1: 45.33%, C2: 32.44%, C3: 22.23% | | | | | |
| | | B | C1: 57.1%, C2: 31.58%, C3: 11.31% | | | | | |
| | Quality | | Class 1: 15.45%, Class 2: 12.29%, Class 3: 72.25% | | | | | |
| CV=0.2 | Speed-avg | | 6210 | 69.95483 | 12.71139 | 14.12 | 99.7 | 0.181709 |
| | Headway-Mean | | 6210 | 3.337593 | 0.565718 | 0.56 | 3.5 | 0.169499 |
| | Curvature-Max | | 6210 | 0.001658 | 0.003192 | 1.00E-10 | 0.063452 | 1.924909 |
| | Lane | | 6210 | 3.499042 | 0.243882 | 3.15 | 3.9 | 0.0697 |
| | Shoulder | | 6210 | 0.524356 | 0.338877 | 0.1 | 1.6 | 0.646274 |
| | RL | | 6210 | 108.7399 | 66.70654 | 40 | 415 | 0.61345 |
| | RL Class | A | C1: 44.46%, C2: 32.95%, C3: 22.59% | | | | | |
| | | B | C1: 56.38%, C2: 32.11%, C3: 11.51% | | | | | |
| | Quality | | Class 1: 15.09%, Class 2: 12.25%, Class 3: 72.66% | | | | | |
| CV=0.1 | Speed-avg | | 5583 | 70.40846 | 12.67568 | 14.12 | 99.7 | 0.180031 |
| | Headway-Mean | | 5583 | 3.331315 | 0.577759 | 0.56 | 3.5 | 0.173433 |
| | Curvature-Max | | 5583 | 0.001638 | 0.003206 | 1.00E-10 | 0.063452 | 1.957742 |
| | Lane | | 5583 | 3.508732 | 0.243608 | 3.15 | 3.9 | 0.069429 |
| | Shoulder | | 5583 | 0.528157 | 0.340889 | 0.1 | 1.6 | 0.645432 |
| | RL | | 5583 | 113.314 | 67.80544 | 40 | 415 | 0.598385 |
| | RL Class | A | C1: 40.98%, C2: 34.28%, C3: 24.74% | | | | | |
| | | B | C1: 53.22%, C2: 34.14%, C3: 12.65% | | | | | |
| | Quality | | Class 1: 13.70%, Class 2: 11.88%, Class 3: 74.42% | | | | | |

## Table 26 RLmin environmental datasets summary statistics

| RLmin | | Count | Mean | Std | Min | Max | CV |
|---|---|---|---|---|---|---|---|
| General (Day-Wet) | Speed-avg | 6340 | 69.8144 | 12.79009 | 14.12 | 99.7 | 0.183201 |
| | Headway-Mean | 6340 | 3.338737 | 0.563277 | 0.56 | 3.5 | 0.16871 |
| | Curvature-Max | 6340 | 0.001666 | 0.003217 | 1.00E-10 | 0.063452 | 1.931031 |
| | Lane | 6340 | 3.497808 | 0.243861 | 3.15 | 3.9 | 0.069718 |
| | Shoulder | 6340 | 0.527058 | 0.341058 | 0.1 | 1.6 | 0.647097 |
| | RL | 6340 | 107.6467 | 66.57054 | 40 | 415 | 0.618417 |
| | RL Class B | C1: 57.18%, C2: 31.53%, C3: 11.29% | | | | | |
| | Quality | Class 1: 15.50%, Class 2: 12.33%, Class 3: 72.16% | | | | | |
| General (Dry) | Speed-avg | 4722 | 71.59508 | 12.69648 | 18.42 | 99.7 | 0.177337 |
| | Headway-Mean | 4722 | 3.312124 | 0.61185 | 0.56 | 3.5 | 0.18473 |
| | Curvature-Max | 4722 | 0.00161 | 0.003039 | 1.00E-10 | 0.063452 | 1.887946 |
| | Lane | 4722 | 3.515205 | 0.264158 | 3.15 | 3.9 | 0.075147 |
| | Shoulder | 4722 | 0.50323 | 0.253279 | 0.1 | 1.1 | 0.503307 |
| | RL | 4722 | 107.7478 | 64.34836 | 40 | 359 | 0.597213 |
| | RL Class B | C1: 56.14%, C2: 32.91%, C3: 10.95% | | | | | |
| | Quality | Class 1: 12.24%, Class 2: 12.20%, Class 3: 75.56% | | | | | |
| Day (Dry-Wet) | Speed-avg | 3575 | 69.68347 | 13.33693 | 14.12 | 99.7 | 0.191393 |
| | Headway-Mean | 3575 | 3.322713 | 0.571286 | 0.56 | 3.5 | 0.171934 |
| | Curvature-Max | 3575 | 0.00183 | 0.003538 | 1.00E-10 | 0.063452 | 1.933432 |
| | Lane | 3575 | 3.482476 | 0.239386 | 3.15 | 3.9 | 0.06874 |
| | Shoulder | 3575 | 0.574937 | 0.393179 | 0.1 | 1.6 | 0.683865 |
| | RL | 3575 | 106.1645 | 67.26308 | 40 | 415 | 0.633574 |
| | RL Class B | C1: 57.79%, C2: 31.69%, C3: 10.52% | | | | | |
| | Quality | Class 1: 14.97%, Class 2: 15.08%, Class 3: 69.96% | | | | | |
| Day (Dry) | Speed-avg | 3005 | 70.76757 | 12.69045 | 18.42 | 99.7 | 0.179326 |
| | Headway-Mean | 3005 | 3.331018 | 0.565793 | 0.56 | 3.5 | 0.169856 |
| | Curvature-Max | 3005 | 0.001776 | 0.00342 | 1.00E-10 | 0.063452 | 1.925345 |
| | Lane | 3005 | 3.473394 | 0.247713 | 3.15 | 3.9 | 0.071317 |
| | Shoulder | 3005 | 0.470882 | 0.271261 | 0.1 | 1.1 | 0.57607 |
| | RL | 3005 | 101.196 | 58.76434 | 40 | 355 | 0.580698 |
| | RL Class B | C1: 59%, C2: 33.34%, C3: 7.65% | | | | | |
| | Quality | Class 1: 14.48%, Class 2: 14.51%, Class 3: 71.01% | | | | | |
| Night (Dry-Wet) | Speed-avg | 2765 | 69.98369 | 12.04659 | 23.1 | 96.26 | 0.172134 |
| | Headway-Mean | 2765 | 3.359454 | 0.552164 | 0.6 | 3.5 | 0.164361 |
| | Curvature-Max | 2765 | 0.001454 | 0.002734 | 1.00E-10 | 0.035791 | 1.87987 |
| | Lane | 2765 | 3.517631 | 0.248172 | 3.15 | 3.9 | 0.070551 |
| | Shoulder | 2765 | 0.465154 | 0.245111 | 0.1 | 1.1 | 0.526947 |
| | RL | 2765 | 109.5631 | 65.62681 | 40 | 359 | 0.598986 |
| | RL Class B | C1: 56.38%, C2: 31.32%, C3: 12.3% | | | | | |
| | Quality | Class 1: 16.20%, Class 2: 8.79%, Class 3: 75.01% | | | | | |
| Night (Dry) | Speed-avg | 1717 | 73.04335 | 12.58034 | 27.51 | 96.26 | 0.172231 |
| | Headway-Mean | 1717 | 3.279056 | 0.683965 | 0.6 | 3.5 | 0.208586 |
| | Curvature-Max | 1717 | 0.001318 | 0.00219 | 1.00E-10 | 0.014786 | 1.661788 |
| | Lane | 1717 | 3.588381 | 0.275929 | 3.25 | 3.9 | 0.076895 |
| | Shoulder | 1717 | 0.559843 | 0.206485 | 0.25 | 0.75 | 0.368827 |
| | RL | 1717 | 119.2143 | 71.6928 | 40 | 359 | 0.601377 |
| | RL Class B | C1: 51.14%, C2: 32.15%, C3: 16.72% | | | | | |
| | Quality | Class 1: 8.33%, Class 2: 8.15%, Class 3: 83.52% | | | | | |

## Table 27 RL3 datasets summary statistics under different segmentation

| RL3 | | | Count | Mean | Std | Min | Max | CV |
|---|---|---|---|---|---|---|---|---|
| General | Speed-avg | | 6340 | 69.8144 | 12.79009 | 14.12 | 99.7 | 0.183201 |
| | Headway-Mean | | 6340 | 3.338737 | 0.563277 | 0.56 | 3.5 | 0.16871 |
| | Curvature-Max | | 6340 | 0.001666 | 0.003217 | 1.00E-10 | 0.063452 | 1.931031 |
| | Lane | | 6340 | 3.497808 | 0.243861 | 3.15 | 3.9 | 0.069718 |
| | Shoulder | | 6340 | 0.527058 | 0.341058 | 0.1 | 1.6 | 0.647097 |
| | RL | | 6340 | 163.7405 | 86.93862 | 40 | 554 | 0.530954 |
| | RL Class | A | C1: 19.61%, C2: 29.94%, C3: 50.46% | | | | | |
| | | B | C1: 28.85%, C2: 39.13%, C3: 32.02% | | | | | |
| | Quality | | Class 1: 15.50%, Class 2: 12.33%, Class 3: 72.16% | | | | | |
| CU=0.005 | Speed-avg | | 5642 | 71.54268 | 12.05978 | 14.12 | 99.7 | 0.168568 |
| | Headway-Mean | | 5642 | 3.327506 | 0.582181 | 0.56 | 3.5 | 0.17496 |
| | Curvature-Max | | 5642 | 0.000798 | 0.001381 | 1.00E-10 | 0.004963 | 1.730688 |
| | Lane | | 5642 | 3.517698 | 0.246272 | 3.15 | 3.9 | 0.070009 |
| | Shoulder | | 5642 | 0.539197 | 0.34068 | 0.1 | 1.6 | 0.631828 |
| | RL | | 5642 | 163.8905 | 87.10781 | 40 | 554 | 0.5315 |
| | RL Class | A | C1: 19.37%, C2: 30.18%, C3: 50.44% | | | | | |
| | | B | C1: 28.73%, C2: 39.05%, C3: 32.22% | | | | | |
| | Quality | | Class 1: 11.22%, Class 2: 11.31%, Class 3: 77.47% | | | | | |
| CU=0.006 | Speed-avg | | 5833 | 71.2264 | 12.0664 | 14.12 | 99.7 | 0.169409 |
| | Headway-Mean | | 5833 | 3.328347 | 0.581524 | 0.56 | 3.5 | 0.174719 |
| | Curvature-Max | | 5833 | 0.000953 | 0.0016 | 1.00E-10 | 0.005999 | 1.6782 |
| | Lane | | 5833 | 3.512909 | 0.245719 | 3.15 | 3.9 | 0.069947 |
| | Shoulder | | 5833 | 0.538136 | 0.341484 | 0.1 | 1.6 | 0.634569 |
| | RL | | 5833 | 164.4608 | 87.06294 | 40 | 554 | 0.529384 |
| | RL Class | A | C1: 19.22%, C2: 29.86%, C3: 50.92% | | | | | |
| | | B | C1: 28.48%, C2: 39.07%, C3: 32.45% | | | | | |
| | Quality | | Class 1: 11.78%, Class 2: 11.61%, Class 3: 76.62% | | | | | |
| CV=0.6 | Speed-avg | | 6329 | 69.84069 | 12.76933 | 14.12 | 99.7 | 0.182835 |
| | Headway-Mean | | 6329 | 3.339009 | 0.563127 | 0.56 | 3.5 | 0.168651 |
| | Curvature-Max | | 6329 | 0.001657 | 0.003191 | 1.00E-10 | 0.063452 | 1.925973 |
| | Lane | | 6329 | 3.497843 | 0.243802 | 3.15 | 3.9 | 0.069701 |
| | Shoulder | | 6329 | 0.526339 | 0.340306 | 0.1 | 1.6 | 0.646553 |
| | RL | | 6329 | 163.9452 | 86.87517 | 40 | 554 | 0.529904 |
| | RL Class | A | C1: 19.47%, C2: 29.99%, C3: 50.55% | | | | | |
| | | B | C1: 28.72%, C2: 39.2%, C3: 32.07% | | | | | |
| | Quality | | Class 1: 15.45%, Class 2: 12.29%, Class 3: 72.25% | | | | | |
| CV=0.2 | Speed-avg | | 6210 | 69.95483 | 12.71139 | 14.12 | 99.7 | 0.181709 |
| | Headway-Mean | | 6210 | 3.337593 | 0.565718 | 0.56 | 3.5 | 0.169499 |
| | Curvature-Max | | 6210 | 0.001658 | 0.003192 | 1.00E-10 | 0.063452 | 1.924909 |
| | Lane | | 6210 | 3.499042 | 0.243882 | 3.15 | 3.9 | 0.0697 |
| | Shoulder | | 6210 | 0.524356 | 0.338877 | 0.1 | 1.6 | 0.646274 |
| | RL | | 6210 | 165.948 | 86.37178 | 40 | 554 | 0.520475 |
| | RL Class | A | C1: 18.29%, C2: 30.32%, C3: 51.38% | | | | | |
| | | B | C1: 27.47%, C2: 39.86%, C3: 32.67% | | | | | |
| | Quality | | Class 1: 15.09%, Class 2: 12.25%, Class 3: 72.66% | | | | | |
| CV=0.1 | Speed-avg | | 5583 | 70.40846 | 12.67568 | 14.12 | 99.7 | 0.180031 |
| | Headway-Mean | | 5583 | 3.331315 | 0.577759 | 0.56 | 3.5 | 0.173433 |
| | Curvature-Max | | 5583 | 0.001638 | 0.003206 | 1.00E-10 | 0.063452 | 1.957742 |
| | Lane | | 5583 | 3.508732 | 0.243608 | 3.15 | 3.9 | 0.069429 |
| | Shoulder | | 5583 | 0.528157 | 0.340889 | 0.1 | 1.6 | 0.645432 |
| | RL | | 5583 | 173.7766 | 86.09444 | 40 | 554 | 0.495432 |
| | RL Class | A | C1: 14.81%, C2: 29.57%, C3: 55.62% | | | | | |
| | | B | C1: 23.39%, C2: 40.8%, C3: 35.81% | | | | | |
| | Quality | | Class 1: 13.70%, Class 2: 11.88%, Class 3: 74.42% | | | | | |

## Table 28 RL3 environmental datasets summary statistics

| RL3 | | Count | Mean | Std | Min | Max | CV |
|---|---|---|---|---|---|---|---|
| General (Day-Wet) | Speed-avg | 6329 | 69.84069 | 12.76933 | 14.12 | 99.7 | 0.182835 |
| | Headway-Mean | 6329 | 3.339009 | 0.563127 | 0.56 | 3.5 | 0.168651 |
| | Curvature-Max | 6329 | 0.001657 | 0.003191 | 1.00E-10 | 0.063452 | 1.925973 |
| | Lane | 6329 | 3.497843 | 0.243802 | 3.15 | 3.9 | 0.069701 |
| | Shoulder | 6329 | 0.526339 | 0.340306 | 0.1 | 1.6 | 0.646553 |
| | RL | 6329 | 163.9452 | 86.87517 | 40 | 554 | 0.529904 |
| | RL Class B | C1: 28.72%, C2: 39.2%, C3: 32.07% | | | | | |
| | Quality | Class 1: 15.45%, Class 2: 12.29%, Class 3: 72.25% | | | | | |
| General (Dry) | Speed-avg | 4718 | 71.59864 | 12.69501 | 18.42 | 99.7 | 0.177308 |
| | Headway-Mean | 4718 | 3.311965 | 0.612085 | 0.56 | 3.5 | 0.18481 |
| | Curvature-Max | 4718 | 0.001606 | 0.003035 | 1.00E-10 | 0.063452 | 1.890347 |
| | Lane | 4718 | 3.515356 | 0.26405 | 3.15 | 3.9 | 0.075113 |
| | Shoulder | 4718 | 0.503264 | 0.253364 | 0.1 | 1.1 | 0.503441 |
| | RL | 4718 | 164.699 | 83.65491 | 40 | 460 | 0.507926 |
| | RL Class B | C1: 27.66%, C2: 39.59%, C3: 32.75% | | | | | |
| | Quality | Class 1: 12.23%, Class 2: 12.19%, Class 3: 75.58% | | | | | |
| Day (Dry-Wet) | Speed-avg | 3566 | 69.73176 | 13.30639 | 18.42 | 99.7 | 0.190822 |
| | Headway-Mean | 3566 | 3.323247 | 0.570916 | 0.56 | 3.5 | 0.171795 |
| | Curvature-Max | 3566 | 0.001816 | 0.0035 | 1.00E-10 | 0.063452 | 1.927031 |
| | Lane | 3566 | 3.482515 | 0.239367 | 3.15 | 3.9 | 0.068734 |
| | Shoulder | 3566 | 0.57378 | 0.39222 | 0.1 | 1.6 | 0.683573 |
| | RL | 3566 | 163.7067 | 90.0567 | 40 | 554 | 0.55011 |
| | RL Class B | C1: 30.62%, C2: 37.66%, C3: 31.72% | | | | | |
| | Quality | Class 1: 14.86%, Class 2: 15.03%, Class 3: 70.11% | | | | | |
| Day (Dry) | Speed-avg | 3002 | 70.77862 | 12.69144 | 18.42 | 99.7 | 0.179312 |
| | Headway-Mean | 3002 | 3.330849 | 0.566051 | 0.56 | 3.5 | 0.169942 |
| | Curvature-Max | 3002 | 0.00177 | 0.003416 | 1.00E-10 | 0.063452 | 1.929855 |
| | Lane | 3002 | 3.473718 | 0.247625 | 3.15 | 3.9 | 0.071285 |
| | Shoulder | 3002 | 0.470953 | 0.271387 | 0.1 | 1.1 | 0.576252 |
| | RL | 3002 | 158.3767 | 80.94162 | 40 | 460 | 0.51107 |
| | RL Class B | C1: 29.98%, C2: 40.04%, C3: 29.98% | | | | | |
| | Quality | Class 1: 14.46%, Class 2: 14.49%, Class 3: 71.05% | | | | | |
| Night (Dry-Wet) | Speed-avg | 2763 | 69.98127 | 12.04177 | 23.1 | 96.26 | 0.172071 |
| | Headway-Mean | 2763 | 3.359352 | 0.552351 | 0.6 | 3.5 | 0.164422 |
| | Curvature-Max | 2763 | 0.001452 | 0.002729 | 1.00E-10 | 0.035791 | 1.880263 |
| | Lane | 2763 | 3.517626 | 0.248057 | 3.15 | 3.9 | 0.070518 |
| | Shoulder | 2763 | 0.46511 | 0.245172 | 0.1 | 1.1 | 0.527126 |
| | RL | 2763 | 164.253 | 82.60319 | 40 | 460 | 0.502902 |
| | RL Class B | C1: 26.28%, C2: 41.19%, C3: 32.54% | | | | | |
| | Quality | Class 1: 16.21%, Class 2: 8.76%, Class 3: 75.03% | | | | | |
| Night (Dry) | Speed-avg | 1716 | 73.03319 | 12.57695 | 27.51 | 96.26 | 0.172209 |
| | Headway-Mean | 1716 | 3.278928 | 0.684143 | 0.6 | 3.5 | 0.208648 |
| | Curvature-Max | 1716 | 0.001319 | 0.00219 | 1.00E-10 | 0.014786 | 1.661129 |
| | Lane | 1716 | 3.588199 | 0.275907 | 3.25 | 3.9 | 0.076893 |
| | Shoulder | 1716 | 0.55979 | 0.206534 | 0.25 | 0.75 | 0.368949 |
| | RL | 1716 | 175.7593 | 87.12829 | 40 | 460 | 0.495725 |
| | RL Class B | C1: 23.6%, C2: 38.81%, C3: 37.59% | | | | | |
| | Quality | Class 1: 8.33%, Class 2: 8.16%, Class 3: 83.51% | | | | | |

## Table 29 RLavg datasets summary statistics under different segmentation

| RLavg | | | Count | Mean | Std | Min | Max | CV |
|---|---|---|---|---|---|---|---|---|
| General | Speed-avg | | 6340 | 69.8144 | 12.79009 | 14.12 | 99.7 | 0.183201 |
| | Headway-Mean | | 6340 | 3.338737 | 0.563277 | 0.56 | 3.5 | 0.16871 |
| | Curvature-Max | | 6340 | 0.001666 | 0.003217 | 1.00E-10 | 0.063452 | 1.931031 |
| | Lane | | 6340 | 3.497808 | 0.243861 | 3.15 | 3.9 | 0.069718 |
| | Shoulder | | 6340 | 0.527058 | 0.341058 | 0.1 | 1.6 | 0.647097 |
| | RL | | 6340 | 193.6793 | 94.01498 | 42 | 614 | 0.485416 |
| | RL Class | A | C1: 9.29%, C2: 28.91%, C3: 61.8% | | | | | |
| | | B | C1: 18.45%, C2: 37.67%, C3: 43.88% | | | | | |
| | Quality | | Class 1: 7.56%, Class 2: 11.01%, Class 3: 81.44% | | | | | |
| CU=0.005 | Speed-avg | | 5642 | 71.54268 | 12.05978 | 14.12 | 99.7 | 0.168568 |
| | Headway-Mean | | 5642 | 3.327506 | 0.582181 | 0.56 | 3.5 | 0.17496 |
| | Curvature-Max | | 5642 | 0.000798 | 0.001381 | 1.00E-10 | 0.004963 | 1.730688 |
| | Lane | | 5642 | 3.517698 | 0.246272 | 3.15 | 3.9 | 0.070009 |
| | Shoulder | | 5642 | 0.539197 | 0.34068 | 0.1 | 1.6 | 0.631828 |
| | RL | | 5642 | 192.8538 | 93.75535 | 42 | 614 | 0.486147 |
| | RL Class | A | C1: 9.38%, C2: 29.32%, C3: 61.31% | | | | | |
| | | B | C1: 18.52%, C2: 38.04%, C3: 43.44% | | | | | |
| | Quality | | Class 1: 5.87%, Class 2: 9.39%, Class 3: 84.74% | | | | | |
| CU=0.006 | Speed-avg | | 5833 | 71.2264 | 12.0664 | 14.12 | 99.7 | 0.169409 |
| | Headway-Mean | | 5833 | 3.328347 | 0.581524 | 0.56 | 3.5 | 0.174719 |
| | Curvature-Max | | 5833 | 0.000953 | 0.0016 | 1.00E-10 | 0.005999 | 1.6782 |
| | Lane | | 5833 | 3.512909 | 0.245719 | 3.15 | 3.9 | 0.069947 |
| | Shoulder | | 5833 | 0.538136 | 0.341484 | 0.1 | 1.6 | 0.634569 |
| | RL | | 5833 | 193.8478 | 94.01556 | 42 | 614 | 0.484997 |
| | RL Class | A | C1: 9.22%, C2: 29.06%, C3: 61.72% | | | | | |
| | | B | C1: 18.31%, C2: 37.75%, C3: 43.94% | | | | | |
| | Quality | | Class 1: 5.98%, Class 2: 9.72%, Class 3: 84.3% | | | | | |
| CV=0.6 | Speed-avg | | 6329 | 69.84069 | 12.76933 | 14.12 | 99.7 | 0.182835 |
| | Headway-Mean | | 6329 | 3.339009 | 0.563127 | 0.56 | 3.5 | 0.168651 |
| | Curvature-Max | | 6329 | 0.001657 | 0.003191 | 1.00E-10 | 0.063452 | 1.925973 |
| | Lane | | 6329 | 3.497843 | 0.243802 | 3.15 | 3.9 | 0.069701 |
| | Shoulder | | 6329 | 0.526339 | 0.340306 | 0.1 | 1.6 | 0.646553 |
| | RL | | 6329 | 193.7252 | 94.05053 | 42 | 614 | 0.485484 |
| | RL Class | A | C1: 9.31%, C2: 28.87%, C3: 61.83% | | | | | |
| | | B | C1: 18.47%, C2: 37.62%, C3: 43.91% | | | | | |
| | Quality | | Class 1: 7.55%, Class 2: 10.95%, Class 3: 81.5% | | | | | |
| CV=0.2 | Speed-avg | | 6210 | 69.95483 | 12.71139 | 14.12 | 99.7 | 0.181709 |
| | Headway-Mean | | 6210 | 3.337593 | 0.565718 | 0.56 | 3.5 | 0.169499 |
| | Curvature-Max | | 6210 | 0.001658 | 0.003192 | 1.00E-10 | 0.063452 | 1.924909 |
| | Lane | | 6210 | 3.499042 | 0.243882 | 3.15 | 3.9 | 0.0697 |
| | Shoulder | | 6210 | 0.524356 | 0.338877 | 0.1 | 1.6 | 0.646274 |
| | RL | | 6210 | 194.6746 | 94.13417 | 42 | 614 | 0.483546 |
| | RL Class | A | C1: 9.29%, C2: 28.33%, C3: 62.38% | | | | | |
| | | B | C1: 18.18%, C2: 37.42%, C3: 44.4% | | | | | |
| | Quality | | Class 1: 7.29%, Class 2: 10.77%, Class 3: 81.93% | | | | | |
| CV=0.1 | Speed-avg | | 5583 | 70.40846 | 12.67568 | 14.12 | 99.7 | 0.180031 |
| | Headway-Mean | | 5583 | 3.331315 | 0.577759 | 0.56 | 3.5 | 0.173433 |
| | Curvature-Max | | 5583 | 0.001638 | 0.003206 | 1.00E-10 | 0.063452 | 1.957742 |
| | Lane | | 5583 | 3.508732 | 0.243608 | 3.15 | 3.9 | 0.069429 |
| | Shoulder | | 5583 | 0.528157 | 0.340889 | 0.1 | 1.6 | 0.645432 |
| | RL | | 5583 | 198.8805 | 94.88502 | 42 | 614 | 0.477096 |
| | RL Class | A | C1: 9.15%, C2: 26.42%, C3: 64.43% | | | | | |
| | | B | C1: 17.05%, C2: 36.29%, C3: 46.66% | | | | | |
| | Quality | | Class 1: 6.45%, Class 2: 10.25%, Class 3: 83.31% | | | | | |

## Table 30 RLavg environmental datasets summary statistics

| RLavg | | Count | Mean | Std | Min | Max | CV |
|---|---|---|---|---|---|---|---|
| General (Day-Wet) | Speed-avg | 6340 | 69.8144 | 12.79009 | 14.12 | 99.7 | 0.183201 |
| | Headway-Mean | 6340 | 3.338737 | 0.563277 | 0.56 | 3.5 | 0.16871 |
| | Curvature-Max | 6340 | 0.001666 | 0.003217 | 1.00E-10 | 0.063452 | 1.931031 |
| | Lane | 6340 | 3.497808 | 0.243861 | 3.15 | 3.9 | 0.069718 |
| | Shoulder | 6340 | 0.527058 | 0.341058 | 0.1 | 1.6 | 0.647097 |
| | RL | 6340 | 193.6793 | 94.01498 | 42 | 614 | 0.485416 |
| | RL Class B | C1: 18.45%, C2: 37.67%, C3: 43.88% | | | | | |
| | Quality | Class 1: 7.56%, Class 2: 11.01%, Class 3: 81.44% | | | | | |
| General (Dry) | Speed-avg | 4722 | 71.59508 | 12.69648 | 18.42 | 99.7 | 0.177337 |
| | Headway-Mean | 4722 | 3.312124 | 0.61185 | 0.56 | 3.5 | 0.18473 |
| | Curvature-Max | 4722 | 0.00161 | 0.003039 | 1.00E-10 | 0.063452 | 1.887946 |
| | Lane | 4722 | 3.515205 | 0.264158 | 3.15 | 3.9 | 0.075147 |
| | Shoulder | 4722 | 0.50323 | 0.253279 | 0.1 | 1.1 | 0.503307 |
| | RL | 4722 | 194.3405 | 90.56206 | 42 | 491 | 0.465997 |
| | RL Class B | C1: 17.85%, C2: 37.04%, C3: 45.11% | | | | | |
| | Quality | Class 1: 5.32%, Class 2: 10.59%, Class 3: 84.1% | | | | | |
| Day (Dry-Wet) | Speed-avg | 3575 | 69.68347 | 13.33693 | 14.12 | 99.7 | 0.191393 |
| | Headway-Mean | 3575 | 3.322713 | 0.571286 | 0.56 | 3.5 | 0.171934 |
| | Curvature-Max | 3575 | 0.00183 | 0.003538 | 1.00E-10 | 0.063452 | 1.933432 |
| | Lane | 3575 | 3.482476 | 0.239386 | 3.15 | 3.9 | 0.06874 |
| | Shoulder | 3575 | 0.574937 | 0.393179 | 0.1 | 1.6 | 0.683865 |
| | RL | 3575 | 195.0895 | 98.83473 | 44 | 614 | 0.506612 |
| | RL Class B | C1: 20.2%, C2: 35.75%, C3: 44.06% | | | | | |
| | Quality | Class 1: 7.3%, Class 2: 14.4%, Class 3: 78.66% | | | | | |
| Day (Dry) | Speed-avg | 3005 | 70.76757 | 12.69045 | 18.42 | 99.7 | 0.179326 |
| | Headway-Mean | 3005 | 3.331018 | 0.565793 | 0.56 | 3.5 | 0.169856 |
| | Curvature-Max | 3005 | 0.001776 | 0.00342 | 1.00E-10 | 0.063452 | 1.925345 |
| | Lane | 3005 | 3.473394 | 0.247713 | 3.15 | 3.9 | 0.071317 |
| | Shoulder | 3005 | 0.470882 | 0.271261 | 0.1 | 1.1 | 0.57607 |
| | RL | 3005 | 189.7055 | 89.32432 | 44 | 487 | 0.470858 |
| | RL Class B | C1: 19.1%, C2: 37.5%, C3: 43.39% | | | | | |
| | Quality | Class 1: 7.09%, Class 2: 13.71%, Class 3: 79.2% | | | | | |
| Night (Dry-Wet) | Speed-avg | 2765 | 69.98369 | 12.04659 | 23.1 | 96.26 | 0.172134 |
| | Headway-Mean | 2765 | 3.359454 | 0.552164 | 0.6 | 3.5 | 0.164361 |
| | Curvature-Max | 2765 | 0.001454 | 0.002734 | 1.00E-10 | 0.035791 | 1.87987 |
| | Lane | 2765 | 3.517631 | 0.248172 | 3.15 | 3.9 | 0.070551 |
| | Shoulder | 2765 | 0.465154 | 0.245111 | 0.1 | 1.1 | 0.526947 |
| | RL | 2765 | 191.8561 | 87.37412 | 42 | 491 | 0.455415 |
| | RL Class B | C1: 16.2%, C2: 40.14%, C3: 43.65% | | | | | |
| | Quality | Class 1: 7.88%, Class 2: 7.09%, Class 3: 85.03% | | | | | |
| Night (Dry) | Speed-avg | 1717 | 73.04335 | 12.58034 | 27.51 | 96.26 | 0.172231 |
| | Headway-Mean | 1717 | 3.279056 | 0.683965 | 0.6 | 3.5 | 0.208586 |
| | Curvature-Max | 1717 | 0.001318 | 0.00219 | 1.00E-10 | 0.014786 | 1.661788 |
| | Lane | 1717 | 3.588381 | 0.275929 | 3.25 | 3.9 | 0.076895 |
| | Shoulder | 1717 | 0.559843 | 0.206485 | 0.25 | 0.75 | 0.368827 |
| | RL | 1717 | 202.4525 | 92.15518 | 42 | 491 | 0.455194 |
| | RL Class B | C1: 15.67%, C2: 36.23%, C3: 48.11% | | | | | |
| | Quality | Class 1: 2.21%, Class 2: 5.13%, Class 3: 92.66% | | | | | |